

# The Institute of Paper Chemistry

Appleton, Wisconsin

## Doctor's Dissertation

The Reaction Between Tetrahydroabietic Acid  
Monolayers and Aluminum Ions.

I. The Influence of Oxalate

Eugene Hartwell Major, Jr.

June, 1969

ERRATA

Eugene Hartwell Major, Jr., Doctoral Dissertation

Fig. 4 (p. 32) and Fig. 10 (p. 49) are to be transposed.

Captions are to remain where they are.

THE REACTION BETWEEN TETRAHYDROABIETIC ACID MONOLAYERS  
AND ALUMINUM IONS. I. THE INFLUENCE OF OXALATE

A thesis submitted by

Eugene Hartwell Major, Jr.

B.S. 1964, North Carolina State University  
M.S. 1966, Lawrence University

in partial fulfillment of the requirements  
of The Institute of Paper Chemistry  
for the degree of Doctor of Philosophy  
from Lawrence University,  
Appleton, Wisconsin

Publication Rights Reserved by  
The Institute of Paper Chemistry

June, 1969

## TABLE OF CONTENTS

	Page
SUMMARY	1
INTRODUCTION	3
Objective of Internal Sizing	3
Modification of the Cellulosic Fiber Surface	5
Internal Sizing with Rosin-Alum System	7
General Description	7
Papermaker's Alum	7
Rosin	8
Interrelated Phenomena	9
Formation of Size Precipitate	9
Retention of Size Precipitate	11
Stabilization of Size Precipitate	12
Effect of Oxalate on Internal Sizing with Rosin-Alum System	12
Aluminum Oxalate Complexes	14
Surface Chemical Model of Rosin-Alum System	14
Monolayers from Oxalate-Alum Substrates	16
PRESENTATION OF THE THESIS PROBLEM	17
APPROACH TO THE THESIS PROBLEM	18
EXPERIMENTAL PROCEDURES	19
Experimental Design of Surface Chemical Model System	19
Determination of $\pi$ - <u>A</u> Isotherms	20
Apparatus	20
Technique	20
Analysis of Collected Monolayer Material	21
Isolation	21
Apparatus	21
Technique	21

Drying	23
Determination of Infrared Spectra	23
Determination of Total Carbon	24
Determination of Radioactive Carbon	24
Determination of Aluminum	24
RESULTS AND DISCUSSION	25
Reaction Between TABSH Monolayers and Aluminum Ions	25
Changes in $\pi$ -A Isotherm	25
Changes in Infrared Spectrum	31
Changes in Free Acid Mole Fraction	34
Composition of Collected Monolayer Material	39
Changes in Structure of Surface Region	40
Nature of the Reaction	41
Effect of Oxalate on the Reaction Between TABSH Monolayers and Aluminum Ions	43
Changes in $\pi$ -A Isotherm	43
Changes in Infrared Spectrum	48
Changes in Free Acid Mole Fraction	50
Composition of Collected Monolayer Material	51
Changes in Structure of Surface Region	53
Nature of the Effect	53
CONCLUSIONS	55
GLOSSARY	56
SUGGESTIONS FOR FURTHER WORK	59
ACKNOWLEDGMENTS	60
LITERATURE CITED	61
APPENDIX I. MATERIALS	66

APPENDIX II. SOLUTIONS	74
Buffer Solution	74
TABSH Spreading Solutions	74
Substrate Solutions	76
Sulfuric Acid	76
Aluminum Sulfate	76
Oxalic Acid	76
Aluminum Sulfate Plus Oxalic Acid	77
Carbon Analysis Solutions	77
Combustion	77
CO <sub>2</sub> -Absorption	77
CO <sub>2</sub> -Liberation	78
Cleaning Solution	78
APPENDIX III. DETERMINATION OF $\pi$ - <u>A</u> ISOTHERMS	79
Monolayers at the Liquid-Air Interface	79
Criteria for Monolayer Formation	79
Definition of $\pi$	80
Manual Measurement of $\pi$	81
Manual Measurement of <u>A</u>	82
Construction of $\pi$ - <u>A</u> Isotherm	82
Design of Automatic Recording Surface Balance	82
Operation of Automatic Recording Surface Balance	88
Determination of $\pi$ - <u>A</u> Isotherm	88
Calibration	89
Sample $\pi$ - <u>A</u> Isotherms	90
Effect of Area Reduction Rate on $\pi$ - <u>A</u> Measurements	90
Reproducibility of $\pi$ - <u>A</u> Measurements	92

APPENDIX IV. ANALYSIS OF COLLECTED MONOLAYER MATERIAL	95
Isolation	95
Collection Trough	95
Effect of Washing on Free Acid Mole Fraction	96
Effect of Number of Skimmings and Substrate Age on Free Acid Mole Fraction	97
Effect of Number of Skimmings on [Al] of Substrate	97
Effect of Number of Skimmings and Substrate Age on Substrate pH	99
Vacuum Drying Chamber	100
Reproducibility of Infrared Absorbance Ratio Values	100
Determination of Total Carbon	102
General Description	102
Recovery and Reproducibility	102
Determination of Optimum Operating Voltage of Bernstein-Ballentine Tube	102
APPENDIX V. DATA	105
APPENDIX VI. SAMPLE CALCULATIONS	108

## SUMMARY

The active species in the rosin-alum sizing process is basic aluminum resinate. This material and/or charged aluminum resinate are formed at the surface of colloidal resin acid particles when aluminum sulfate is added to a suspension. Before this colloidal reaction mechanism was presented, Cobb and Lowe hypothesized that oxalate prevents sizing by inhibiting the reaction between resinate and aluminum ions. The purpose of this work was to test their hypothesis in a quantitative manner for an isolated colloidal system.

A tetrahydroabietic acid (TABSH) monolayer was spread on the liquid-air interface of an aluminum sulfate solution - with and without oxalate. This monolayer was used to simulate the surface of colloidal resin acid particles in suspension. The interfacial reaction was monitored by measuring changes in physical and chemical properties of the monolayer when changes were made in the composition of the substrate. The physical properties (surface pressure,  $\pi$ , and molecular area,  $\underline{A}$ ) measured were the average molecular area of the monolayer molecules at  $\pi = 10$  dyne  $\text{cm}^{-1}$  ( $\underline{A}_{10}$ ), the average molecular area of the monolayer molecules at the extrapolated collapse point ( $\underline{A}_{\underline{K}, \underline{EX}}$ ), and the surface pressure of the monolayer at the extrapolated collapse point ( $\underline{\pi}_{\underline{K}, \underline{EX}}$ ). These quantities were obtained from monolayer  $\pi$ - $\underline{A}$  isotherms determined with an automatic recording surface balance of the Langmuir type. The free acid mole fraction ( $\underline{X}_{\underline{TABSH}}$ ) values and the aluminum and carbon contents of samples of collected monolayer material were also determined. The  $\underline{X}_{\underline{TABSH}}$  values were calculated from infrared data and the aluminum contents were obtained by an emission spectroscopy technique. The carbon contents were determined manometrically by the Van Slyke procedure.

Monolayers skimmed from the surface of aluminum sulfate solutions at pH 4.00 with no added sodium hydroxide consisted of monobasic aluminum ditetrahydroabietate ( $\text{Al}(\text{TABS})_2\text{OH}$ ) and TABSH. This compares favorably with the recent identification of

monobasic aluminum diresinate and free resin acid in the commercial size precipitate isolated from suspension.

The concentration dependence of the interfacial reaction and the existence of an apparent monolayer capacity indicate that the salt formation involves cation-exchange.

For aluminum sulfate systems that contained oxalate, the aluminum concentration,  $[Al]$ , (total molar concentration of aluminum species in the system) was constant at  $3.16 \times 10^{-3} M$ . (With an oxalate-free system, this  $[Al]$  gave a monolayer with a free acid mole fraction of 0.51.) As the oxalate concentration,  $[C_2O_4]$ , (total molar concentration of oxalate species in the system) was increased in these systems, changes in the properties of the monolayers signified that the interfacial reaction was inhibited. When  $[C_2O_4]/[Al]$  approached 2.0 for the model systems, the reaction was completely prevented. In the  $[C_2O_4]/[Al]$  range between 0.0 and 0.75,  $Al(C_2O_4)_3$  appeared to be formed in approximately stoichiometric amounts. Little if any of this complex reacted with the TABSH monolayer.

The  $\pi$ ,  $A$ , and  $X_{TABSH}$  data obtained with the monolayer system indicate that oxalate inhibits the reaction between colloidal resin acid and aluminum ions. This is in agreement with the hypothesis of Cobb and Lowe.

## INTRODUCTION

## OBJECTIVE OF INTERNAL SIZING

Often the resistance of paper or paperboard to the penetration of water and various aqueous liquids must be increased for the material to fit its end-use requirements. One process by which the paper product is modified to give it the desired resistance is termed internal sizing. The nature of this modification can best be understood by analyzing the penetration of a liquid into a capillary tube. The extent of such penetration is given by Equation (1)

$$L^2 = (\gamma_{LV} r \cos \theta) / (2\eta) \quad (1)$$

where

$L$  = depth of penetration

$r$  = capillary radius

$\gamma_{LV}$  = specific free-surface energy of the liquid-vapor interface

$\theta$  = contact angle between liquid and solid

$t$  = time of penetration

$\eta$  = coefficient of viscosity of the liquid.

Differentiation of Equation (1) with respect to time yields Equation (2) which describes the rate of penetration of a liquid into a capillary tube. This is the Washburn equation (1) and it is valid

$$dL/dt = (\gamma_{LV} r \cos \theta) / (4\eta L) \quad (2)$$

under the following conditions:

1. The driving pressure is limited to the capillary pressure;
2. The contact angle is acute;
3. The flow is laminar;

4. The air resistance and gravitational and inertial effects may be excluded or neglected.

These equations apply strictly for a single, uniform, cylindrical capillary. The structure of paper is not assumed to be composed of uniform capillaries. However, examination of Equation (2) for a single capillary can provide order of magnitude information about the factors involved in penetration.

For a given liquid and a given paper sample, this analysis suggests that one way to decrease the rate of penetration is to increase the contact angle. The surface chemical factors which determine the contact angle on a smooth solid surface are related by the Young-Dupre Equation (3) (2)

$$\cos \theta_A = (\gamma_{SV} - \gamma_{SL}) / (\gamma_{LV}) \quad (3)$$

where

$\theta_A$  = advancing contact angle between liquid and solid

$\gamma_{SV}$  = specific free-surface energy (erg cm.<sup>-2</sup>) of the solid-vapor interface

$\gamma_{SL}$  = specific free-surface energy of the solid-liquid interface

$\gamma_{LV}$  = specific free-surface energy of the liquid-vapor interface.

According to Equation (3),  $\theta_A$  may be increased by increasing  $\gamma_{LV}$  and/or by decreasing the difference between  $\gamma_{SV}$  and  $\gamma_{SL}$ . Moreover, if the difference between  $\gamma_{SV}$  and  $\gamma_{SL}$  is made negative,  $\theta_A$  will be  $>90^\circ$  ( $\cos \theta_A$  will be negative) and the liquid will not spontaneously penetrate the paper structure. In practice,  $\gamma_{LV}$  and  $\gamma_{SL}$  are difficult to increase and the objective of internal sizing is to lower the value of  $\gamma_{SV}$  (the specific free-surface energy of the solid-vapor interface).

## MODIFICATION OF THE CELLULOSIC FIBER SURFACE

The specific free-surface energy of the solid-vapor interface can be changed significantly by altering the molecular species in the first layer of the solid. This layer may be modified by a number of factors. Among these are the following as summarized by Swanson (3):

1. The chemical composition of the molecule;
2. The structure of the molecule;
3. The orientation of the molecule on the solid surface;
4. The degree of packing of the molecules on the solid surface;
5. The strength of anchorage of amphipathic (polar-nonpolar) molecules in an oriented position;
6. The nature of the underlying solid molecules;
7. Possible electrical charge effects.

Langmuir (4) conducted pioneering studies on the behavior of various plane solid surfaces in contact with water. He found that drops of water placed on clean surfaces of glass, platinum, mica calcite, sphalerite, and galena spread over these surfaces and wetted them completely. Consequently, the contact angle between water and the clean surfaces of these materials is zero and they possess high free-surface energies.

When a fatty acid monolayer was deposited on each of the solid surfaces studied, a marked change occurred in its behavior toward water. Without exception, each of the modified surfaces became hydrophobic, and the contact angle between water and these new surfaces was observed to depend on the character of the underlying solid. The difference in contact angles for the various solids was attributed to the difference in the strength of anchorage of the amphipathic fatty acid molecule to the solid surfaces.

The hydrocarbon end of the fatty acid molecule has a low free-surface energy and tends to promote a high contact angle with water. The carboxyl group on the opposite end of the molecule has a high intrinsic free-surface energy and tends to promote wetting or a low contact angle with water. The attraction between the carboxyl group and the solid surfaces is probably sufficient to orient the hydrocarbon portion of the molecule away from the solid surface initially. However, a drop of water possesses attraction for the carboxyl groups and it competes with the solid surface for these groups. Consequently, the contact angle between water and the monolayer deposited on the solid surface depends on the strength of anchorage of monolayer molecules to the solid surface. It also depends on the proportion of amphipathic molecules in the monolayer which can be overturned and brought into contact with the water surface.

Later work by Rideal and Tadayon (5, 6) showed that the contact angle between water and solid crystalline stearic acid decreases with time. The mobility of stearic acid molecules in the solid state is apparently sufficient to allow the orientation of the carboxyl groups into the interface between the solid acid and water. Yiannos (7) measured the reorientation of stearic acid, myristic acid, and lauric acid monolayers when in contact with water. He found that the rate at which these monolayers approached an equilibrium contact angle depended inversely on the size of the molecules involved.

By using basic concepts of surface chemistry, the problem of improving sizing reduces to one of decreasing the free-surface energy of the cellulosic fiber surface. This reduction can be accomplished by covering a significant proportion of the surface with properly oriented and anchored bulky amphipathic molecules. The advantage of using the amphipathic molecules is that they have a better chance of being retained through chemical and physical interactions than nonpolar molecules.

## INTERNAL SIZING WITH THE ROSIN-ALUM SYSTEM

## GENERAL DESCRIPTION

The rosin-alum internal sizing process has been in use since 1807 and it is still widely used (8). The active sizing species in this process is the amphipathic molecule, basic aluminum resinate (3, 9-12). This material and/or charged aluminum resinate are produced in a pulp suspension by reacting papermaker's alum ( $\text{Al}_2(\text{SO}_4)_3 \cdot \text{ca. } 14 \text{ H}_2\text{O}$ ) with rosin (in the free, partially saponified, or saponified form) in the pH range between 4 and 7 (3, 9-15). These aluminum resinates exist with free resin acid in colloidal aggregations which are retained on the fibers during formation of the paper web (3, 11-15). During drying, these aggregations develop resistance to being wetted by water, and sizing is thereby achieved. Evidence was obtained by Guide (11) and Watkins (12) that the basic aluminum resinate molecules (charged aluminum resinate is converted to basic aluminum resinate during drying) in the aggregations are oriented and anchored with their hydrocarbon portion pointing away from the fiber surface. The position of the free resin acid molecules is not clear. Two investigators believe that they are on the interior of the precipitate particle after drying (14). Others have pictured them as randomly spaced and oriented molecules on the surface of the precipitate particle (11, 12).

Papermaker's Alum

Papermaker's alum is primarily a mixture of aluminum sulfate hydrates and its average composition is represented by the formula  $\text{Al}_2(\text{SO}_4)_3 \cdot \text{ca. } 14 \text{ H}_2\text{O}$  (16). For freshly prepared, dilute, acidic aluminum sulfate solutions, Miceli and Stuehr (17) reported that the coupled equilibria in Fig. 1 fitted pressure-jump relaxation data.

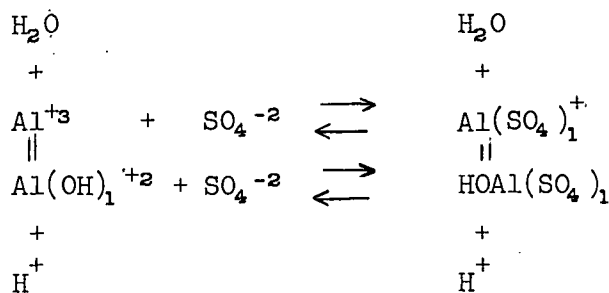


Figure 1. Coupled Equilibria Scheme for Freshly Prepared, Dilute, Acidic Aluminum Sulfate Solutions (17)

These authors used solutions with  $\text{Al}_2(\text{SO}_4)_3$  concentrations ranging from  $1.0 \times 10^{-2}$  to  $2.0 \times 10^{-1} \text{ M}$ . The pH of the systems was maintained between 1 and 3 and the ionic strength was not held constant. The zero ionic strength equilibrium constant for the reaction given in Equation (4) is  $1.59 \times 10^3 \text{ l. mole}^{-1}$ .



Likewise, the zero ionic strength equilibrium constant for the reaction given in Equation (5) is  $6.46 \times 10^{-6} \text{ l. mole}^{-1}$ .



Miceli and Stuehr found that the proportion of hydrated  $\text{Al}^{+3}$  in the solutions increases with dilution and that the fraction of  $\text{Al}(\text{OH})_1^{+2}$  remains very low. For the  $1.0 \times 10^{-2} \text{ M}$   $\text{Al}_2(\text{SO}_4)_3$  solution,  $\text{Al}^{+3}$  comprises approximately 50% of the total aluminum species concentration. For  $\text{Al}(\text{ClO}_4)_3$  solutions with small amounts of added base, evidence of  $\text{Al}(\text{H}_2\text{O})_5\text{OH}^{+2}$  dimerization was obtained (18). Likewise for  $\text{Al}(\text{Cl})_3$  solutions with small amounts of added base, the formation of  $\text{Al}(\text{H}_2\text{O})_4(\text{OH})_2^{+1}$  (19) has been proposed as has the formation of colloidal particles (13).

### Rosin

Rosin is composed of a mixture of resin acids and about 10% nonacidic material. The resin acids (monocarboxylic acids of alkylated hydrophenanthrene nuclei) are

further divided into two types, the abietic acid type and the pimaric acid type. Commercial rosin contains 59 to 75% abietic acid type resin acids; the exact amount depends on the source and the method of isolation (20-22).

#### INTERRELATED PHENOMENA

An exact mechanism of rosin sizing has not yet been defined that explains the results obtained for all sizing conditions. The difficulty to formulate an iron-clad mechanism probably arises because the system possesses both colloidal and ionic characteristics (8).

This dual nature of the system makes it extremely sensitive to the everyday variables in the papermaking process (12, 13). Regardless of the complexity of the rosin-alum sizing system, three primary interrelated factors that must be in proper balance can be recognized (3). These factors are as follows: 1. the preparation of a size precipitate which has a potentially low free-surface energy; 2. the retention of the size precipitate upon the fiber surfaces; and 3. the conversion of the wet sizing compounds on the solid surface to a stable low free-surface energy configuration which remains fixed even though aqueous fluids are brought into contact with it.

#### Formation of Size Precipitate

The active sizing species in the rosin-alum system is the amphipathic molecule, basic aluminum resinate (3, 9-12). Whether this is the dibasic aluminum mono-resinate, the monobasic aluminum diresinate, or a mixture of the two is still subject to debate. Likewise, the mechanism of formation is not yet settled.

Guide (11) used solvent extraction and chemical analysis techniques to determine the products formed when perchloric acid is added to alkaline sodium aluminate-sodium

abietate systems. He concluded that the size precipitates are not stoichiometric compounds and that they consist of coprecipitates of aluminum abietates, abietic acid, and aluminum hydroxide. Guide considered the precipitation reaction to be ionic. Davidson (15) also used the ionic mechanism to explain the reaction between rosin size and alum. He employed infrared, analytical pyrolysis, and chemical analysis techniques to determine the composition of the precipitates formed by adding alum or alum and sulfuric acid to alkaline rosin size solutions. He found that the precipitate is approximately an equimolar mixture of monobasic aluminum diresinate and free resin acid. This composition is the same as that reported by Price (23-24) for the rosin size-alum system and Back and Steenberg (25) for the sodium abietate-alum system. These latter three authors used solvent extraction and chemical analysis techniques to determine the composition of the size precipitate. They also explained their results on the assumption that the reaction between sodium resinate and alum is ionic.

On the contrary, Watkins (12) and Strazdins (13) reported that rosin is colloidal within the normal pH range used in commercial rosin-alum sizing. Watkins postulated that the aluminum ion reacts with carboxyl groups available on the surface of the colloidal particle to give dibasic aluminum monoresinate and monobasic aluminum diresinate. The interpretation made by Strazdins is that complex aluminum species (colloidal or ionic) react with colloidal rosin to give an aggregated size precipitate. Vandenberg and Spurlin (14) determined that in acid systems the size precipitate consists of colloidal particles composed of monobasic aluminum diresinate and resin acid.

Thode, et al. (26), and Ninck Blok (27) reported earlier that rosin is colloidal within the normal pH range used in sizing. Consequently, the colloidal mechanism of basic aluminum resinate (12, 13) and/or charged aluminum resinate (14) formation seems more reasonable than the ionic mechanism for the actual sizing system.

### Retention of Size Precipitate

The theories and variations of theories concerning the retention of the size precipitate can be reduced to two main ones - the coordination theory and the electrostatic theory.

The basis of the coordination theory is that the aluminum ion acts as an interconnecting link between rosin and the cellulose fiber. Wilson (28) pictured the aluminum ion as the replacement for the cations of the saponified rosin size and the cations of cellulose in an ion exchange reaction. Thomas (29) and Cobb and Lowe (30) assumed that aluminum resinate forms coordination bonds with cellulose hydroxyl groups.

The electrostatic theory is based on the mutual attraction of colloidal particles with opposite electrokinetic potentials. Work by Rowland and coworkers (31) showed that the electrokinetic potential of size precipitates is affected by the pH of the system and the composition of the precipitates. Thode, et al., (32) confirmed these results and, in later studies, he and his coworkers (33) determined that cellulose fibers dispersed in water have a negative potential. This latter observation was confirmed by Ninck Blok (34). Thode, et al., (32) proposed that size precipitates are attracted to negatively charged fibers because the precipitate has a positive electrokinetic potential which can be attributed to the aluminum ion. The difference in the potential of the two particles causes the mutual coalescence of the size precipitate and the fiber (3). Work by Guide (11) confirmed these charge effects. According to Guide (11) and Strazdins (13), the mechanism of retention of the size particles is a physical adsorption phenomenon. In their scheme, the short range van der Waals forces are operative and electrostatic attraction aids in the union of suspended particles. Later work by Vandenberg and Spurlin (14) is in general agreement with the importance of electrostatic attraction.

### Stabilization of Size Precipitate

The coordination theory and the reorientation theory are used to explain the stabilization of the size precipitate. Cobb and Lowe (30) proposed that the basic aluminum resinate fraction is stabilized by coordination with cellulose hydroxyl groups. Meanwhile, Guide (11) postulated that the conversion process involves the association of molecules of aluminum hydroxide, aluminum resinate, and cellulose hydroxyl groups by olation (Al-OH-Al linkage). The olation immobilizes the individual precipitate molecules so that they are effectively bound to the cellulose fiber in a nonwetting configuration. Vandenberg and Spurlin (14) reasoned that monobasic aluminum diresinate partially ionizes to give the aluminum diresinate ion which reacts directly with the hemicellulose portion of the fiber.

The reorientation of basic aluminum resinate molecules at sheet drying temperatures was proposed by Watkins (12) for deposited aggregations of these molecules and resin acid molecules. He hypothesized that as a result of this reorientation, the hydrocarbon portions of the basic aluminum resinate molecules are on the surface of the particles. This places the aluminum hydroxyl portions of the molecules inside the particles where they can undergo olation. Vandenberg and Spurlin (14) also proposed that the size precipitate particles reorient at sheet drying temperatures and form stable Al-O-Al bonds which retard molecular overturning.

#### EFFECT OF OXALATE ON INTERNAL SIZING WITH ROSIN-ALUM SYSTEM

Papermakers often find that satisfactory sizing cannot be obtained during hot weather with the rosin-alum sizing system (30). Cobb and Lowe (30) noted that this is also the period of the year during which bacterial fermentation is at its height in the normal mill system. Consequently, these workers postulated that oxalic and other di- and tricarboxylic acid anions present in the mill system because of bacterial action compete with resinate for aluminum ions.

Thomas (29) reported that certain common anions replace the hydroxyl group from hydrated aluminum complexes. The order of effectiveness among the anions is as follows: oxalate = citrate > tartrate > acetate > sulfate > chloride > nitrate. This has been called the order of coordination affinity of these anions for the aluminum ion (30). Based on this order of anion replacement, Cobb and Lowe hypothesized that oxalate in the mill system will greatly reduce or prevent aluminum resinate formation by sequestering aluminum ions.

Cobb and Lowe tested their theory concerning the competition between oxalate and resinate ions for aluminum ions on laboratory handsheets. They found that normally sized sheets that were dipped in dilute oxalic acid before drying showed little or no sizing after drying. Likewise, when aluminum tartrate and aluminum citrate were substituted for alum in the normal sizing procedure, poor sizing occurred. Thode and Gorham (35) reported that when sodium citrate is added to the rosin-alum sizing system, the sizing that can be attained with the system decreases. These workers also noted that the electrophoretic mobility of size precipitates is reduced from positive to negative as the concentration of sodium citrate in the rosin-aluminum chloride system is increased. Later work by Thode and Htoo (33) showed that the surface potential of size precipitates changes from positive to negative when the concentration of sodium oxalate in the system increases.

Swanson (36) noted that oxalic acid can enter the mill system by other means than bacterial fermentation. Some of these other sources are as follows: 1. fiber degradation during cooking and bleaching, 2. water supply, and 3. wood supply.

## ALUMINUM OXALATE COMPLEXES

The existence of aluminum oxalate complexes in solution has been indicated by the isolation of mixed crystalline salts of aluminum oxalate and by studies of aluminum oxalate solutions.

Rosenheim (37) and Fujita, *et al.*, (38) reported the isolation of crystalline salts of the type  $\text{MeAl}(\text{C}_2\text{O}_4)_2 \cdot n\text{H}_2\text{O}$  and  $\text{Me}_3\text{Al}(\text{C}_2\text{O}_4)_3 \cdot n\text{H}_2\text{O}$  where  $\text{Me} = \text{K}^+, \text{Na}^+$ , or  $\text{NH}_4^+$ . The infrared spectrum of  $\text{K}_3\text{Al}(\text{C}_2\text{O}_4)_3 \cdot 3\text{H}_2\text{O}$  was determined by Fujita, *et al.*, (38) and the Al-O stretching bands in the range between 600 and 300  $\text{cm}^{-1}$  for this compound were assigned by these authors. These assignments were made on the basis of a normal coordinate treatment of the 1:1 metal:ligand model of the chelate ring of tris-(oxalato)-Cr(III).

Lacroix (39) reported evidence for the presence of  $\text{Al}(\text{C}_2\text{O}_4)_2^{-1}$  and  $\text{Al}(\text{C}_2\text{O}_4)_3^{-3}$  complex ions in solution at pH values greater than 3.0. Later Babko and Dubovenko (40) used the isomolar series method to study the formation of aluminum oxalate complexes at various hydrogen ion concentrations. They found that only the simple complex,  $\text{Al}(\text{C}_2\text{O}_4)^{+1}$ , is formed in solutions which are 0.5N in HCl. For aluminum-oxalate solutions with successively lower hydrogen ion concentrations, Babko and Dubovenko obtained evidence of the stepwise formation of  $\text{Al}(\text{C}_2\text{O}_4)_2^{-1}$  and  $\text{Al}(\text{C}_2\text{O}_4)_3^{-3}$ . The concentration of each species present in the system was shown to depend on the concentration of oxalate and the pH of the solution. Some mixed complexes have also been reported in which oxalate is one of several anions complexed with aluminum (41).

## SURFACE CHEMICAL MODEL OF ROSIN-ALUM SYSTEM

A number of investigators (12-14, 26-27) have indicated that resin acids exist in a colloidal form under the normal conditions used in commercial rosin-alum sizing. As a result, the formation of basic aluminum resinate involves the

surface reaction between hydrated aluminum ions and colloidal resin acid particles (12-14). The success of the rosin-alum sizing operation depends on this surface reaction. Both the retention and stabilization of the size precipitate on the fiber surface are functions of the basic aluminum resinate content of the precipitate.

Ekwall (42) noted that the behavior of substances in monolayers is directly connected with their behavior in colloidal aggregations. The packing of molecules in the surface of a colloidal particle can be no closer than in a condensed monolayer of the same substance on an aqueous substrate. This correlation has been proven for the alkali salts of n-long paraffin chain fatty acids by x-ray investigation (43). The molecular packing area is the average cross-sectional area of the molecules ( $\underline{A_K}$ ,  $A \cdot \text{molecule}^{-1}$ ) at the point of film collapse for a monolayer under lateral compression. Likewise, the lateral force per unit width of the monolayer ( $\underline{\pi_K}$ , dynes  $\text{cm.}^{-1}$ ) needed to collapse the film is related to the stability of a colloidal particle of the same substance (42).

Ekwall and Bruun (42, 44-46) first used the surface chemical model for the reaction between hydrated aluminum ions and colloidal resin acid. These workers found that  $\underline{\pi_K}$  and  $\underline{A_K}$  values can be used to follow the reaction between resin acid monolayer molecules and aluminum ions in the substrate. Ekwall and Bruun (46) reported that when  $\underline{\pi_K}$  reached a maximum for a system, the aluminum content of the collected monolayer corresponded to that of dibasic aluminum monoresinate. However, absorption at  $1700 \text{ cm.}^{-1}$  in the infrared spectrum of the collected material indicated that substantial free resin acid was still present in the sample (47). This absorption and the fact that the collected monolayer material was not immediately isolated from aluminum salt solution weakened Ekwall and Bruun's identification (46, 48).

Strazdins (49) also used a surface chemical model system to determine the aluminum counterion shielding effect on the colloidal surface. He was able to show that aluminum salt formation and counterion data for resin acid monolayer-aluminum chloride systems correlate with actual handsheet sizing results.

Carboxylic acid molecules in a monolayer on an aqueous substrate are oriented so that the polar carboxyl groups are in the substrate (50). The reaction between multivalent metal ions and this layer of carboxyls has been compared to a chelation reaction between metal ions and multidentate ligands in aqueous solution. Ferroni, *et al.*, (51, 52) obtained evidence that the molecular areas for certain monolayer salts are similar to those for planar chelates.

#### MONOLAYERS FROM OXALATE-ALUM SUBSTRATES

Major and Swanson (53) studied the wettability of monolayers of free resin acid plus basic aluminum resinate cast on silver-coated glass slides by the Langmuir-Blodgett technique (54). These authors found that as the oxalate:aluminum mole ratio in the substrate of the casting trough increased (at constant pH and alum concentration), the rate at which the deposited monolayers wetted increased. Likewise, the final contact angle between water and the monolayer decreased. These results indicate that a change in the composition of the model monolayer occurs with oxalate addition to the aqueous aluminum sulfate substrate.

## PRESENTATION OF THE THESIS PROBLEM

Successful rosin sizing depends on the formation of a size precipitate that contains sufficient basic aluminum resinate to insure its retention and stabilization on the fiber surface. When oxalate is present in the mill system, sizing with rosin and alum is seriously impaired. The detrimental effect of oxalate is ascribed to aluminum oxalate formation at the expense of basic aluminum resinate formation. This hypothesis was used to explain the results of handsheet sizing, size precipitate surface potential, and monolayer stability studies where oxalate was present in model rosin sizing systems. The hypothesis is based on an ionic reaction mechanism for resin ions and aluminum ions. However, recent workers have indicated that the resin acids exist in commercial systems as colloidal aggregations that can behave as multidentate ligands. Likewise, the hypothesis does not take into consideration the possibility of the formation of mixed aluminum resinate oxalate complexes.

No evidence has been presented in the literature to confirm or deny the direct effect of oxalate on the reaction between colloidal resin acid aggregations and aluminum ions. Consequently, the purpose of this thesis is to test the following hypothesis: aluminum oxalate is formed in preference to aluminum resinate when oxalate is present in an acidic colloidal resin acid-aluminum ion system.

## APPROACH TO THE THESIS PROBLEM

The effect of oxalate on the reaction between colloidal resin acid agglomerates and aluminum ions is difficult to determine in a quantitative manner for a suspension. However, the surface chemical model of the system can be used to circumvent the problems associated with a suspension. The resin acid monolayer is pictured as similar to the surface of a colloidal resin acid particle with an infinite radius. The effect of oxalate on the interfacial reaction will be quantitatively determined from changes in the physical and chemical properties of the monolayer. In addition, the possibility that aluminum resinate oxalate complexes exist will be checked with a surface chemical system that contains carbon-14 enriched oxalate.

The presence of various proportions of dibasic aluminum monoresinate and free resin acid in collected monolayer material has been reported (46). Likewise, the complete conversion of the monolayer to dibasic aluminum monoresinate has been proposed for certain combinations of substrate pH and aluminum ion concentration (46). However, both of these conclusions have been questioned recently because of the method used to collect the monolayer material for chemical and infrared analyses (48). Before further use of the surface chemical model, the aluminum resinate formed and the extent of salt formation at the interface must be determined. These characteristics of the model system will be used to help clarify the nature of the reaction between resin acid monolayers and aluminum ions.

## EXPERIMENTAL PROCEDURES

## EXPERIMENTAL DESIGN OF SURFACE CHEMICAL MODEL SYSTEM

The surface chemical model consisted of a monolayer of tetrahydroabietic acid spread on an aqueous substrate at pH 4.00. All work with the model system was done in a room maintained at  $20 \pm 1^\circ\text{C}$ . The various substrates used were prepared with sulfuric acid, aluminum sulfate, oxalic acid, or aluminum sulfate plus oxalic acid. The pH of the substrates was controlled by the addition of sodium hydroxide or sulfuric acid before the resin acid monolayer was spread.

The predominant resin acid in commercial rosin is abietic acid (21, 22); but monolayers of this material are not convenient to study because they oxidize rapidly (44). Tetrahydroabietic acid (the fully saturated abietic acid-type resin acid (44, 55) monolayers give the same type of  $\pi$ -A isotherm as unoxidized abietic acid monolayers and they are not subject to rapid oxidation (44). The sample of tetrahydroabietic acid obtained consisted of approximately equal quantities of the two isomers,  $8\beta$ ,  $9\alpha$ ,  $13\alpha$ -H and  $8\alpha$ ,  $9\alpha$ ,  $13\alpha$ -H, and will be referred to as TABSH. At pH = 4.00 the following are true:

1. Good sizing can be obtained with the rosin-alum system (12).
2. Oxalate ligands are known to complex with aluminum ions (40).
3. Tetrahydroabietic acid monolayers are stable to dissolution (44).
4. The absorption of atmospheric carbon dioxide by the aqueous substrate has no measurable effect on the substrate pH (56).
5. Reacted monolayer material can be removed from the substrate without causing a significant change in the aluminum ion concentration of the substrate (46).
6. The behavior of dilute acidic aluminum sulfate systems can be predicted.

A detailed listing of the thesis materials is given in Appendix I along with purification and evaluation procedures where applicable. Appendix II contains information concerning the preparation of solutions.

#### DETERMINATION OF MONOLAYER $\pi$ -A ISOTHERMS

##### APPARATUS

The  $\pi$ -A isotherms used to determine the values of  $A_{10}$ ,  $A_{\underline{K},\underline{EX}}$ , and  $\pi_{\underline{K},\underline{EX}}$  were obtained with an automatic recording surface balance. This null-deflection balance is similar to the one described by Anderson and Evett (57), and a detailed description of the instrument is given in Appendix III.

##### TECHNIQUE

The test and reference surfaces of the substrate solution were cleaned by sweeping them with movable barriers. A micropipet was used to deposit  $1.0 \times 10^{17}$  molecules of TABSH on the test area from a  $5.0 \times 10^{17}$  molecule ml.<sup>-1</sup> n-hexane solution of TABSH. This spreading solution was placed on the center of the test surface in a dropwise manner and the total amount delivered was reproducible within  $\pm 0.5\%$ . The time allowed for reaction was 6 minutes (evaporation of n-hexane occurs instantaneously).

The average area available to the monolayer molecules was reduced at the rate of  $2.86 \text{ A.}^2 \text{ molecule}^{-1} \text{ minute}^{-1}$ . This was the maximum rate for the balance but it was still lower than that used by Bruun (44). The  $\pi$ -A isotherm for the monolayer was recorded continuously over the range of 56 to 28  $\text{A.}^2 \text{ molecule}^{-1}$ . Calibration of the torsion wire was checked daily.

After each  $\pi$ -A isotherm determination, the test area of the balance was expanded to the initial value. The interfacial material was washed from the trough

by flooding it with pH 4.00 sulfuric acid solution. The remaining liquid was removed from the trough by suction and the edges of the trough were cleaned with n-hexane. The trough was then filled and flooded with distilled water and emptied by suction. After the use of each aluminum sulfate or aluminum sulfate plus oxalic acid substrate in the balance, the effectiveness of the cleaning procedure was checked. This was accomplished by determining the  $\pi$ -A isotherm of a monolayer of TABSH on a sulfuric acid substrate.

The standard error was less than  $\pm 0.03$  for  $A_{10}$ ,  $A_{\underline{K}, \underline{EX}}$ , and  $\pi_{\underline{K}, \underline{EX}}$  measurements obtained for replicate monolayers on sulfuric acid substrates. The standard error was less than  $\pm 0.1$  for the corresponding three quantities obtained for replicate monolayers on aluminum sulfate substrates with  $[Al] = 3.16 \times 10^{-3} M$ . The quantity,  $[Al]$ , represents the total molar concentration of aluminum species in the system.

#### ANALYSIS OF COLLECTED MONOLAYER MATERIAL

##### ISOLATION

##### Apparatus

Monolayers to be collected for analysis were prepared at the liquid-air interfaces of two large shallow troughs equipped with compression barriers and Teflon spatulas. These troughs are similar to the one described by Langmuir and Schaefer (58). The brass and glass components used by these workers were replaced by Lucite and polyfluorocarbon tape. A detailed description of the troughs is given in Appendix IV.

##### Technique

The surface of the substrate solution was cleaned by sweeping it with movable barriers. Monolayer spreading solution was placed on the center of the surface in

a dropwise manner with a micropipet. With the smaller trough,  $3.20 \times 10^{17}$  molecules of TABSH were spread from a  $1.28 \times 10^{18}$  molecule ml.<sup>-1</sup> solution. For the larger trough,  $1.39 \times 10^{18}$  molecules of TABSH were spread from a  $5.56 \times 10^{18}$  molecule ml.<sup>-1</sup> solution.

Six minutes were allowed for reaction before the two inside compression barriers were moved to within 3 mm. (small trough) or 1 cm. (large trough) of each other. The appropriate spatula was used to skim the crumpled monolayer from the surface bounded by these barriers and the trough edges. This technique was similar to the one used by Langmuir and Schaefer (58) except that here the surface of the substrate was above the trough edges.

The monolayer material was transferred to a microfilter and allowed to drain. Six to 18 monolayers were deposited, collapsed, collected, and drained in this manner for each substrate. After the collection of the last monolayer in a set, the material was washed three times with pH 4.00 HCl solution. During the washes, the material was agitated with a Teflon microspatula.

The troughs were cleaned between sets in the same manner as that used for the automatic recording surface balance.

The free acid mole fraction ( $X_{\text{TABSH}}$ ) values of washed and unwashed material collected from an aluminum sulfate substrate with  $[Al] = 3.16 \times 10^{-3} M$  were not significantly different (Appendix IV). Likewise, the  $X_{\text{TABSH}}$  values of the first and last monolayers of a series collected from an aluminum sulfate substrate with  $[Al] = 3.16 \times 10^{-3} M$  were not significantly different (Appendix IV). Similar results were obtained for the first and last monolayers collected from an aluminum sulfate plus oxalic acid substrate with  $[Al] = [C_2O_4] = 3.16 \times 10^{-3} M$  (Appendix IV). The quantity,  $[C_2O_4]$ , represents the total molar concentration of oxalate species in

the system. Depletion of the [Al] caused by removal of reacted monolayer material was calculated to be 0.06% or less for all substrates. This quantity was based on the original [Al] (Appendix IV). The pH values of substrates after 6 to 18 skimmings were essentially unchanged (Appendix IV).

#### DRYING

The collected material was air-dried for 12 hours and then dried over  $P_2O_5$  under 29 inches Hg vacuum for 60 hours. The temperature for both of these steps was  $20 \pm 1^\circ C$ . For higher temperature drying a glass vacuum chamber (Appendix IV) in an oven was used.

Samples for free acid analysis were taken from the material dried under vacuum at  $20^\circ C$ . Portions of each of these were analyzed immediately. The remaining portions were dried for 2 hours at  $40^\circ C$ . under 29 inches Hg vacuum. This material was again split and one portion was dried for 2 hours at  $100^\circ C$ . under 29 inches Hg vacuum. Part of the material collected from aluminum sulfate substrates was dried twice at  $100^\circ C$ . for 2 hours under 29 inches Hg vacuum.

#### DETERMINATION OF INFRARED SPECTRA

The infrared spectra of the collected monolayer samples were determined by the ultramicro KBr disk technique with a model 21 Perkin-Elmer recording spectrophotometer. This instrument was equipped with a 4X beam condenser and NaCl optics.

The disks were 0.5 mm. in diameter and the sample weight for each ranged from 5 to 10 g. The spectra for the samples were determined between 2.0 and 15.0  $\mu m$ . For replicate samples of TABSH dried at  $20^\circ \pm 1^\circ C$ ., the standard error was  $\pm 0.01$ . for the absorbance ratio,  $\frac{A_{COOH}}{A_{CH}}$ . Here,  $A_{COOH}$  is the absorbance of the disk at  $1700\text{ cm.}^{-1}$  and  $A_{CH}$  is the absorbance of the disk at  $2910\text{ cm.}^{-1}$  (Appendix IV).

## DETERMINATION OF TOTAL CARBON

The total carbon content of the collected monolayer material was determined manometrically with a Thomas-Van Slyke apparatus similar to that described by Van Slyke and Folch (59). The amount of carbon in the organic material was determined from pressure-volume-temperature measurements after the sample had been oxidized to carbon dioxide. The technique is thoroughly described in the original papers (59-62) and it is outlined in Appendix IV. For sodium carbonate, the recovery of carbon was 99.35% and the standard error for replicate samples was  $\pm 0.41$ .

## DETERMINATION OF RADIOACTIVE CARBON

The liberated carbon dioxide obtained from the combustion of the sample was transferred to a Bernstein-Ballentine counting tube (63) with methane (62). The radioactive portion of this gas was determined with a model 182 Nuclear-Chicago scaling unit. The optimum operating voltage of the tube was 3600 v. and the fraction of the tube which was effective in counting was 0.842.

## DETERMINATION OF ALUMINUM

The aluminum content of the samples was determined by an emission spectroscopy technique developed by the Institute Analytical Department. It was based on the methods described by Pienaar (64) and ASTM (65). A Bausch and Lomb 1.5 meter grating spectrograph and a Jarrell-Ash microphotometer were used in the analysis. The 5680 A. emission line of tin was used as the reference and the 5304 A. line of aluminum was measured. Aluminum sulfate ( $\text{Al}_2(\text{SO}_4)_3 \cdot 18\text{H}_2\text{O}$ ) was the aluminum standard and the limit of detection of aluminum by this method was 0.05% based on the sample weight.

## RESULTS AND DISCUSSION

## REACTION BETWEEN TABSH MONOLAYERS AND ALUMINUM IONS

CHANGES IN  $\pi$ - $A$  ISOTHERM

The  $\pi$ - $A$  isotherms in Fig. 2 are for the monolayers formed when TABSH is spread on substrates with various aluminum sulfate concentrations. The pH values of the substrates before adjustment are given in Appendix V for values of  $\log_{10} [Al]$  between -3.75 and -1.75.

The  $\pi$ - $A$  isotherm for the monolayer formed on a substrate with  $\log_{10} [Al] = -6.0$  is the same as the one for the TABSH monolayer on sulfuric acid (Appendix III). This isotherm is typical of a liquid condensed monolayer (44) which behaves as a highly oriented liquid (66). The rise of the isotherm results from the decrease in the specific free-surface energy as the area available to each monolayer molecule is reduced (Appendix III). As the area is made smaller, the limiting extent of area reduction is reached where the film is placed in equilibrium with the bulk material. This phenomenon occurs at  $(A_{K,EX}, \pi_{K,EX})$  (see arrow in Fig. 2). Further reduction of the area forces the film material into patches of bulk liquid or solid in the transition region (66). The secondary rise at the left of the transition region is attributed to the flow resistance of these patches of material (67). As the  $[Al]$  increases, the characteristics of the isotherm change; these changes are reflected by the  $A_{10}^1$ ,  $A_{K,EX}$ , and  $\pi_{K,EX}$  values in Table I and Fig. 3.

The average molecular area of the monolayer molecules at  $\pi = 10$  dyne  $cm^{-1}$  is  $A_{10}^1$ . This quantity was picked arbitrarily to use in comparing the isotherms. It decreases gradually from  $46.0 \text{ \AA}^2 \text{ molecule}^{-1}$  at  $\log_{10} [Al] = -6.0$  to  $43.1 \text{ \AA}^2 \text{ molecule}^{-1}$  at  $\log_{10} [Al] = -2.5$  and then rises smoothly as the  $[Al]$  is increased. A portion of the decrease in  $A_{10}^1$  is attributed to the close pairing of hydrocarbon

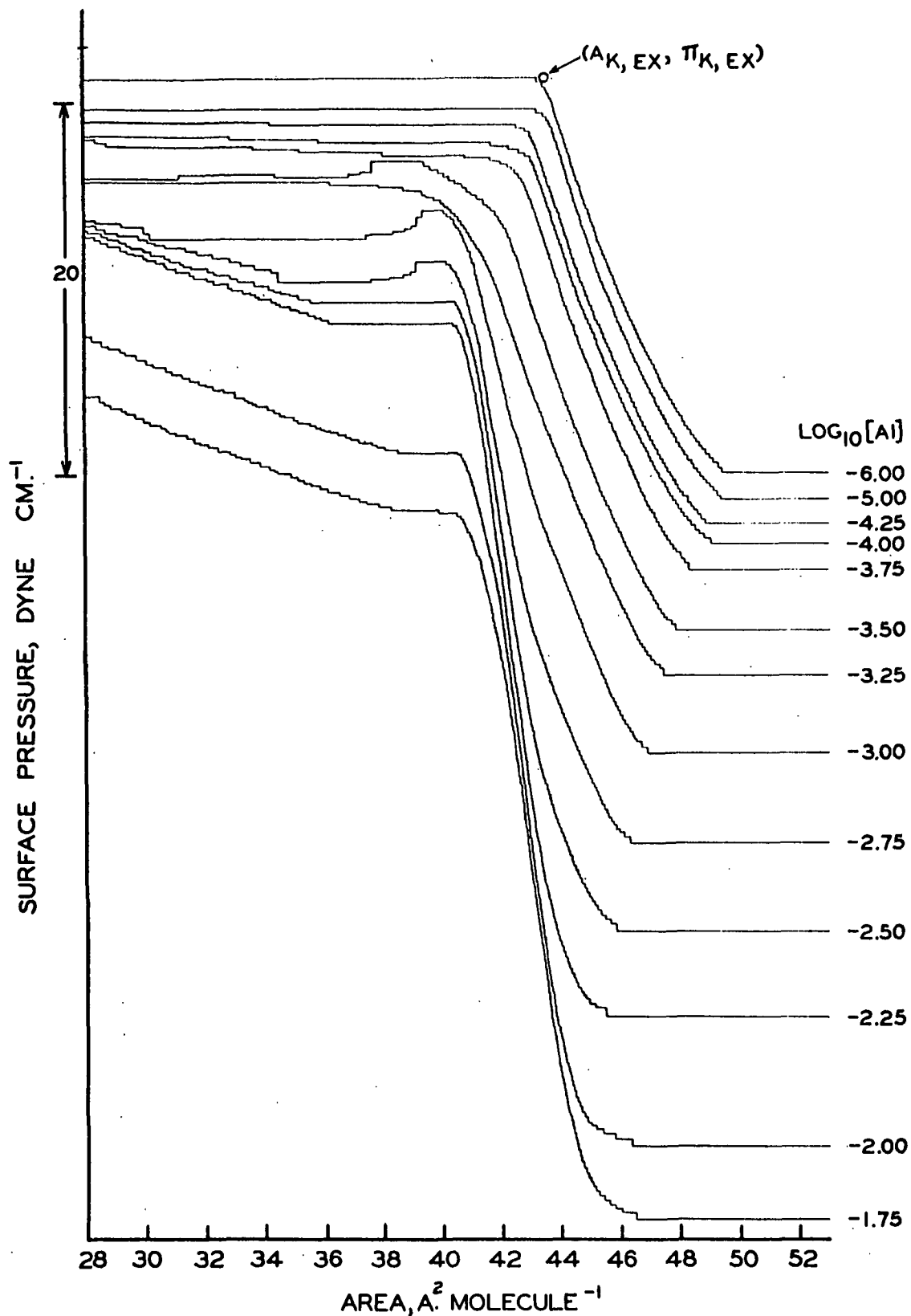


Figure 2. Surface Pressure-Area Isotherms for the Monolayers Formed when TABSH is Spread on Aluminum Sulfate Substrates. These Substrates were at  $20^{\circ}\text{C}$ . with  $\text{pH} = 4.00$ . Reaction Time = 6 Minutes, and  $\frac{dA}{dt} = 2.86 \text{ A.}^2 \text{ Molecule}^{-1} \text{ Minute}^{-1}$ . Note that the Surface Pressure Axes of the Isotherms are Shifted and that the Area Reduction Proceeds from Right to Left

TABLE I

$\underline{A}_{10}$ ,  $\underline{A}_{\underline{K},\underline{EX}}$ , AND  $\underline{\pi}_{\underline{K},\underline{EX}}$  VALUES FOR THE MONOLAYERS FORMED WHEN  
TABSH IS SPREAD ON ALUMINUM SULFATE SUBSTRATES<sup>a</sup>

$\text{Log}_{10} [\text{Al}]$ in Substrate	$\underline{A}_{10}$ , A. <sup>2</sup> molecule <sup>-1</sup>	$\underline{A}_{\underline{K},\underline{EX}}$ , A. <sup>2</sup> molecule <sup>-1</sup>	$\underline{\pi}_{\underline{K},\underline{EX}}$ , dyne cm. <sup>-1</sup>
-6.00	45.9	43.5	20.8
-5.00	45.8	43.6	20.6
-4.25	45.4	43.0	21.1
-4.00	45.3	42.9	21.2
-3.75	45.2	42.6	22.0
-3.50	44.6	--	--
-3.25	44.3	40.7	26.4
-3.00	44.0	40.6	29.0
-2.75	43.4	40.8	31.1
-2.50	43.1	41.0	33.7
-2.25	43.2	41.0	37.2
-2.00	43.6	41.4	37.3
-1.75	43.8	41.4	37.9

<sup>a</sup>Substrates were at 20°C. with pH = 4.00, reaction time = 6 minutes, and  $\underline{dA}/\underline{dt} = 2.86 \text{ A.}^2 \text{ molecule}^{-1} \text{ minute}^{-1}$ .

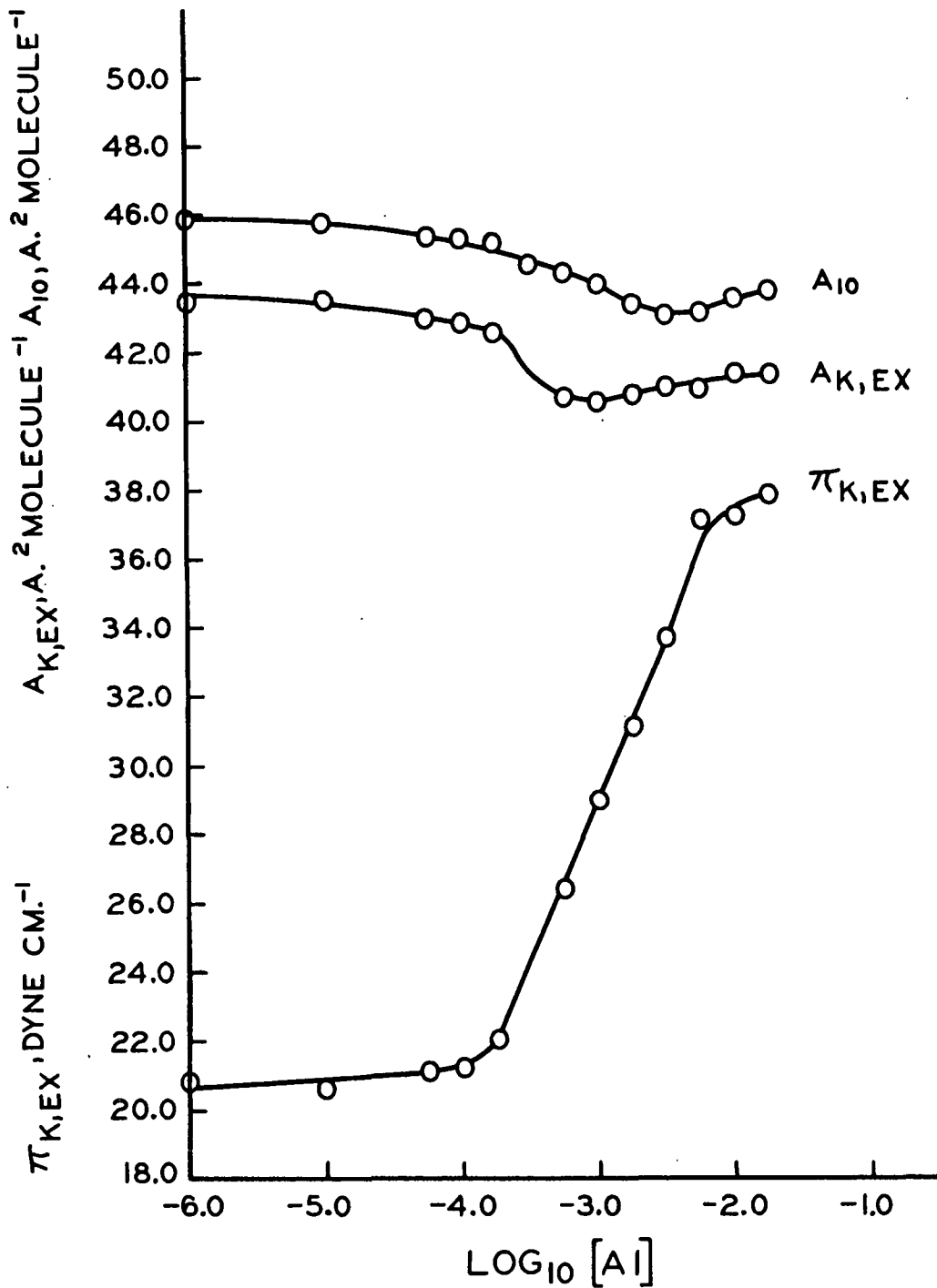


Figure 3.  $A_{10}$ ,  $A_{K,EX}$ , and  $\pi_{K,EX}$  Values for the Monolayers Formed when TABSH is Spread on Aluminum Sulfate Substrates. These Substrates were at 20°C. with pH = 4.00. Reaction Time = 6 Minutes, and  $\frac{dA}{dt} = 2.86 \text{ A.}^2 \text{ Molecule}^{-1} \text{ Minute}^{-1}$ . Data Points at a Given  $\text{Log}_{10} [\text{Al}]$  were Obtained from One  $\pi_A$  Isotherm.

ring structures. This results when two TABSH molecules react with  $Al^{+3}$  [or  $Al(OH)_2^{+2}$ ] to form the diresinate in the film [analytical results presented later indicate that the collected monolayer material consists of  $Al(TABS)_2OH$  and TABSH]. Part of the decrease is ascribed to the formation of a hydrogen-bonded network under the monolayer. This network probably involves the hydroxyls and water molecules associated with the aluminum portions of the salt in the film. The reduction of  $A_{10}$  as the substrate concentration of a cation is increased has been reported for fatty acid monolayer-divalent metal cation systems (68). This behavior was limited to the pH and concentration range where cation hydrolysis complexes were not formed. It was attributed to hydrocarbon chain packing in the disalt. Numerous workers have used the network concept for fatty acids spread on solutions of divalent and trivalent cations that can form hydrolysis complexes (69-74).

The rise in  $A_{10}$  corresponds to the aluminum concentrations where sodium hydroxide was necessary to raise the pH of the substrate to 4.00 (Appendix V). This increase in  $A_{10}$  is probably caused by expansion of the network under the film by the base. As a result, the experimental  $A_{10}$  values in this region reflect the competing effects of hydrocarbon pairing and network expansion.

The quantity,  $A_{K,EX}$ , is the average molecular area of the monolayer molecules in  $A^2$  molecule<sup>-1</sup> at the extrapolated collapse point (see arrow in Fig. 2). This point is obtained by extending the steepest portion of the first rise in the isotherm and the approximately horizontal portion of the isotherm. This latter portion of the isotherm is termed the phase transition region. It indicates the formation of groups of closely associated particles that are in equilibrium with the film (75, 66). With isotherms which have two distinct portions approximately parallel to the area axis, the portion with the higher  $\pi$  was used in the extrapolation. The monolayers on aluminum sulfate substrates with  $\log_{10} [Al] = -3.0$  and  $-2.75$  have

isotherms of this type. The high pressure plateau is attributed to 2-dimensional supersaturation (76). The plot of  $\underline{A}_{\underline{K},\underline{EX}}$  versus  $\log_{10} [Al]$  has a minimum at  $\log_{10} [Al] = -3.0$ . The decrease in  $\underline{A}_{\underline{K},\underline{EX}}$  is again ascribed to pairing in the hydrocarbon portion and favorable spacing in the hydroxyl-water network. The increase in  $\underline{A}_{\underline{K},\underline{EX}}$  values is attributed to crowding in the network that outweighs the pairing phenomenon.  $\underline{A}_{\underline{K},\underline{EX}}$  represents a closer molecular packing arrangement in the monolayer than  $\underline{A}_{10}$ . The natural crowding in the hydroxyl-water structure becomes apparent at this spacing even before base is added to the substrate.

The surface pressure of the monolayer at the extrapolated collapse point is  $\underline{\pi}_{\underline{K},\underline{EX}}$ . This quantity increases smoothly between  $\log_{10} [Al] = -4.25$  and  $-1.75$  as shown in Fig. 3. The increase in  $\underline{\pi}_{\underline{K},\underline{EX}}$  results from a decrease in the specific free-surface energy of the film-covered surface (Appendix III). A decrease in the free-surface energy is usually associated with the optimization of size and spacing in the surface (50). In the model sizing systems, this is attributed to the formation of aluminum diresinate in the monolayer accompanied by the simultaneous formation of a hydroxyl-water network under the film. The relative increase of  $\underline{\pi}_{\underline{K},\underline{EX}}$  with an increase in  $\log_{10} [Al]$  is noticeably reduced for the substrate with  $\log_{10} [Al] = -1.75$ . This behavior is ascribed to the attainment of limiting spacing in the network.

In Fig. 2 the slope of the first rise increases numerically with the  $[Al]$  up to  $\log_{10} [Al] = -2.25$  and then decreases slightly. The increase in slope indicates an increase in rigidity of the film. This behavior is consistent with the formation of a network of hydroxyls and water molecules under the monolayer. The decrease in the slope occurs when sodium hydroxide is added to the substrate.

The  $\underline{\pi}$ - $\underline{A}$  isotherms in Fig. 2 are similar to those obtained by Strazdins (49) for the monolayers formed when tall oil rosin is spread on aluminum chloride

substrates. The transition regions in the  $\pi$ -A isotherms are better defined than in the isotherms presented by Bruun (44) for the tetrahydroabietic acid monolayer-potassium aluminum sulfate system. The area reduction rate used by Bruun may have been high enough to influence the sharpness of the transition region. Likewise, differences in the isomeric composition of the tetrahydroabietic acid samples used in Bruun's study and in this work could explain the  $\pi$ -A isotherm differences. The samples were obtained from the same supplier but Bruun did not determine the isomeric composition of his sample.

The behavior of monolayers on substrates free of sodium hydroxide (Fig. 2 and 3) is consistent with the existence of appreciable proportions of  $Al^{+3}$  in these substrates. The surface tension of an aluminum sulfate solution is not significantly different from that of water up to  $[Al] = 1.0 \times 10^{-1} M$  (77).

A sodium chloride concentration of  $2.0M$  has a slight beneficial effect on the reaction between tetrahydroabietic acid monolayers and aluminum ions (45). In addition, the reaction between fatty acid monolayers and di- and trivalent cations reaches equilibrium in 5 minutes or less (71, 78, 79).

#### CHANGES IN INFRARED SPECTRUM

The bottom eight infrared spectra in Fig. 4 are for samples of monolayer material collected from substrates with various aluminum concentrations. The spectrum for the TABSH starting material is also included in the figure for comparison.

As the  $[Al]$  is raised, the following absorption bands attributed to the acid fraction (80) decrease in intensity relative to the hydrocarbon band at  $2910 \text{ cm.}^{-1}$ :

1. The broad band at  $2650 \text{ cm.}^{-1}$  for the strongly hydrogen-bonded OH group.
2. The band at  $1700 \text{ cm.}^{-1}$  for the C=O stretching vibration.

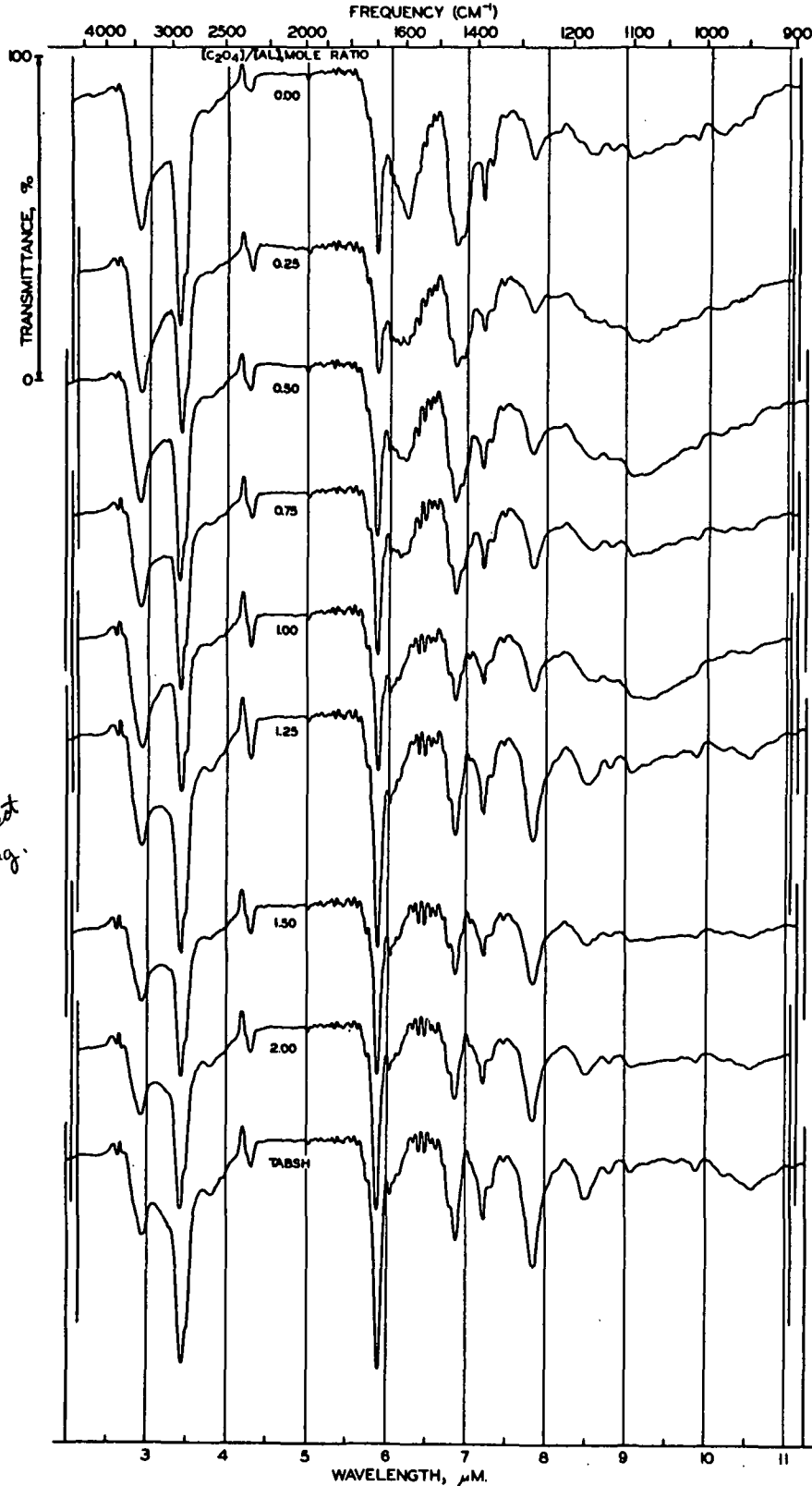


*Fig is wrong.  
see Fig 10 for correct  
Caption is OK.*

Figure 4. Infrared Spectra of TABSH Starting Material and Monolayer Material Collected from Aluminum Sulfate Substrates at 20°C. with pH = 4.00. Reaction Time = 6 Minutes. These Materials were Washed and Dried at 20°C.

3. The broad band at  $1275 \text{ cm.}^{-1}$  for the coupled C-O stretching and OH deformation vibration.

The following absorption bands that are usually ascribed to salt formation (80) increase as the [Al] in the substrate is raised:

1. The band at  $1590 \text{ cm.}^{-1}$  for the antisymmetrical vibration of the ionized carboxyl group.
2. The band at  $1435 \text{ cm.}^{-1}$  for the symmetrical vibration of the ionized carboxyl group.

Absorption bands for the hydrocarbon portion of the material are as follows:

1. The band at  $2910 \text{ cm.}^{-1}$  for the stretching of the  $\text{CH}_2$  and OH groups.
2. The band at  $1455 \text{ cm.}^{-1}$  for the C- $\text{CH}_3$  antisymmetrical deformation.
3. The band at  $1385 \text{ cm.}^{-1}$  for the C- $\text{CH}_3$  symmetrical deformation.

The primary changes in the spectrum are attributed to the presence of increasing proportions of salt in the collected material as [Al] is increased. The band at  $3400 \text{ cm.}^{-1}$  is assigned to the stretching of hydroxyl groups attached to aluminum (47, 81). A transmittance loss between  $1250 \text{ cm.}^{-1}$  and  $950 \text{ cm.}^{-1}$  has been noted before for mixed basic aluminum resinate-resin acid material. This is associated with the amorphous nature of the aluminum-hydroxyl portion of the basic aluminum resinate (47, 81). The absence of a distinctive new absorption band between  $980 \text{ cm.}^{-1}$  and  $1000 \text{ cm.}^{-1}$  indicates that no regular aluminum-hydroxyl chain structure is present (81). However, the presence of a random aluminum-hydroxyl structure is not ruled out.

Sadtler (82) reported that glass contamination can cause the transmittance base line for ultramicro samples to have a convex curvature between  $1250 \text{ cm.}^{-1}$  and  $860 \text{ cm.}^{-1}$ . This phenomenon and the amorphous nature of the aluminum salt contribute to the broad bands for material from substrates with  $\log_{10} [\text{Al}] = -2.25$  and  $-2.00$ . The

absence of a distinctive absorption band between  $1080 \text{ cm.}^{-1}$  and  $1110 \text{ cm.}^{-1}$  indicates that no appreciable  $\text{Al}(\text{SO}_4)_1^{+1}$  reacted with the monolayer molecules.

Bagg, et al., (83) prepared mixed monolayers of calcium stearate and stearic acid for infrared analysis by two methods. One was similar to the technique employed here and the other involved casting monolayers directly on silver chloride plates by the Langmuir-Blodgett technique (54). Samples prepared by the two techniques gave the same infrared spectra for a given mixture.

When samples of basic aluminum resinate-resin acid mixtures were dried at  $40^\circ\text{C}$ . and at  $100^\circ\text{C}$ ., no distinctive changes in their infrared spectra were noted.

#### CHANGES IN FREE ACID MOLE FRACTION

The free acid mole fractions of the samples of collected monolayer material were ascertained from a quantitative treatment of the infrared spectra. The relationship between the concentration of a substance in a KBr disk and the absorbance of a disk at a given wavelength may be expressed by Equation (6)

$$A_S = a_S b_d c_S \quad (6)$$

where

$A_S$  = absorbance of disk at a given wavelength

$a_S$  = absorptivity of substance at a given wavelength,  $\text{cm.}^{-1} \text{ mole}^{-1} \text{ g}$ .

$b_d$  = thickness of disk, cm.

$c_S$  = concentration of substance in disk, moles  $\text{g.}^{-1}$ .

This is Beer's law (84) and it is written in terms convenient for use with solid samples (85). With this equation, the total concentration of tetrahydroabiatic acid (nonionized and ionized) in a disk can be related to the absorbance of hydrocarbon at  $2910 \text{ cm.}^{-1}$  as shown by Equation (7)

$$A_{\text{CH}} = a_{\text{R}} b_1 c_1 \quad (7)$$

where

$A_{\text{CH}}$  = absorbance of disk at 2910  $\text{cm}^{-1}$

$a_{\text{R}}$  = absorptivity of TABSH and  $\text{TABS}^-$  at 2910  $\text{cm}^{-1}$ ,  $\text{cm}^{-1} \text{ mole}^{-1} \text{ g}$ .

$b_1$  = thickness of disk, cm.

$c_1$  = concentration of TABSH plus  $\text{TABS}^-$  in disk,  $\text{mole g}^{-1}$ .

Equation (7) is based on the assumption that the absorptivities of TABSH and  $\text{TABS}^-$  [in  $\text{Al}(\text{TABS})_2\text{OH}$ ] are equal at 2910  $\text{cm}^{-1}$ . Equation (6) can also be used to relate the concentration of TABSH in a disk to the absorbance of nonionized carboxyl at 1700  $\text{cm}^{-1}$  as shown in Equation (8)

$$A_{\text{COOH}} = a_{\text{TABSH}} b_2 c_2 \quad (8)$$

where

$A_{\text{COOH}}$  = absorbance of disk at 1700  $\text{cm}^{-1}$

$a_{\text{TABSH}}$  = absorptivity of TABSH at 1700  $\text{cm}^{-1}$ ,  $\text{cm}^{-1} \text{ mole}^{-1} \text{ g}$ .

$b_2$  = thickness of disk, cm.

$c_2$  = concentration of TABSH in disk,  $\text{mole g}^{-1}$ .

Equation (8) is based on the assumption that the absorptivity of TABSH at 1700  $\text{cm}^{-1}$  is constant for various mixtures of TABSH and  $\text{TABS}^-$  in a disk.

The mole fraction of TABSH in a disk may be represented by Equation (9)

$$X_{\text{TABSH}} = \frac{N_{\text{TABSH}}}{(N_{\text{TABSH}} + N_{\text{TABS}^-})} \quad (9)$$

where

$X_{\text{TABSH}}$  = mole fraction of TABSH

$N_{\text{TABSH}}$  = number of moles of TABSH

$N_{\text{TABS}^-}$  = number of moles of  $\text{TABS}^-$ .

Likewise, the concentration of a substance in a disk can be obtained with Equation (10)

$$c_S = N_S/w_d \quad (10)$$

where

$\underline{c}_S$  = concentration of substance in disk, mole g.<sup>-1</sup>

$\underline{N}_S$  = number of moles of substance in disk

$\underline{w}_d$  = weight of disk, g.

As a result, the mole fraction expression [Equation (9)] can be written in terms of concentration as shown in Equation (11).

$$X_{\text{TABSH}} = c_2 w_2 / c_1 w_1 \quad (11)$$

The combination of Equations (7), (8), and (11) yields Equation (12) upon simplification.

$$X_{\text{TABSH}} = (A_{\text{COOH}}/A_{\text{CH}})(a_{\text{R}}/a_{\text{TABSH}}) \quad (12)$$

For each spectrum, base lines were drawn between 2.25 and 4.65  $\mu\text{m}$ . and 4.65 and 11.0  $\mu\text{m}$ . Peak heights at 2910  $\text{cm}^{-1}$  and 1700  $\text{cm}^{-1}$  were measured for use in Equation (12) (85). With the base lines selected, the average value of  $a_{\text{TABSH}}/a_{\text{R}}$  was 1.08 for pure TABSH ( $X_{\text{TABSH}} = 1$ ) (Appendix IV). With the assumptions that  $a_{\text{TABSH}}/a_{\text{R}}$  does not vary with composition and that Beer's law is obeyed, Equation (12) was used to calculate  $X_{\text{TABSH}}$  values.

The assumption concerning the absorptivity ratio was also used by Bagg, *et al.*, (83) for calcium stearate plus stearic acid monolayer material. Stearic acid or stearate monolayers deposited on calcium fluoride plates showed only slight negative deviation from Beer's law at 2900  $\text{cm}^{-1}$  and 1716  $\text{cm}^{-1}$  (78).

The  $X_{\text{TABSH}}$  values for basic aluminum resinate plus resin acid samples are given in Table II and Fig. 5. These results indicate that the regular conversion

of acid to salt in the monolayer occurs as  $\log_{10} [Al]$  is increased between -3.75 and -2.00. The appearance of salt was not measured directly because water adsorbed from the atmosphere by potassium bromide affects the absorption bands of the ionized material (86). Known mixtures of free acid and monobasic aluminum diresinate were not prepared because the pure salt was not available. Davidson (15) was not able to prepare pure monobasic aluminum diresinate in aqueous systems. Attempts to obtain it by acetone extraction of free acid-salt mixtures were unsuccessful.

TABLE II

FREE ACID MOLE FRACTIONS AND SALT MOLE FRACTIONS OF MONOLAYER MATERIAL COLLECTED FROM ALUMINUM SULFATE SUBSTRATES<sup>a, b</sup>

$\log_{10} [Al]$ in Substrate	$X_{TABS}^c$	$X_{TABS}^{-d}$
-3.75	0.82	0.18
-3.50	0.75	0.25
-3.25	0.69	0.31
-3.00	0.63	0.37
-2.75	0.57	0.43
-2.50	0.52	0.48
-2.25	0.46	0.54
-2.00	0.40	0.60

<sup>a</sup>Substrates were at 20°C. with pH = 4.00.

<sup>b</sup>Material washed and dried at 20°C.

<sup>c</sup>Calculated with Equation (12).

<sup>d</sup>Obtained by difference.

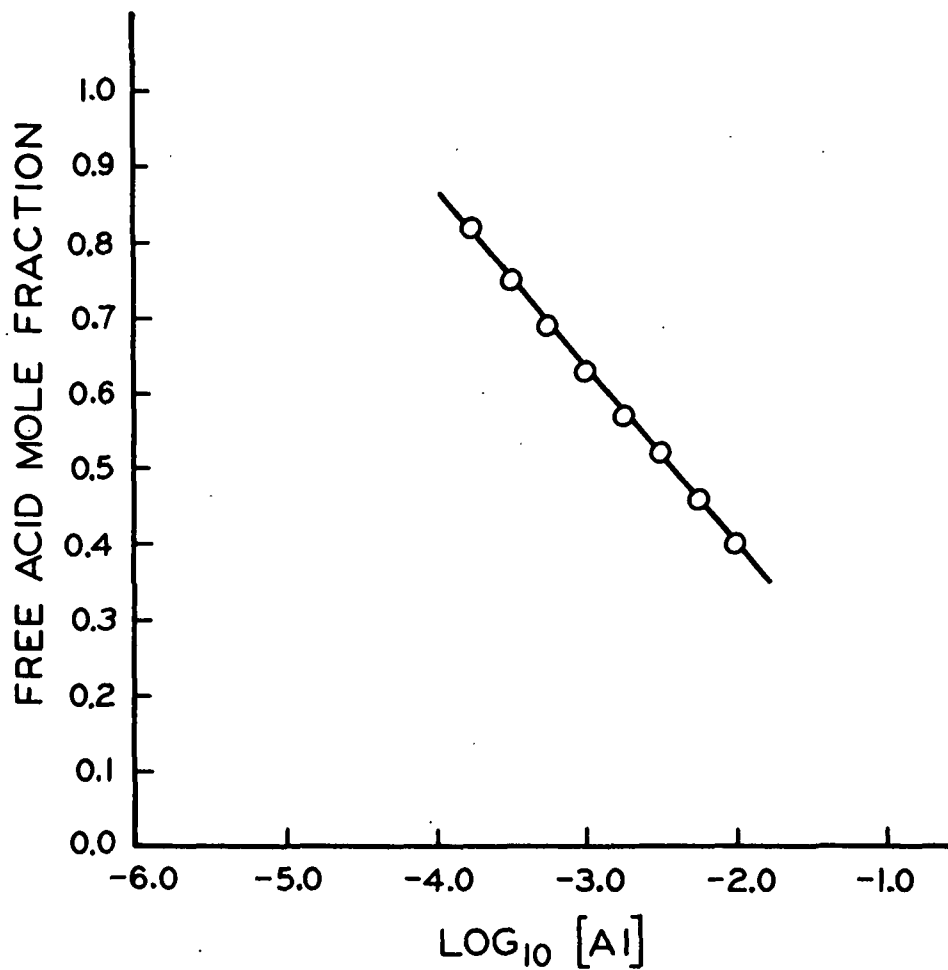


Figure 5. Free Acid Mole Fractions of Monolayer Material Collected from Aluminum Sulfate Substrates at 20°C. with pH = 4.00. Reaction Time = 6 Minutes. This Material was Washed and Dried at 20°C.

## COMPOSITION OF COLLECTED MONOLAYER MATERIAL

The  $\bar{X}_{\text{TABSH}}$  values and aluminum and carbon contents of two samples of collected monolayer material are given in Table III.

TABLE III

$\bar{X}_{\text{TABSH}}^a$ , Al, AND C CONTENTS OF COLLECTED MONOLAYER MATERIAL<sup>b</sup>

Substrate <sup>c</sup>	$\bar{X}_{\text{TABSH}}$	Al, %	C, %
[Al] = $3.16 \times 10^{-3}\text{M}$	0.50 <sup>d</sup>	2.30	74.0
[Al] = [C <sub>2</sub> O <sub>4</sub> ] = $3.16 \times 10^{-3}\text{M}$	0.84 <sup>d</sup>	0.67 <sup>e</sup>	78.4 <sup>e</sup>

<sup>a</sup>Calculated from Equation (12) with  $\frac{a_{\text{TABSH}}}{a_{\text{R}}} = 1.08$

<sup>b</sup>Samples washed and dried at 20°.

<sup>c</sup>Both substrates were at 20°C. with pH = 4.00.

<sup>d</sup>Standard error =  $\pm 0.01$ .

<sup>e</sup>Corrected for small amount of oxalate in sample indicated by radiochemistry results reported in Table VII.

Theoretical aluminum and carbon contents of aluminum tetrahydroabietate plus TABSH mixtures with the same free acid mole fractions reported in Table III are given in Table IV.

The experimental aluminum contents in Table III agree - within expected accuracy - with those calculated for a mixture of  $\text{Al}(\text{TABS})_2\text{OH}$  and TABSH.

Ekwall and Bruun (46) reported that monolayers collected from potassium aluminum sulfate solutions consisted of dibasic aluminum monoresinate and tetrahydroabietic acid. Their analytical results were based on the assumption that the acid was completely converted to the salt at a given combination of substrate pH

and [Al]. However, the infrared spectrum for their collected material contained absorption bands that are commonly attributed to free acid (78, 80, 83). Ekwall and Bruun (46) also allowed the collected monolayer material to stand in contact with a small volume of substrate for an unspecified length of time. This step in their isolation procedure was questioned by Motomura and Matuura (48) because of the possibility of aluminum being trapped in the material.

TABLE IV  
THEORETICAL Al AND C CONTENTS OF COLLECTED MONOLAYER MATERIAL

Mixture	$X_{\text{TABSH}}$	Al, %	C, %
Al(TABS)(OH) <sub>2</sub> plus TABSH	0.50	4.01	71.5
Al(TABS) <sub>2</sub> OH plus TABSH	0.50	2.14	75.7
Al(TABS) <sub>3</sub> plus TABSH	0.50	1.45	77.4
Al(TABS)(OH) <sub>2</sub> plus TABSH	0.84	1.37	76.0
Al(TABS) <sub>2</sub> OH plus TABSH	0.84	0.70	77.6
Al(TABS) <sub>3</sub> plus TABSH	0.84	0.47	78.0

The composition of the aluminum resinate formed in the present system agrees with that recently reported for the size precipitate isolated from suspension (14, 15). Likewise, the analytical results parallel those reported for the erucic acid-copper (II) chloride system (79). In that system, the bis-salt and the free acid were found in monolayer material collected from substrates free of complex copper ion hydrolysis products.

#### CHANGES IN STRUCTURE OF SURFACE REGION

Two changes in the structure of the surface region appear to be associated with aluminum ditetrahydroabietate formation in the monolayer. First, the aluminum salt improves the packing of the hydrocarbon portions of the molecules in the

monolayer. Second, the hydroxyls and water molecules associated with the salt appear to be involved in a random network beneath the monolayer that improves its stability.

#### NATURE OF THE REACTION

The  $X_{\text{TABSH}}$  data presented in Table II were used to calculate the mole fractions of salt in the collected monolayer material. These results are shown in Fig. 6. The concentration dependence of the reaction is typical of that observed for weak acid ion exchange resins with carboxylic acid groups (87).

Ekwall and Bruun (46) reported that the reaction between tetrahydroabietic acid monolayers and aluminum ions depends on the pH and the aluminum salt concentration in the substrate. They found that resin acid monolayers appear to have a definite capacity and that this capacity is increased slightly when the substrate is 2.0M in NaCl. These properties are consistent with an ion-exchange mechanism for the reaction.

The reaction between phospholipid monolayers and metal cations was attributed to ion-exchange by Rojas and Tobias (88) and Lettvin and Pickard (89). These workers found that the adsorption of ions by pure phospholipid monolayers (*in situ*) depends on pH, cation concentration, exchange of adsorbed cations, and site accessibility. The dependence of the reaction on these parameters strongly indicates that cation-exchange occurs between monolayer carboxyl groups and the cations of the substrate.

In the present study, the salt mole fraction ( $X_{\text{TABS}^-}$ ) is not expected to increase significantly for aluminum concentrations above  $1.0 \times 10^{-2} \text{M}$ . The value of  $A_{\text{K,EX}}$  does not increase for the next increment of  $[Al]$  beyond  $\log_{10} [Al] = -2.0$  (Fig. 3). This indicates that the spacing in the surface region at the point of

extrapolated film collapse has attained a limiting value. A limiting value for  $X_{\text{TABS}^-}$  of 0.60 compares favorably with 0.61 reported by Davison for the rosin-alum size precipitate isolated from suspension (15).

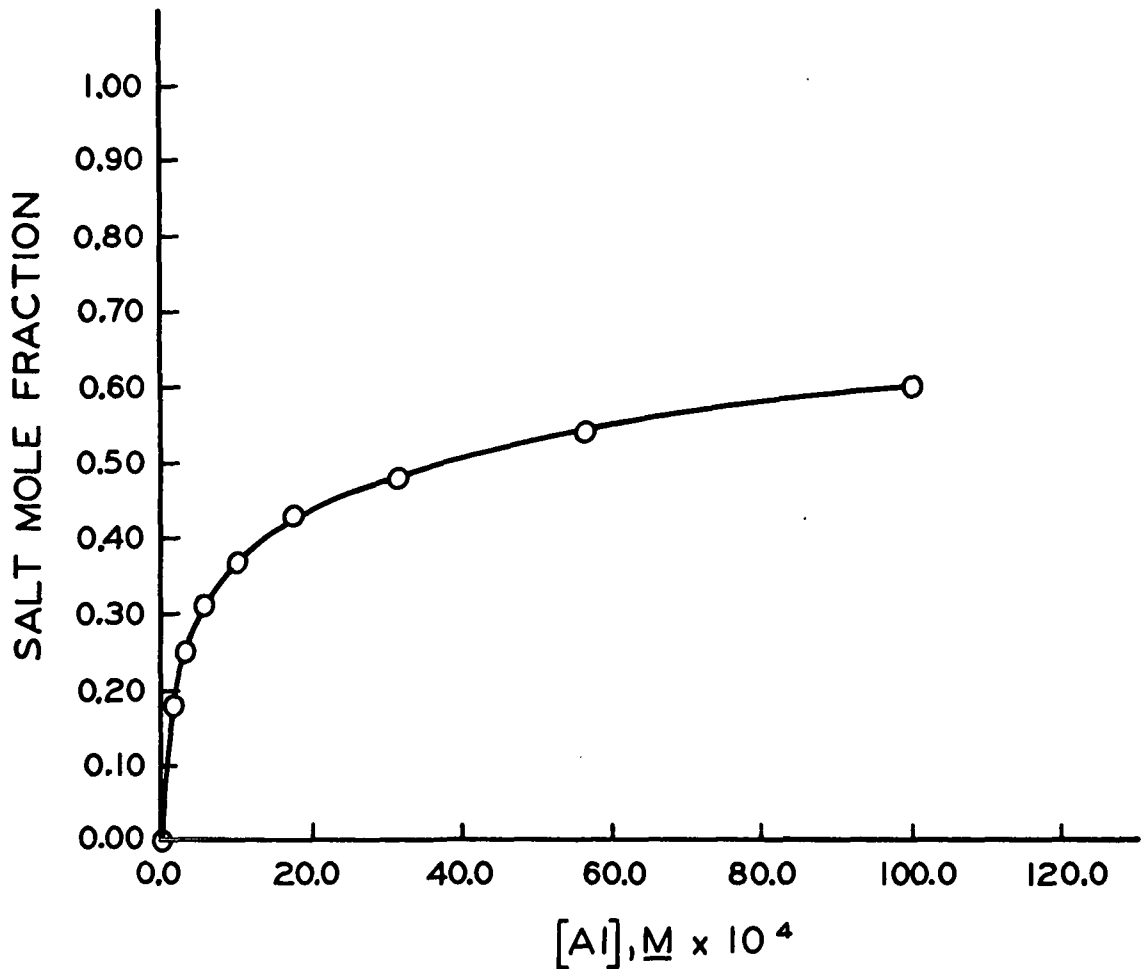


Figure 6. Salt Mole Fractions of Monolayer Material Collected from Aluminum Sulfate Substrates at  $20^\circ C$ . with  $pH = 4.00$ . Reaction Time = 6 Minutes. This Material was Washed and Dried at  $20^\circ C$ .

EFFECT OF OXALATE ON THE REACTION BETWEEN  
TABSH MONOLAYERS AND ALUMINUM IONS

CHANGES IN  $\pi$ -A ISOTHERM

The top eight  $\pi$ -A isotherms shown in Fig. 7 are for the monolayers formed when TABSH is spread on aluminum sulfate plus oxalic acid substrates. The  $[Al]$  was held constant at  $3.16 \times 10^{-3} M$  and the  $[C_2O_4]$  was varied. The pH of the substrates was adjusted to 4.00 by the addition of sodium hydroxide. The pH of each solution before adjustment is listed in Appendix V.

The bottom  $\pi$ -A isotherm in the figure is for the aluminum ditetrahydroacetate plus TABSH monolayer on a substrate with  $\log_{10} [Al] = -2.50$  and no oxalate. As  $[C_2O_4]/[Al]$  increases, the isotherms lose the characteristics associated with the presence of aluminum ditetrahydroacetate in the monolayer. When  $[C_2O_4]/[Al] = 2.00$ , the  $\pi$ -A isotherm is the same as the one for the TABSH monolayer on sulfuric acid (Fig. 2,  $\log_{10} [Al] = -6.00$ ). These changes are reflected in the  $A_{10}$ ,  $A_{K,EX}$ , and  $\pi_{K,EX}$  values of the  $\pi$ -A isotherms given in Table V and shown in Fig. 8 (data points). The dotted lines in Fig. 8 represent the  $A_{10}$ ,  $A_{K,EX}$ , and  $\pi_{K,EX}$  values for the TABSH monolayer on sulfuric acid. These data indicate that the aluminum ions in the system are strongly sequestered by oxalate. Essentially no aluminum ions react with the TABSH monolayer when  $[C_2O_4]/[Al] = 2.00$ .

Since the bulk of the reversion has occurred when  $[C_2O_4]/[Al] = 1.00$ , the formation of primarily  $Al(C_2O_4)_1^{-1}$  in the substrate between  $[C_2O_4]/[Al] = 0.00$  and 1.00 is proposed. The dashed lines in Fig. 8 are based on the  $A_{10}$ ,  $A_{K,EX}$ , and  $\pi_{K,EX}$  data in Fig. 3 and the assumptions that oxalate reacts stoichiometrically with the aluminum ions in the substrate, that the TABSH monolayer does not compete

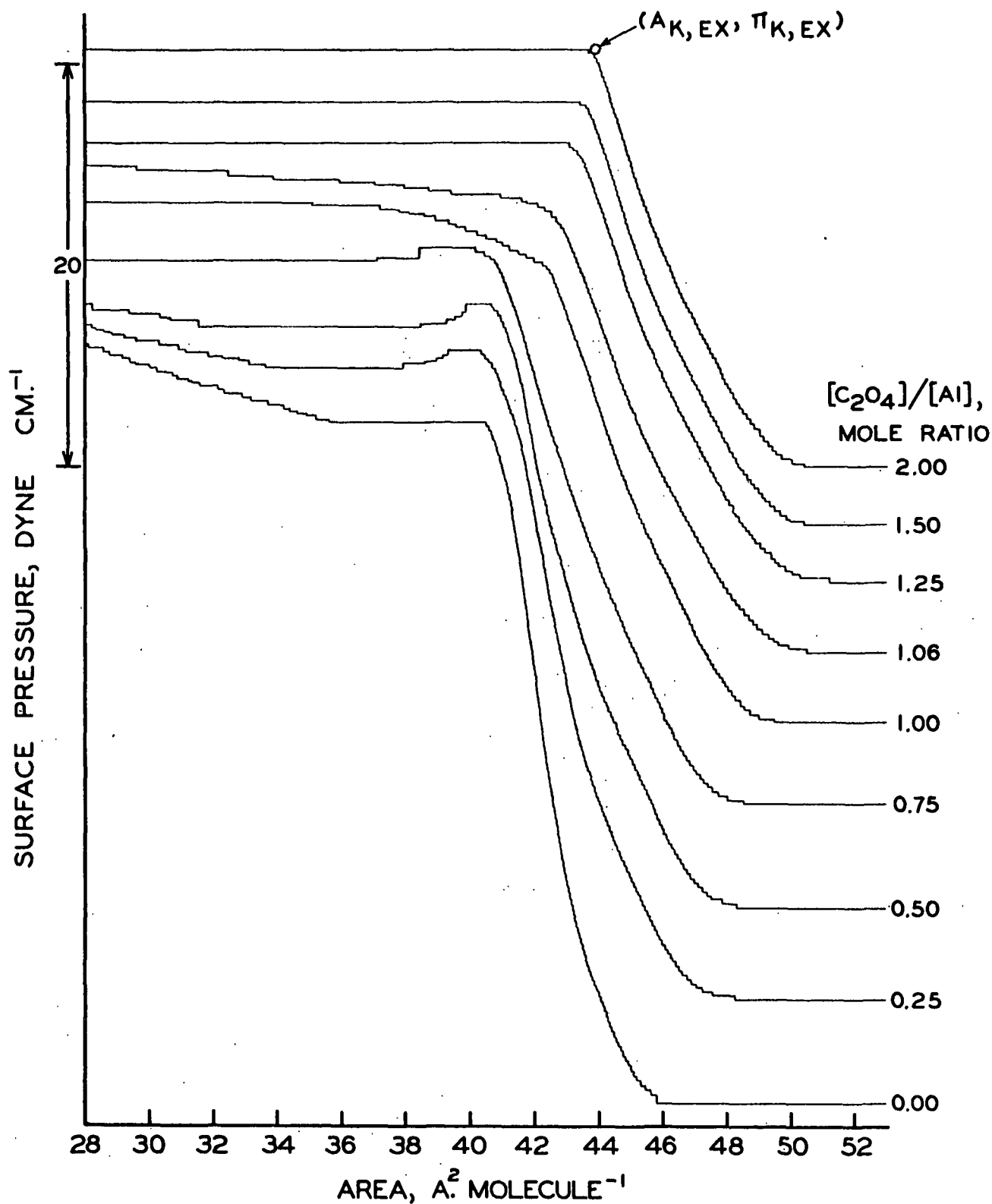


Figure 7. Surface Pressure-Area Isotherms for the Monolayers Formed when TABSH is Spread on Aluminum Sulfate Plus Oxalic Acid Substrates with  $[Al] = 3.16 \times 10^{-3} M$ . These Substrates were at  $20^\circ C$ . with  $pH = 4.00$ . Reaction Time = 6 Minutes, and  $dA/dt = 2.86 \text{ \AA}^2 \text{ Molecule}^{-1} \text{ Minute}^{-1}$ .

TABLE V

$\underline{A}_{10}$ ,  $\underline{A}_{K,EX}$ , AND  $\underline{\pi}_{K,EX}$  VALUES FOR THE MONOLAYERS FORMED WHEN TABSH IS SPREAD ON ALUMINUM SULFATE PLUS OXALIC ACID SUBSTRATES<sup>a</sup>

$[C_2O_4]/[Al]$ <sup>b</sup> in Substrate, mole ratio	$\underline{A}_{10}$ , A. <sup>2</sup> molecule <sup>-1</sup>	$\underline{A}_{K,EX}$ , A. <sup>2</sup> molecule <sup>-1</sup>	$\underline{\pi}_{K,EX}$ , dyne cm. <sup>-1</sup>
0.00	43.1	41.0	33.5
0.25	44.0	41.2	32.2
0.50	44.3	41.2	30.0
0.75	44.5	40.9	27.6
1.00	45.3	42.5	22.5
1.06	45.6	42.7	22.3
1.25	46.1	43.4	21.8
1.50	46.1	43.7	21.0
2.00	46.2	43.8	20.7

<sup>a</sup>Substrates were at 20°C. with pH = 4.00, reaction time = 6 minutes, and  $\underline{dA}/\underline{dt} = 2.86$  A.<sup>2</sup> molecule<sup>-1</sup> minute<sup>-1</sup>.

<sup>b</sup>[Al] =  $3.16 \times 10^{-3}$  M in all substrates.

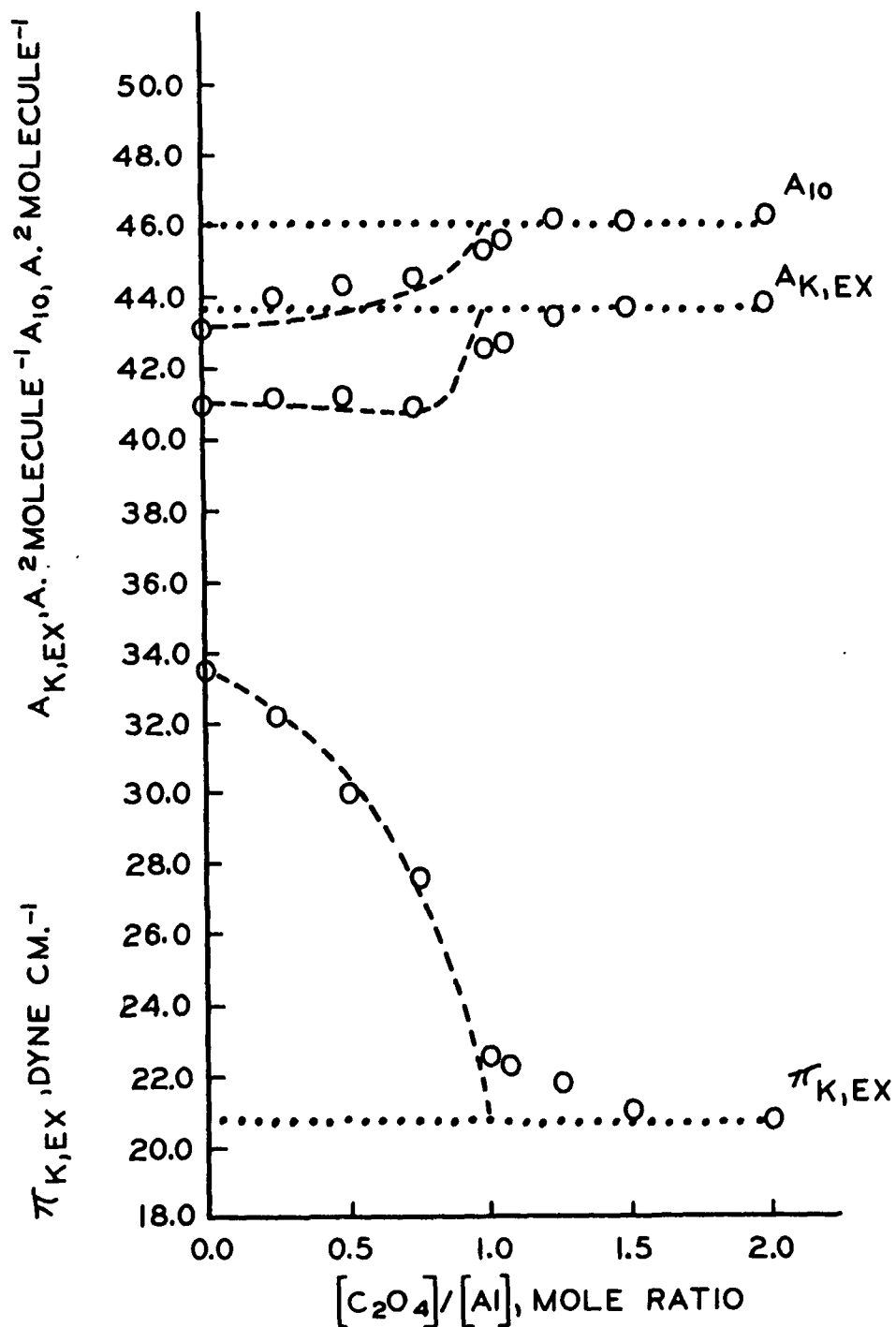
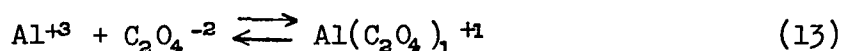


Figure. 8.  $A_{10}$ ,  $A_{K,EX}$ , and  $\pi_{K,EX}$  Values for the Monolayers Formed when TABSH is Spread on Aluminum Sulfate Plus Oxalic Acid Substrates with  $[Al] = 3.16 \times 10^{-3} M$ . These Substrates were at  $20^\circ C$ . with  $pH = 4.00$ . Reaction Time = 6 Minutes, and  $\frac{dA}{dt} = 2.86 A. 2 \text{ Molecule}^{-1} \text{ Minute}^{-1}$ . Data Points at a Given  $[C_2O_4]/[Al]$  were Obtained from One  $\pi$ -A Isotherm. Dashed Lines are for Stoichiometric Formation of  $Al(C_2O_4)_3$ . Dotted Lines are for TABSH Monolayer on Sulfuric Acid Substrate at  $20^\circ C$ . with  $pH = 4.00$ . Reaction Time = 6 Minutes, and  $\frac{dA}{dt} = 2.86 A. 2 \text{ Molecule}^{-1} \text{ Minute}^{-1}$

effectively with  $\text{Al}(\text{C}_2\text{O}_4)_1^{+1}$  for aluminum ions, and that  $\text{Al}(\text{C}_2\text{O}_4)_1^{+1}$  does not react with the TABSH monolayer.

Babko and Dubovenko (40) reported that aluminum oxalate complexes are formed in stepwise manner in the aluminum chloride plus oxalic acid system. They found that  $\text{Al}(\text{C}_2\text{O}_4)_1^{+1}$  is the first complex formed. The formation of this complex is given by Equation (13) where  $\text{Al}^{+3}$  represents the hydrated aluminum ions.



The formation constant for the reaction is given in Equation (14). The brackets represent the molar concentrations of the species and  $K_F$  is the formation constant. At pH < 1, the value of  $K_F$  is  $1.82 \times 10^7 \text{ l mole}^{-1}$  (40).

$$[\text{Al}(\text{C}_2\text{O}_4)_1^{+1}] / [\text{Al}^{+3}][\text{C}_2\text{O}_4^{-2}] = K_F \quad (14)$$

The structure of  $\text{Al}(\text{C}_2\text{O}_4)_1^{+1}$  (38) is shown in Fig. 9.

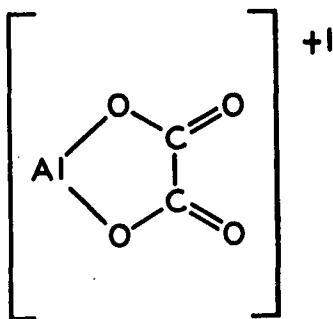


Figure 9. Structure of  $\text{Al}(\text{C}_2\text{O}_4)_1^{+1}$  (38).

This planar five-membered ring structure is stable and only a ligand that forms a complex of equivalent stability can compete effectively with it for aluminum (90).

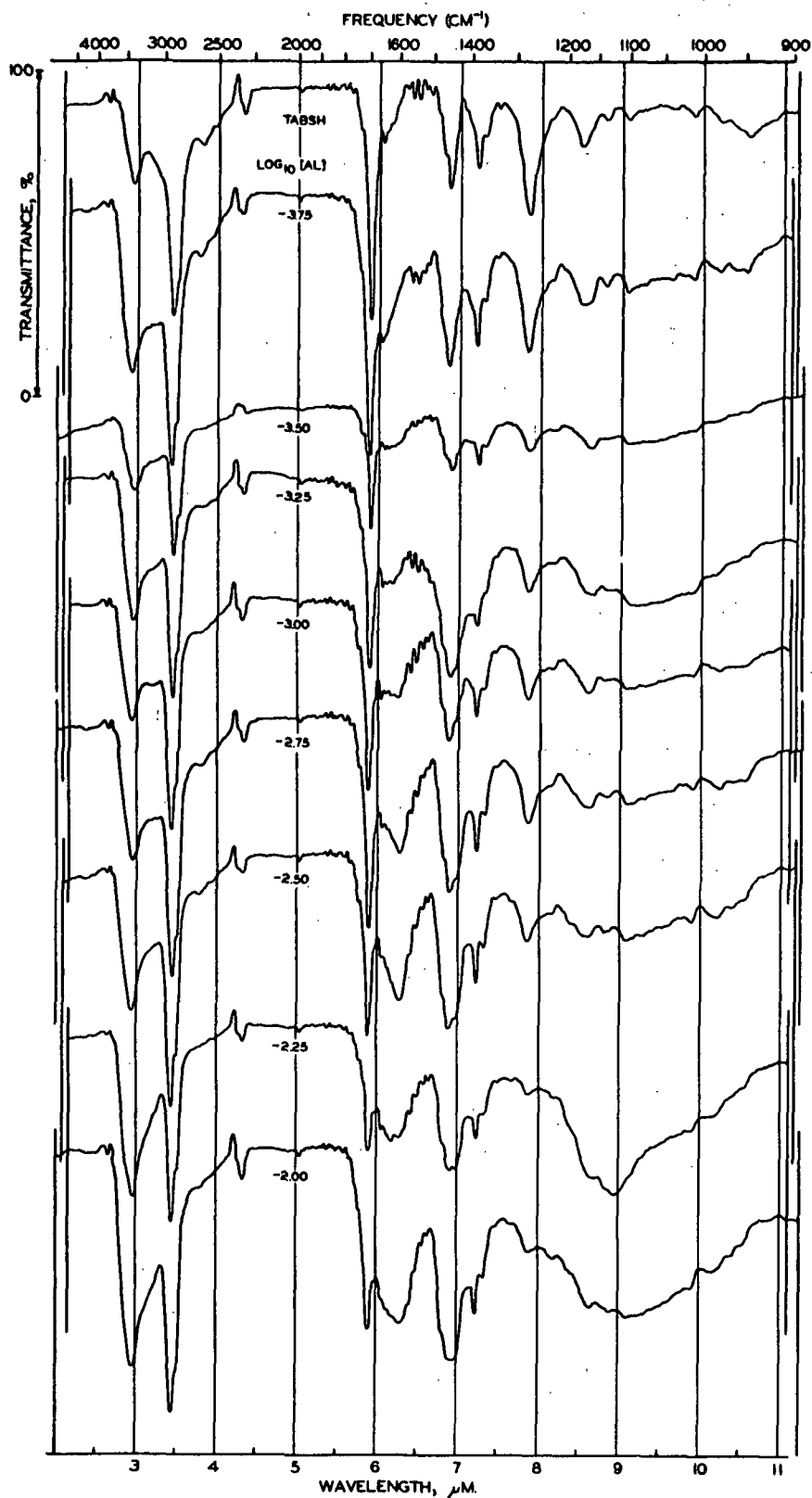
Sears and Schulman (91) reported that cations with large charge to radius ratios are favored over those with small ratios in reactions with fatty acid monolayers. The  $\text{Al}(\text{C}_2\text{O}_4)_1^{+1}$  species has a smaller charge and a larger radius than the  $\text{Al}^{+3}$  species. As a result, the charge to radius ratio for  $\text{Al}(\text{C}_2\text{O}_4)_1^{+1}$  is less than that for  $\text{Al}^{+3}$ .

The experimental values of  $A_{10}$ ,  $A_{\underline{K},\underline{EX}}$ , and  $\pi_{\underline{K},\underline{EX}}$  agree reasonably well with the dashed lines in Fig. 8 based on the assumptions outlined above. Deviations from the lines are attributed to the complex equilibria involving the monolayer molecule and hydroxide, sulfate, oxalate, and aluminum ions. (Radiochemistry data presented in Table VII indicate that only a small amount of oxalate is present in the sample of monolayer material collected at  $[\text{C}_2\text{O}_4]/[\text{Al}] = 1.00$ .) The formation constant reported by Babko and Dubovenko (40) is for the aluminum chloride plus oxalic acid system at  $\text{pH} < 1$ . However, the present work was done at  $\text{pH} 4.00$  where  $\text{Al}(\text{C}_2\text{O}_4)_1^{+1}$ ,  $\text{Al}(\text{C}_2\text{O}_4)_3^{-1}$ , and  $\text{Al}(\text{C}_2\text{O}_4)_3^{-3}$  may exist in stepwise equilibrium (40).

The  $\pi$ - $A$  isotherms for TABSH on oxalic acid and sulfuric acid substrates were the same within the  $[\text{C}_2\text{O}_4]$  range used in aluminum sulfate plus oxalic acid substrates (Appendix V). This indicates that oxalate alone has no effect on the monolayers on these mixed substrates.

#### CHANGES IN INFRARED SPECTRUM

Monolayer material was collected from aluminum sulfate plus oxalic acid substrates in which the  $[\text{Al}]$  was held constant at  $3.16 \times 10^{-3}\text{M}$  and the  $[\text{C}_2\text{O}_4]$  was varied. The middle seven infrared spectra shown in Fig. 10 are for samples of this material.



*should be in  
Fig 4  
location  
caption ok here*

Figure 10. Infrared Spectra of TABSH Starting Material and Monolayer Material Collected from Aluminum Sulfate Plus Oxalic Acid Substrates with  $[Al] = 3.16 \times 10^{-3} M$  at  $20^\circ C$ . with  $pH = 4.00$ . Reaction Time = 6 Minutes. These Materials were Washed and Dried at  $20^\circ C$ .

The spectra of the TABSH starting material and the material collected from an aluminum sulfate substrate with  $[Al] = 3.16 \times 10^{-3} M$  are also shown in the figure.

As  $[C_2O_4]/[Al]$  is increased, the acid absorption bands at  $2650 \text{ cm.}^{-1}$ ,  $1700 \text{ cm.}^{-1}$ , and  $1275 \text{ cm.}^{-1}$  increase in intensity relative to the hydrocarbon band at  $2910 \text{ cm.}^{-1}$ . Likewise, the salt absorption bands at  $1590 \text{ cm.}^{-1}$  and  $1435 \text{ cm.}^{-1}$  decrease in relative intensity. When  $[C_2O_4]/[Al] = 2.00$ , the spectrum for the sample of collected monolayer material is practically the same as that for the TABSH starting material.

These results indicate that the proportion of free acid in the collected monolayer material is steadily increased as  $[C_2O_4]/[Al]$  in the substrate is increased. This trend in the monolayer composition is attributed to the sequestering action of oxalate on aluminum ions.

#### CHANGES IN FREE ACID MOLE FRACTION

The  $X_{\text{TABSH}}$  values of monolayer material collected from aluminum sulfate plus oxalic acid substrates are given in Table VI and shown in Fig. 11 (data points). These results were calculated with Equation (12) for data taken from the infrared spectra shown in Fig. 10. The dotted line is for pure TABSH. The dashed curve between  $[C_2O_4]/[Al] = 0.00$  and  $1.00$  is based on the  $X_{\text{TABSH}}$  data in Fig. 5 and the assumptions outlined in the section on  $\pi$ -A isotherms.

Between  $[C_2O_4]/[Al] = 1.00$  and  $1.50$ , the experimental values of  $X_{\text{TABSH}}$  are measurably lower than the predicted values. This deviation is attributed to the complex equilibria involving the monolayer molecules and hydroxide, sulfate, oxalate, and aluminum ions.

TABLE VI

FREE ACID MOLE FRACTIONS OF MONOLAYER MATERIAL COLLECTED  
FROM ALUMINUM SULFATE PLUS OXALIC ACID SUBSTRATES<sup>a, b</sup>.

$[C_2O_4]/[Al]^c$ in Substrate, mole ratio	$X_{TABS^H}^d$
0.00	0.51
0.25	0.52
0.50	0.62
0.75	0.68
1.00	0.79
1.25	0.89
1.50	0.94
2.00	0.97

<sup>a</sup>Substrates were at 20°C. with pH = 4.00

<sup>b</sup>Material washed and dried at 20°C.

<sup>c</sup> $[Al] = 3.16 \times 10^{-3}$  in all substrates.

<sup>d</sup>Calculated with Equation (12).

#### COMPOSITION OF COLLECTED MONOLAYER MATERIAL

The  $X_{TABS^H}$  and aluminum and carbon contents of monolayer material collected from an aluminum sulfate plus oxalic acid substrate are reported in Table III. The  $[OXALATE]/[TABS^H \text{ plus } TABS^-]$  mole ratios for that sample and for material collected from an oxalic acid substrate are given in Table VII.

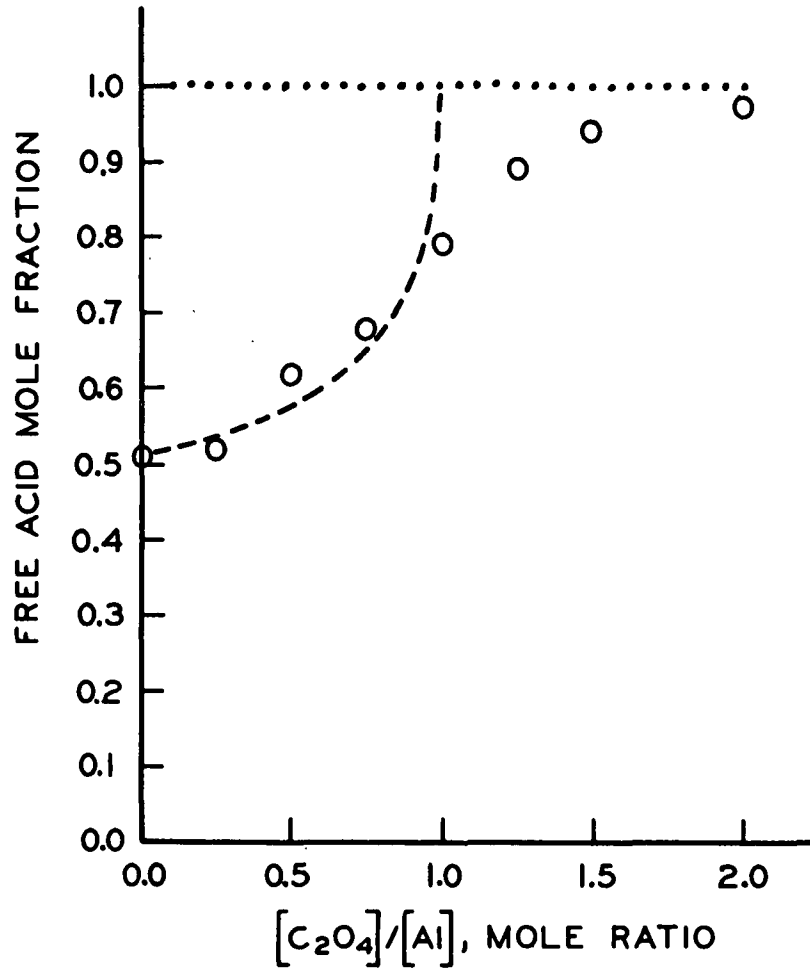


Figure 11. Free Acid Mole Fractions of Monolayer Material Collected from Aluminum Sulfate Plus Oxalic Acid Substrates with  $[Al] = 3.16 \times 10^{-3}M$  at  $20^\circ$  with  $pH = 4.00$ . Reaction Time = 6 Minutes. This Material was Washed and Dried at  $20^\circ C$ . Dashed Line is for Stoichiometric Formation of  $Al(C_2O_4)_1^{+1}$ . Dotted Line is for TABSH Starting Material Dried at  $20^\circ C$ .

TABLE VII

[OXALATE]<sup>a</sup>/[TABSH PLUS TABS<sup>-</sup>]<sup>b</sup> MOLE RATIOS  
OF COLLECTED MONOLAYER MATERIAL<sup>c</sup>

Substrate <sup>d</sup>	[OXALATE] <sup>a</sup> /[TABSH plus TABS <sup>-</sup> ] <sup>b</sup> , mole ratio
[C <sub>2</sub> O <sub>4</sub> ] = 3.16 x 10 <sup>-3</sup> M	0.01
[Al] = [C <sub>2</sub> O <sub>4</sub> ] = 3.16 x 10 <sup>-3</sup> M	0.02

<sup>a</sup>Moles of oxalate in collected sample.

<sup>b</sup>Total moles of TABSH and TABS<sup>-</sup> in collected sample.

<sup>c</sup>Material washed and dried at 20°C.

<sup>d</sup>Carbon-14 enriched oxalic acid was used to prepare substrates at 20°C. with pH = 4.00.

The [OXALATE]/[TABSH plus TABS<sup>-</sup>] mole ratios for both samples are small and these amounts of oxalate can be attributed to entrapment.

#### CHANGES IN STRUCTURE OF SURFACE REGION

The evidence for hydrocarbon packing and for a hydrogen-bonded structure beneath the monolayer diminish sharply as [C<sub>2</sub>O<sub>4</sub>]/[Al] increases between 0.00 and 1.00. When [C<sub>2</sub>O<sub>4</sub>]/[Al] = 2.00, no significant aluminum ditetrahydroacetate is present in the monolayer and the structuring in the surface region associated with this species has disappeared.

#### NATURE OF THE EFFECT

The results presented in Fig. 7, 8, 10, and 11 indicate that oxalate inhibits the reaction between TABSH monolayers and aluminum ions by strongly sequestering the cations. Analysis of these data indicates that Al(C<sub>2</sub>O<sub>4</sub>)<sub>1</sub><sup>+1</sup> is the first

aluminum oxalate species formed in the mixed substrates. Furthermore, this complex does not react with the monolayer molecules.

The masking action of oxalate has been reported previously for the chrome-tanning system (92). Ethylenediamine tetraacetate (EDTA) has also been shown to inhibit the reaction between fatty acid monolayers and multivalent metal cations (73, 93).

## CONCLUSIONS

Aluminum ions react with TABSH (tetrahydroabiatic acid) monolayer molecules at the liquid-air interface of acidic aluminum sulfate solutions to form aluminum ditetrahydroabietate. The resulting salt mole fraction ( $X_{\text{TABS}^-}$ ) in the monolayers appears to approach a limiting value just above 0.60 as the  $[\text{Al}]$  (total molar aluminum species concentration in system) is increased. The aluminum resinate composition and apparent limiting  $X_{\text{TABS}^-}$  in the monolayer agree with the corresponding quantities for the commercial size precipitate reported by other authors. The concentration dependence of the monolayer reaction and the indication of a capacity for the monolayer strongly suggest that the reaction involves ion-exchange. Salt formation at the interface causes the rigidity of the monolayer to increase. This indicates the formation of a hydrogen-bonded network of hydroxyls and water molecules associated with the aluminum portion of the salt.

For aluminum sulfate substrates with added oxalate, the reaction between TABSH monolayers and aluminum ions is completely prevented when  $[\text{C}_2\text{O}_4]/[\text{Al}]$  approaches 2.00 ( $[\text{C}_2\text{O}_4]$  = total molar oxalate species concentration in system and  $[\text{Al}] = 3.16 \times 10^{-3}\text{M}$  in these substrates). Up to  $[\text{C}_2\text{O}_4]/[\text{Al}] = 0.75$ ,  $\text{Al}(\text{C}_2\text{O}_4)_1^{+1}$  appears to be formed in the substrate and little if any of this complex reacts with the TABSH monolayer. Between 0.75 and 2.00 deviation from the stoichiometric formation of  $\text{Al}(\text{C}_2\text{O}_4)_1^{+1}$  is noted. This can be explained by the complex equilibria involving the monolayer molecules and hydroxide, sulfate, oxalate, and aluminum ions. The inhibition of the monolayer reaction indicates that oxalate can prevent the formation of aluminum resinate in suspension by sequestering aluminum ions. This evidence for a colloidal system is in agreement with the hypothesis that Cobb and Lowe originally proposed for an ionic system.

## GLOSSARY

$\underline{L}$  = depth of penetration

$\underline{r}$  = capillary radius

$\gamma_{\underline{LV}}$  = specific free-surface energy of the liquid-vapor interface

$\theta$  = contact angle between liquid and solid

$\underline{t}$  = time of penetration

$\eta$  = coefficient of viscosity of the liquid

$\underline{dL/dt}$  = rate of penetration

$\theta_{\underline{A}}$  = advancing contact angle between liquid and solid

$\gamma_{\underline{SV}}$  = specific free-surface energy of the solid-vapor interface

$\gamma_{\underline{SL}}$  = specific free-surface energy of the solid-liquid interface

$H^+$  = hydrogen ion

$Al(R)(OH)_2$  = dibasic aluminum monoresinate

$Al(R)_2(OH)$  = monobasic aluminum diresinate

Me =  $K^+$ ,  $Na^+$ , or  $NH_4^+$

$\underline{A}_{\underline{K}}$  = average cross-sectional area of monolayer molecules when the monolayer collapses,  $A.^2$  molecule $^{-1}$

$\underline{\pi}_{\underline{K}}$  = lateral force per unit width of the monolayer (surface pressure) when the monolayer collapses, dyne cm. $^{-1}$

TABSH= sample of tetrahydroabiatic acid used in this work

$\underline{A}$  = average cross-sectional area of monolayer molecules,  $A.^2$  molecule $^{-1}$

$\pi$  = surface pressure of monolayer, dyne cm. $^{-1}$

$\underline{A}_{\underline{K}0}$  = average cross-sectional area of monolayer molecules when  $\pi = 10$  dyne cm. $^{-1}$ ,  $A.^2$  molecule $^{-1}$

$\underline{A}_{\underline{K},\underline{EX}}$  = average cross-sectional area of monolayer molecules at the extrapolated collapse point of the monolayer,  $A.^2$  molecule $^{-1}$

$\underline{\pi}_{\underline{K},\underline{EX}}$  = surface pressure at extrapolated collapse point of the monolayer, dyne cm. $^{-1}$

$\frac{dA}{dt}$  = rate of reduction of average area available to monolayer molecules,  $A^2$   
molecule<sup>-1</sup> minute<sup>-1</sup>

$\sigma$  = standard deviation

[Al] = total molar concentration of aluminum species in system

= moles of aluminum added to system

[C<sub>2</sub>O<sub>4</sub>] = total molar concentration of oxalate species in system

= moles of oxalate added to system

$A_{-COOH}$  = absorbance of disk at 1700 cm.<sup>-1</sup>

$A_{-CH}$  = absorbance of disk at 2910 cm.<sup>-1</sup>

Al(TABS)(OH)<sub>2</sub> = dibasic aluminum monotetrahydroabietate

Al(TABS)<sub>2</sub>(OH) = monobasic aluminum ditetrahydroabietate

Al(TABS)<sub>3</sub> = aluminum tritetrahydroabietate

TABS<sup>-</sup> = tetrahydroabietate ion

$A_{-S}$  = absorbance of disk at a given wavelength

$a_{-S}$  = absorptivity of substance at a given wavelength, cm.<sup>-1</sup> mole<sup>-1</sup> g.

$b_{-d}$  = thickness of disk, cm.

$c_{-S}$  = concentration of substance in disk, moles g.<sup>-1</sup>

$a_{-R}$  = absorptivity of TABSH and TABS<sup>-</sup> at 2910 cm.<sup>-1</sup>, cm.<sup>-1</sup> mole<sup>-1</sup> g.

$b_{-1}$  = thickness of disk, cm.

$c_{-1}$  = concentration of TABSH plus TABS<sup>-</sup> in disk, mole g.<sup>-1</sup>

$a_{-TABS\ H}$  = absorptivity of TABSH at 1700 cm.<sup>-1</sup>, cm.<sup>-1</sup> mole<sup>-1</sup> g.

$b_{-2}$  = thickness of disk, cm.

$c_{-2}$  = concentration of TABSH in disk, mole g.<sup>-1</sup>

$X_{-TABS\ H}$  = mole fraction of TABSH

$N_{-TABS\ H}$  = number of moles of TABSH

$N_{-TABS\ -}$  = number of moles of TABS<sup>-</sup>

$N_{-S}$  = number of moles of substance in disk

$w_{-d}$  = weight of disk, g.

$K_F$  = formation constant

$[Al^{+3}]$  = molar concentration of aluminum ion

$[H^+]$  = molar concentration of hydronium ion

[OXALATE] = moles of oxalate in collected sample

[TABS<sup>H</sup> plus TABS<sup>-</sup>] = total moles of TABS<sup>H</sup> and TABS<sup>-</sup> in collected sample

DEGS = diethylene glycol succinate

mc. = millicurie

$\gamma_0$  = surface tension of pure liquid, dyne cm.<sup>-1</sup>

$\gamma$  = surface tension of film-covered surface, dyne cm.<sup>-1</sup>

$C$  = torsion wire constant, dyne degree<sup>-1</sup>

$\theta_r$  = rotation of torsion wire, degree

$L_f$  = effective length of float, cm.

$l$  = actual length of float, cm.

$w$  = combined width of gaps occupied by flexible ribbons, cm.

$p$  = test area length, cm.

$g$  = test area width, cm.

$N$  = number of molecules on test area

$c$  = A.-cm. equivalence, 10<sup>-8</sup> cm. A.<sup>-1</sup>

A. = Angstrom unit

## SUGGESTIONS FOR FURTHER WORK

Citrate and tartrate are reported to be detrimental to sizing (30). These ligands probably affect the interfacial reaction between colloidal resin acid agglomerates and aluminum ions. This hypothesis should be tested with the surface chemical model of the rosin-alum sizing system.

The influence of high surface pressures on the configuration of bulky monolayer molecules is not clear (66). Tetrahydroabietic acid monolayers appear to be ideally suited for investigating this influence. The molecules of this resin acid are relatively simple and they are resistant to air oxidation. Likewise, they can be prepared in three configurations or the three isomers may be separated from a mixture by gas chromatography.

## ACKNOWLEDGMENTS

The author expresses sincere thanks for the guidance and interest of his Thesis Advisory Committee: J. W. Swanson (chairman), B. L. Browning, and M. A. Buchanan. J. W. Swanson suggested the thesis topic and he was tireless in his efforts to help the author obtain, build, and perfect necessary equipment. B. L. Browning and M. A. Buchanan provided pertinent criticism and advice concerning the analytical techniques employed in the course of the thesis work.

The tetrahydroabiatic acid was obtained from S. H. Watkins of Hercules Incorporated and the pimaric acid was supplied by C. Bordenca of the Glidden Company.

K. W. Hardacker designed and built the electrical system for the automatic recording surface balance. He also prepared Table XII and Figure 16. The mechanical system of the balance was designed by the author and modified and built by L. E. Dambruch, M. C. Filz, and P. F. Van Rossum.

B. D. Andrews, H. J. Grady, and L. M. Wittman were instrumental in providing distilled water and L. O. Sell skillfully determined the infrared spectra. L. G. Borcharadt determined the emission spectra and H. F. Hanel obtained the gas chromatographic data.

The author is indebted to all of these people for their assistance during the course of his thesis work.

## LITERATURE CITED

1. Washburn, E. W., Phys. Rev. 17:273-83(1921).
2. Dupre, A. Theorie Mecanique de la Chaleur. Paris, 1869. 368 p.; Cited in Adamson, A. W. Physical chemistry of surfaces. New York, Interscience, 1960. 629 p.
3. Swanson, J. W., Tappi 44, no. 1:142A-81A(Jan., 1961).
4. Langmuir, I., Overturning and anchoring of monolayers. In Recent advances in surface chemistry and chemical physics. Edited by F. R. Moulten, Publication no. 7 of the American Association for Advancement of Science, p. 9-18. 1939.
5. Rideal, E. K., and Tadayon, J., Proc. Royal Soc. (London) A225:346-56(1954).
6. Rideal, E. K., and Tadayon, J., Proc. Royal Soc. (London) A225:357-61(1954).
7. Yiannos, P. N. Molecular reorientation of some fatty acids when in contact with water. Doctoral Dissertation. Appleton, Wis., The Institute of Paper Chemistry, 1960. 115 p.
8. Engel, E. M., The internal sizing of paper. In Pulp and paper science and technology. Vol. II: Paper. p. 40-59. Edited by C. E. Libby, New York, McGraw-Hill, 1962.
9. Back, E., and Steenberg, B., Svensk Papperstid. 54, no. 15:510-15(Aug. 15, 1951).
10. Ekwall, P., and Bruun, H., Paper and Timber (Finland) 32, no. 7:194-202(1950).
11. Guide, R. G., A study of the sodium aluminate-abietate size precipitates. Doctoral Dissertation. Appleton, Wis., The Institute of Paper Chemistry, 1959. 102 p.
12. Watkins, S. H., Tappi 45, no. 5:216A-20A(May, 1962).
13. Strazdins, E., Tappi 48, no. 3:157-64(March, 1965).
14. Vandenberg, E. J., and Spurlin, H. M., Tappi 50, no. 5:209-24(May, 1967).
15. Davison, R. W., Tappi 47, no. 10:609-16(Oct., 1964).
16. Casey, J. P., Pulp and paper. Vol. II: Papermaking. 2nd ed. p. 1054. New York, Interscience, 1960.
17. Miceli, J., and Stuehr, J. J. Am. Chem. Soc. 90:6967-72(1968).
18. Kubota, H. Properties and volumetric determination of aluminum ion. Doctoral Dissertation. Madison, Wis., The University of Wisconsin, 1956. 121 p.
19. Schofield, R. K., and Taylor, A. W., J. Chem. Soc. 1954:4445-8.

20. Buchanan, M. A., Extraneous components of wood. In The chemistry of wood. p. 313-67. Edited by B. L. Browning, New York, Interscience, 1963.
21. Lawrence, R. V., Tappi 42, no. 10:867-9(Oct., 1959).
22. Genge, C. A., Anal. Chem. 31:1750-3(1959).
23. Price, D., Paper Trade J. 126, no. 15:61-6(T. S. 191-6) (April 8, 1948).
24. Price, D., Ind. Eng. Chem. 39, no. 9:1143-7(Sept., 1947).
25. Back, E., and Steenberg, B., Svensk Papperstid. 54, no. 15:510-15(Aug. 15, 1951).
26. Thode, E. F., Gorham, J. F., and Atwood, R. H. Tappi 36, no. 7:310-14(July, 1953).
27. Ninck Blok, C. J. J., Pulp Paper Mag. Can. 57, no. 3:208-15(1956).
28. Wilson, W. S., Tech. Assoc. Papers 27:404-7(1944).
29. Thomas, A. W., Paper Trade J. 100, no. 6:36-9(1935).
30. Cobb, R. M. K., and Lowe, D. V., Tappi 38, no. 2:49-65(1955).
31. Collins, T. T., Davis, H. L., and Rowland, B. W., Paper Trade J. 113, no. 13:94-9(Sept. 25, 1941).
32. Thode, E. F., Gorham, J. F., Kumler, R. W., and Woodbury, N. T., Tappi 38, no. 12:710-16(Dec., 1955).
33. Thode, E. F., and Htoo, S., Tappi 38, no. 12:705-9(Dec., 1955).
34. Ninck Blok, C. J. J. The sizing of paper as a colloid-chemical phenomena. Doctoral Dissertation. The Netherlands, The University of Utrecht, 1952.
35. Thode, E. F., and Gorham, J. F., Tappi 36, no. 7:315-19(July, 1953).
36. Swanson, J. W., Course A 235. Colloid chemistry of papermaking materials. Appleton, Wis., The Institute of Paper Chemistry. Fall, 1965.
37. Rosenheim, A., Z. Anorg. Chem. 11:175-248(1896).
38. Fujita, J., Martell, A. E., and Nakamoto, K., J. Chem. Phys. 36, no. 2:324-31 (1962).
39. Lacroix, S., Bull. Soc. Chim. France, no. 5-6:408-15(1947).
40. Babko, A. K., and Dubovenko, L. I., Zh. Neorg. Khim., 2, no. 6:1294-1305(1957).
41. Nakamoto, K., Fujita, J., Tanaka, S., and Kobayashi, M., J. Am. Chem. Soc. 79:4904-8(1957).

42. Ekwall, P., Svensk Kem. Tid. 63:277-307(1951).
43. Harkins, W. D., Mattoon, R. W., and Corrin, M. L., J. Am. Chem. Soc. 68:220-8 (1946).
44. Bruun, H. H. Surface balance studies of rosin acid monolayers. Doctoral Dissertation. Abo, Finland, Abo Akademi, 1954. 111 p.
45. Ekwall, P., and Bruun, H. H., Acta Chem. Scand. 9:412-23(1955).
46. Ekwall, P., and Bruun, H. H., Acta Chem. Scand. 9:424-9(1955).
47. Bruun, H. H., Acta Chem. Scand. 9:1721-3(1955).
48. Motomura, K., and Matuura, R., Bull. Chem. Soc. Japan 35:285-9(1962).
49. Strazdins, E., Tappi 46, no. 7:432-7(July, 1963).
50. Adamson, A. W. The nature and thermodynamics of liquid-gas interfaces. In Physical chemistry of surfaces. p. 51-102. New York, Interscience, 1960.
51. Ferroni, E., Ficalba, A., and Gabrielli, G., Ann. Chim. (Rome) 47:1100-4 (1957); C. A. 52:3583f.
52. Ferroni, E., Ficalba, A., and Gabrielli, G., Ann. Chim. (Rome). 47:1105-18 (1957); C. A. 52:3583h.
53. Major, E. H., and Swanson, J. W. A study of the effect of oxalate ions on the formation of a dibasic aluminum monoresinate. Unpublished work, 1965.
54. Langmuir, I., and Blodgett, K. B. Some new methods for the investigation of monomolecular films. In The collected works of Irving Langmuir. Vol. 9: Surface phenomena. p. 302-11. Edited by C. G. Suits. New York, Pergamon Press, 1961.
55. Marx, J. M., Part I. Synthesis and stereochemistry of fichtelite. Part II. Structure and stereochemistry of some reduction products of abietic-type resin acids. Doctoral Dissertation. Lawrence Kansas, University of Kansas, 1965. 128 p.
56. Goddard, E. D., Smith, S. R., and Kao, O., J. Colloid Interface Sci. 21: 320-30(1966).
57. Anderson, P. A., and Evett, A. A., Rev. Sci. Instr. 23, no. 9:485-8(Sept., 1952).
58. Langmuir, I., and Schaefer, V. T., J. Am. Chem. Soc. 58, no. 2:284-7(Feb., 1936).
59. Van Slyke, D. D., and Folch, J., J. Biol. Chem. 136:509-41(1940).
60. Van Slyke, D. D., Plazin, J., and Weisiger, J. R., J. Biol. Chem. 191:299-304 (1951).

61. Van Slyke, D. D., Steele, R., and Plazin, J., *J. Biol. Chem.* 192:769-805(1951).
62. Van Slyke, D. D., and Plazin, J., *J. Biol. Chem.* 237:3296-8(1962).
63. Bernstein, W., and Ballentine, R., *Rev. Sci. Instr.* 21, no. 2:158-61(Feb., 1950);.
64. Pienaar, W. J. The quantitative spectrographic analysis of plant material with the aid of the direct current arc. Union of South Africa, Dept. of Agr. Scientific Bull. 355:2-16(1955).
65. *Methods for emission spectrochemical analysis.* 3rd ed. p. 564. Philadelphia, Pa., ASTM, 1960.
66. Gaines, G. L., Jr. *Insoluble monolayers at liquid-gas interfaces.* New York, Interscience, 1966. 386 p.
67. Wolstenholme, G. A., and Schulman, J. H. *Trans. Faraday Soc.* 47:788-94(1951).
68. Spink, J. A., and Sanders, J. V., *Trans. Faraday Soc.* 51:1154-65(1955).
69. Matuura, R., *Bull. Chem. Soc. Japan* 24, no. 6:278-81(1951).
70. Thomas, J. G. N., and Schulman, J. H., *Trans. Faraday Soc.* 50:1128-30(1954).
71. Thomas, J. G. N., and Schulman, J. H., *Trans. Faraday Soc.* 50:1131-9(1954).
72. Thomas, J. G. N., and Schulman, J. H., *Trans. Faraday Soc.* 50:1139-47(1954).
73. Kimizuka, H., *Bull. Chem. Soc. Japan* 29, no. 1:123-6(1956).
74. Motomura, K., and Matuura, R., *Bull. Chem. Soc. Japan* 35:285-9(1962).
75. Dervichian, D. G., *J. Chem. Phys.* 7:931-48(Oct., 1939).
76. Defay, R., Prigogine, I., Bellemans, A., and Everett, D. H. *Surface tension and adsorption.* New York, John Wiley and Sons, 1966. 432 p.
77. Cupples, H. L., *J. Phys. Chem.* 50:256-60(1946).
78. Ellis, J. W., and Pauley, J. L., *J. Colloid Sci.* 19:755-64(1964).
79. Smith, T., and Serrins, R., *J. Colloid Interface Sci.* 23:329-40(1967).
80. Bellamy, L. J. *The infra-red spectra of complex molecules.* New York, John Wiley and Sons, 1958. 423 p.
81. Friberg, S., and Bruun, H. H., *Arkiv Kemi* 25, no. 45:491-8(1966).
82. Sadtler, T., *Sadtler Spectrum II*, no. 1:2(Summer, 1968).
83. Bagg, J., Abramson, M. B., Fichman, M., Haber, M. D., and Gregor, H. P., *J. Am. Chem. Soc.* 86, no. 14:2759-63(1964).

84. Hughes, H. K., and Committee. *Anal Chem.* 24, no. 8:1349-54(Aug., 1952).
85. Potts, W. J., Jr. *Chemical infrared spectroscopy*. Vol. 1, Techniques. New York, John Wiley and Sons, 1963. 322 p.
86. Colthup, N. B., Daley, L. H., and Wiberley, S. E. *Introduction to infrared and raman spectroscopy*. New York, Academic Press, 1964. 511 p.
87. Helfferich, F. *Ion exchange*. New York, McGraw Hill, 1962. 624 p.
88. Rojas, E., and Tobias, J. M., *Biochim. Biophys. Acta* 94:394-404(1965).
89. Lettvin, J. Y., and Pickard, W. F., *Nature* 209, no. 5026:886-7(1966).
90. Martell, A. E., and Calvin, M. *Chemistry of the metal chelate compounds*. New York, Prentice-Hall, Inc., 1953. 613 p.
91. Sears, D. F., and Schulman, J. H., *J. Phys. Chem.* 68:3529-34(1964).
92. Thorstensen, T. C., *J. Am. Leather Chemists' Assoc.* 52:489-504(1957).
93. Kimizuka, H. and Koketsu, K., *Nature* 196, no. 4858:995-6(1962).
94. Sanderson, T. F., Personal communication, 1968.
95. Max. Nestler, F. H., and Zinkel, D. F., *Anal. Chem.* 39, no. 10:1118-24(Aug., 1967).
96. Pierce, W. C., Sawyer, D. T., and Haenisch, E. L. *Quantitative analysis*. 4th ed. New York, John Wiley & Sons, 1960. 497 p.
97. Hanser, W. J., Pinching, G. D., and Acree, S. F., *J. Res. Nat. Bur. Stds.* 36:47-62(1946).
98. Langmuir, I., *J. Am. Chem. Soc.* 39:1848-1906(1917).
99. Adam, N. K., and Jessop, G. *Proc. Roy. Soc. (London)* A110:423-43(1926).

## APPENDIX I

## MATERIALS

## WATER

The water used was obtained by a four-step purification of tap water. The steps were as follows: filtration, deionization, filtration, and distillation. Tap water was passed through a Cuno Micro-Klean filter cartridge (50  $\mu\text{m}$ . maximum pore size) and fed to a model MB-590 Illco-Way mixed bed deionizer. The deionizer was charged with number C-211 cation and number A-244 anion exchange resins (Illinois Water Treatment Company numbers). Filtered, deionized water was next passed through a Shriver filter press and fed to an all-tin Barnstead water still. Distilled water was stored in polyethylene carboys. These were cleaned with chromic acid cleaning solution, thoroughly rinsed with distilled water, and filled with distilled water and allowed to stand for two weeks before use. The specific conductance of distilled water stored in these carboys did not change by a detectable amount for the normal period of storage used (1 to 5 days).

The water was evaluated with respect to specific conductance and liquid-air interface cleanliness. The specific conductance was determined with a model MIC 1201 Numinco electrophoretic mass-transport analyzer. Only water with a specific conductance of  $1.2 \times 10^{-6} \text{ ohm}^{-1} \text{ cm.}^{-1}$  or less was used. The liquid-air interface cleanliness of the water was checked by the surface balance technique (66). The trough was filled to the normal operating level with the water. After 30 minutes, the movable barrier was brought as close as possible to the float connected to the torsion balance system. The area reduction rate was  $2.86 \text{ A.}^2 \text{ molecule}^{-1} \text{ minute}^{-1}$  and approximately 98% of the test surface was scanned. No detectable surface pressure was recorded for the distilled water when the operational sensitivity of

the balance was  $0.19 \text{ dyne cm.}^{-1} \text{ mm.}^{-1}$  (Appendix III). This test indicated that the water and the surface balance parts in contact with it were free of significant surface active material (66).

#### PARAFFIN

Sun Oil paraffin wax number 5512 (m.p.  $158-160^{\circ}\text{F.}$ ) was obtained for use in this study. This material was in block form and it was processed to remove possible polar impurities. Portions of the paraffin were melted and passed through a 300 ml. Allihn condenser filled with activated silica gel particles. The condenser jacket was heated with steam and the silica gel was renewed after a 1200 ml. volume of paraffin was passed through the condenser. The first 300 ml. portion of paraffin was discarded and the remainder was collected.

This purified paraffin was checked for spreadable material before use. Small pieces of it were dropped on distilled water surfaces sprinkled with ignited talc (66). No spreading was observed.

#### TETRAHYDROABIETIC ACID

The sample of tetrahydroabietic acids (TABSH) was obtained from Hercules Incorporated. This mixture was prepared by high pressure hydrogenation of an alcohol solution of pure dehydroabietic acid over palladium at  $240^{\circ}\text{C.}$  (94). The sample was further purified by recrystallization from methanol to remove a small fraction of n-hexane insoluble material.

The recrystallized mixture was subjected to gas chromatographic analysis in order to determine its isomeric composition. The relative retention values of the methyl esters of the three known tetrahydroabietic acids (pimarate = 1.00) are

given in Table VIII (95). These values were obtained for a diethylene glycol succinate (DEGS) column.

TABLE VIII

RELATIVE RETENTION VALUES (PIMARATE = 1.00) FOR METHYL ESTERS OF KNOWN TETRAHYDROABIETIC ACIDS ON DEGS (95)

Tetrahydroabietate	Relative Retention Value (Pimarate = 1.00) on DEGS
8 $\beta$ , 9 $\alpha$ , 13 $\alpha$ -H	0.92
8 $\beta$ , 9 $\alpha$ , 13 $\beta$ -H	1.01
8 $\alpha$ , 9 $\alpha$ , 13 $\alpha$ -H	1.12

The methyl esters of TABSH and pimaric acid (supplied by the Glidden Company) were prepared with diazomethane. These were subjected to gas chromatographic analysis with an Aerograph 1520-1B chromatograph under the following conditions: 10  $\mu$ l. injections of benzene solutions of esters; injection and detector temperature at 225°C.; column temperature isothermal at 200°C.; flow rate at 25 ml. min.<sup>-1</sup> for both nitrogen and hydrogen; H<sub>2</sub> flame detector; and 20% DEGS on Anakrom ABS 70/80, 6 feet x 1/8 inch, stainless steel column. The relative retention values for the two peaks given by the methyl esters of the TABSH sample are listed in Table IX. The percentage of total peak area for each peak is also listed in the table.

These results indicate that the sample of TABSH is composed of approximately equal quantities of 8 $\beta$ , 9 $\alpha$ , 13 $\alpha$ -H and 8 $\alpha$ , 9 $\alpha$ , 13 $\alpha$ -H tetrahydroabietic acids. These acids are shown in Fig. 12.

TABLE IX

RELATIVE RETENTION VALUES (PIMARATE = 1.00) AND PERCENTAGES OF TOTAL PEAK AREA FOR METHYL ESTERS OF TABSH SAMPLE ON DEGS

Ester Peak	Relative Retention Value (Pimarate = 1.00) on DEGS	Total Peak Area, %
No. 1	0.91	55
No. 2	1.11	45

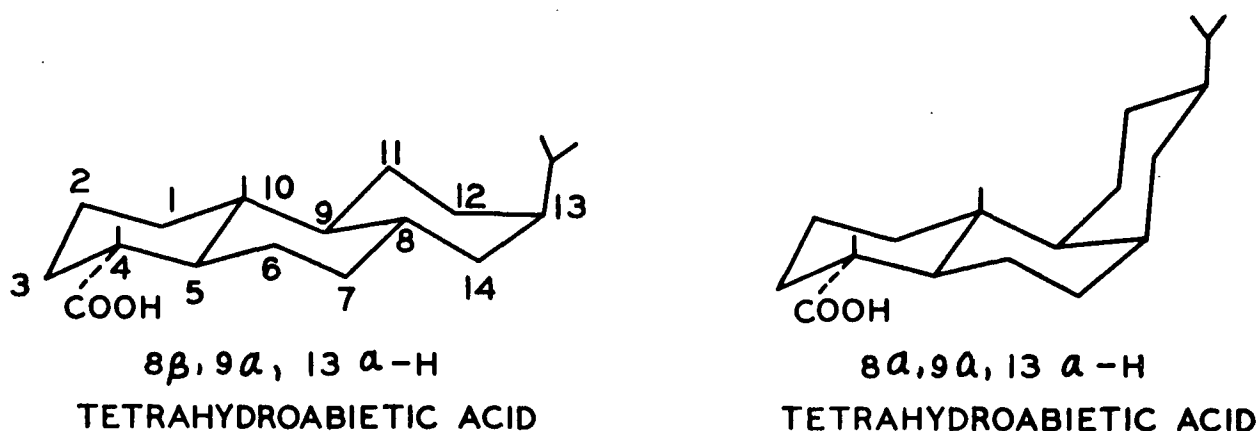


Figure 12. Tetrahydroabietic Acids in TABSH Sample

Sanderson (94) reported that gas chromatographic analysis of the original TABSH sample gave two peaks with approximately equal areas. He also indicated that one of the isomers present in the mixture of acids was  $8\alpha, 9\alpha, 13\alpha\text{-H}$  tetrahydroabietic acid.

#### n-HEXANE

Matheson Coleman & Bell reagent grade n-hexane was used in this thesis work. This material was further purified to remove traces of spreadable

contamination by distillation in a grease-free glass system (66). The fraction with a boiling point between 66.5 and 68.0°C. was collected.

The purified n-hexane was evaluated with respect to its completeness of evaporation at the liquid-air interface. The amount of n-hexane normally used to spread a TABSH monolayer was deposited on the liquid-air interface of the surface balance and allowed to evaporate. The cleanliness of the water surface was then tested in the same manner as for water. Again, no surface pressure was detected.

#### ALUMINUM SULFATE

Merck reagent grade aluminum sulfate,  $\text{Al}_2(\text{SO}_4)_3 \cdot 18\text{H}_2\text{O}$  (crystals), was used as received.

This material was checked for metal salt contamination and for aluminum content. Analysis of the aluminum sulfate by emission spectroscopy showed no significant levels of contamination. The aluminum content of the aluminum sulfate was determined by ignition of the salt to aluminum oxide,  $\text{Al}_2\text{O}_3$ . Before ignition, the samples were dried under a stream of air in a vacuum oven. The vacuum was maintained at 20 inches Hg and the temperature was increased in small increments from 25 to 200°C. The length of time between temperature increases was 1 to 8 hours. After this drying step, the samples were ignited at 1000°C. to constant weight (96). Duplicate samples of aluminum sulfate dried and ignited by this technique gave 8.25% and 8.26% aluminum based on the original sample weight. The theoretical aluminum content of  $\text{Al}_2(\text{SO}_4)_3 \cdot 18\text{H}_2\text{O}$  is 8.10%.

#### OXALIC ACID

Mallinckrodt analytical reagent grade oxalic acid,  $\text{H}_2\text{C}_2\text{O}_4 \cdot 2\text{H}_2\text{O}$  (crystals), was also used as received. The carbon content of this reagent was checked by the

Van Slyke manometric technique (Appendix IV). Duplicate samples of oxalic acid analyzed by this method gave 18.90% and 18.91% carbon based on the original sample weight. The theoretical carbon content of  $\text{H}_2\text{C}_2\text{O}_4 \cdot 2\text{H}_2\text{O}$  is 19.03%.

#### OXALIC- $\text{C}^{14}$ ACID

Oxalic- $\text{C}^{14}$  acid was obtained from Nuclear-Chicago as the crystalline dihydrate. The acid was uniformly tagged at both carbons and its specific activity was 39.7 millicurie/millimole (mc.  $\text{mM}^{-1}$ ). Dilution analysis of the acid by the supplier indicated that the radiochemical purity of the sample was 98%.

#### SODIUM HYDROXIDE

Analytical reagent (pellets), Mallinckrodt.

#### SULFURIC ACID

Analytical reagent, Mallinckrodt.

#### POTASSIUM ACID PHTHALATE

Primary standard (crystals), Mallinckrodt.

#### HYDROCHLORIC ACID

Reagent, Matheson Scientific.

#### POTASSIUM DICHROMATE

Analytical reagent (crystals), Mallinckrodt.

#### PHOSPHORUS PENTOXIDE

(Powder), Mallinckrodt.

## PARAFFIN OIL

U.S.P., white, Matheson Coleman & Bell.

## PRESSURE SENSITIVE PLASTIC (POLYFLUOROCARBON) TAPE

No. 549, 6.5 mil. thick, 2 inches wide, Minnesota Mining and Manufacturing Company.

## PLASTIC FILM

Teflon, 2.4 mil. thick, 12 inches wide, Du Pont.

## POTASSIUM IODATE

Analytical reagent (powder), Mallinckrodt.

## HYDRAZINE SULFATE

Reagent-A.C.S. (crystals), Matheson Coleman & Bell.

## SODIUM HYDROXIDE

5.0N in CO<sub>2</sub>-free water, Harleco.

## LACTIC ACID

2.0N in CO<sub>2</sub>-free water, Harleco.

## MERCURY

Triple distilled, A.C.S., instrument mercury, Bethlehem.

## SILICA GEL

No. Mil-D-3716, Davidson Chemical Company

## METHANOL

Reagent, Matheson Coleman & Bell.

## ACETONE

Reagent, Matheson Coleman & Bell.

## ETHANOL

Reagent, Matheson Coleman & Bell.

## METHANE

C.P. Matheson Coleman & Bell.

## TALC

Mallinckrodt. (Ignited to redness for 1 hour.)

## APPENDIX II

## SOLUTIONS

## BUFFER SOLUTION

Potassium acid phthalate buffer was used to standardize the Model 12 Corning pH meter (equipped with calomel and silver-silver chloride electrodes). The solid reagent was dried for 2 hours at 105°C. and a 0.05M solution was prepared with freshly boiled and cooled distilled water. The pH of the buffer solution at 20°C. is 4.002 (97).

Hanser, et al. (97) reported that 0.05M potassium acid phthalate is stable for 6 months when stored in Pyrex glassware. For this thesis work, fresh buffer was prepared every 52 days or less. The pH values of the fresh buffers relative to previously prepared buffers are shown in Table X.

TABLE X

pH VALUES OF FRESH BUFFER SOLUTIONS OF 0.05M POTASSIUM ACID PHTHALATE

Age of Shelf Solution of 0.05M Potassium Acid Phthalate, days	Temperature, °C	pH of Fresh Buffer	pH of Shelf Buffer, set
13	21.0	4.004	4.003
42	20.6	4.001	4.003
52	19.2	4.001	4.002

## TABSH SPREADING SOLUTIONS

n-Hexane was used to prepare TABSH spreading solutions. This solvent was selected for two reasons. It has a very low solubility in water (66). In addition, its volatility induces satisfactory evaporation from the spread monolayer

but slow evaporation from spreading solutions stored in ground glass-stoppered flasks. The concentration of the TABSH spreading solution used for  $\pi$ -A isotherm monolayers was  $5.0 \times 10^{17}$  molecule ml.<sup>-1</sup> (0.254 mg. ml.<sup>-1</sup>) of solution. The concentrations used for monolayers to be collected were  $1.28 \times 10^{18}$  molecule ml.<sup>-1</sup> (0.650 mg. ml.<sup>-1</sup>) and  $5.56 \times 10^{18}$  molecule ml.<sup>-1</sup> (2.82 mg. ml.<sup>-1</sup>) of solution.

The stability of the concentration of the TABSH spreading solution used for  $\pi$ -A isotherm monolayers was evaluated by a surface chemical technique. This was accomplished by determining the effect of the age of the solution on the average area,  $\frac{A}{K, EX}$ , of the molecules in monolayers cast from the solution (Appendix III). These results are shown in Table XI.

TABLE XI

$\frac{A}{K, EX}$  VALUES FOR TABSH MONOLAYERS SPREAD ON SULFURIC  
ACID SUBSTRATES<sup>a</sup> FROM STORED SPREADING SOLUTION<sup>b</sup>

Time After Preparation of Spreading Solution, days	$\frac{A}{K, EX}$ , A. <sup>2</sup> molecule <sup>-1</sup>
0	43.6
1	43.8
1	43.7
4	43.8
4	43.8
5	43.8
5	43.9
5	43.7

<sup>a</sup>Substrates were at 20°C. with pH = 4.00, reaction time = 6 minutes; and the area reduction rate ( $\frac{dA}{dt}$ ) = 2.86 A.<sup>2</sup> molecule<sup>-1</sup> minute<sup>-1</sup>.

<sup>b</sup>The procedure is described in the experimental section.

These data indicate that the spreading solution can be stored for at least 5 days after preparation without appreciable change in  $\frac{A_{K,EX}}{K,EX}$ . The measurement of  $\frac{A_{K,EX}}{K,EX}$  is based on the original concentration of the spreading solution. Consequently, no significant change in this quantity indicates no significant change in the spreading solution concentration.

#### SUBSTRATE SOLUTIONS

##### Sulfuric Acid

Sulfuric acid substrates were prepared by the addition of sufficient 0.1N  $H_2SO_4$  to distilled water to obtain a pH of 4.00. The pH of these substrates was found not to change by more than  $\pm 0.003$  pH unit when they were allowed to stand in contact with air for 3 hours.

##### Aluminum Sulfate

Aluminum sulfate substrates were prepared with stock solutions of the salt and adjusted to pH 4.00 with sulfuric acid or sodium hydroxide solutions. The stock solutions were prepared with crystalline aluminum sulfate ( $Al_2(SO_4)_3 \cdot 18H_2O$ ) and ranged in concentration from 0.2 to 2.2% based on the hydrate. These solutions were renewed every 48 hours and no solutions that showed any evidence of flocculation were used. The pH of the substrates was adjusted approximately 30 minutes after addition of the stock solutions. It was found not to change by more than  $\pm 0.006$  pH unit when the substrates were allowed to stand in contact with air for 3 hours.

##### Oxalic Acid

Oxalic acid substrates were prepared with stock solutions of the acid and adjusted to pH 4.00 with sodium hydroxide solution. The stock solutions were made up

with crystalline oxalic acid ( $\text{H}_2\text{C}_2\text{O}_4 \cdot 2\text{H}_2\text{O}$ ) and ranged in concentration from 1.66 to 1.83% based on the hydrate. Oxalic- $\text{C}^{14}$  acid enriched oxalic acid substrates were formulated with a stock solution with a specific activity of  $1.72 \times 10^{-4}$  mc.  $\text{mM}^{-1}$ . This stock solution was obtained by the addition of crystalline oxalic- $\text{C}^{14}$  acid (as the dihydrate) to a 1.83% oxalic acid solution. The pH of the oxalic acid substrates was found not to change by more than  $\pm 0.003$  pH unit when they were allowed to stand in contact with air for 3 hours.

#### Aluminum Sulfate Plus Oxalic Acid

Aluminum sulfate plus oxalic acid substrates were prepared with stock solutions similar in concentration to those used for the individual substrates. The aluminum sulfate solution was added before the oxalic acid solution for each substrate. The pH of the mixtures was adjusted to 4.00 with sodium hydroxide approximately 30 minutes after the addition of the oxalic acid stock solution. When these substrates were allowed to stand in contact with air for 3 hours, the pH was observed not to change by more than  $\pm 0.005$  pH unit. This is in agreement with the pH behavior reported by Babko and Dubovenko (40) for similar systems.

#### CARBON ANALYSIS SOLUTIONS

##### Combustion

The liquid combustion reagent for the Van Slyke manometric determination of carbon was made with fuming sulfuric acid, phosphoric acid, and potassium iodate. This material was prepared and stored as recommended by Van Slyke, et al., (60).

##### CO<sub>2</sub>-Absorption

Alkaline hydrazine solution (0.5N NaOH plus 0.3M hydrazine) for the absorption of CO<sub>2</sub> was prepared with 5.0N sodium hydroxide (in CO<sub>2</sub>-free water), hydrazine sulfate,

and boiled distilled water. The 5.0N NaOH stock solution was substituted for 18-20N NaOH used by Van Slyke and Folch (59). Otherwise, the preparation and storage procedures given by these workers were followed.

#### CO<sub>2</sub>-Liberation

Lactic acid solution (2.0N, in CO<sub>2</sub>-free water) for the liberation of CO<sub>2</sub> from the alkaline hydrazine solution was used as received. This material was stored as recommended by Van Slyke and Folch (59).

#### CLEANING SOLUTION

Saturated chromic acid cleaning solution was used for cleaning glassware and polyethylene containers. This solution was prepared with potassium dichromate and concentrated sulfuric acid.

## APPENDIX III

DETERMINATION OF  $\pi$ -A ISOTHERMS

## MONOLAYERS AT THE LIQUID-AIR INTERFACE

Criteria for Monolayer Formation

Only certain types of molecules are capable of forming insoluble monolayers at the liquid-gas interface. The simplest type is composed of a large nonpolar portion and a polar functional group at one extremity. This kind of molecule remains at the interface primarily because the insolubility of the nonpolar portion balances the solubility of the polar functional group. The stability of a monolayer of these molecules depends on the molecular volatility and the intermolecular interactions between the hydrocarbon portions of adjacent molecules. Both of these properties must be below certain levels for the monolayer to be stable enough to study (66). The resin acid molecules are of this simple type and they form stable monolayers on aqueous substrates (44). The orientation of these molecules at the interface is shown schematically in Fig. 13. The polar heads of the molecules are immersed while the nonpolar hydrocarbon portions stick out of the aqueous solution.

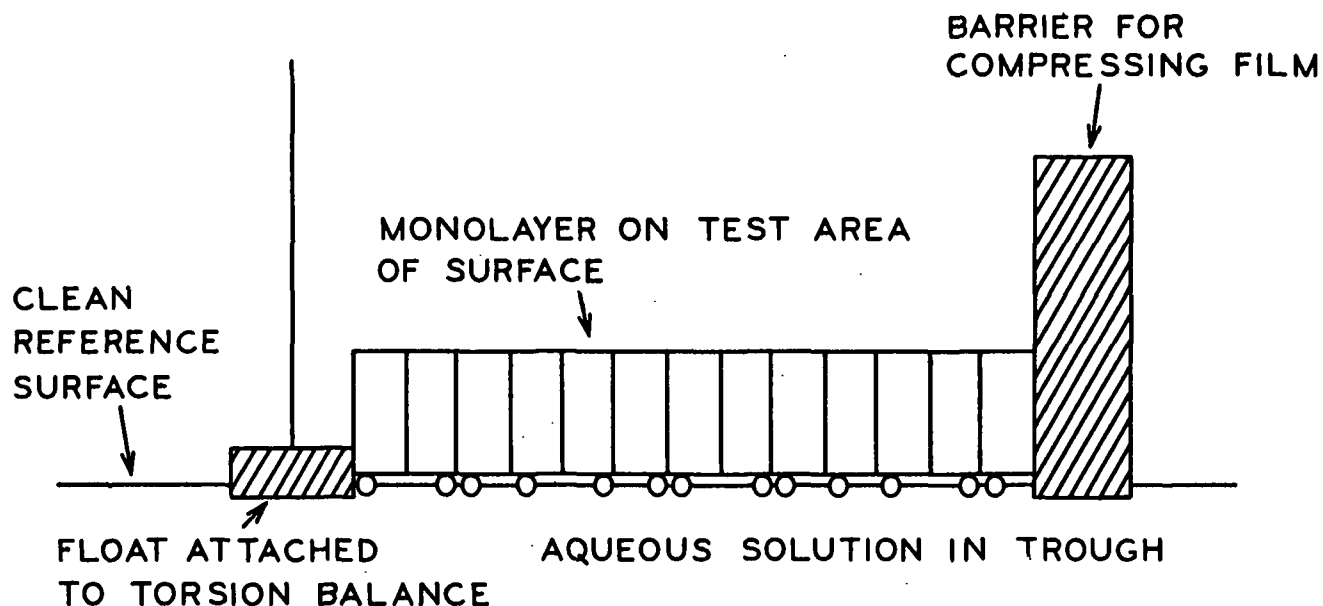


Figure 13. Schematic Diagram of a Resin Acid Monolayer Under Study in a Langmuir Surface Balance.

#### Definition of $\pi$

The surface pressure,  $\pi$ , is generally considered to be equal to the reduction of the pure liquid-surface tension by the film and it is defined mathematically by Equation (15)

$$\pi = \gamma_0 - \gamma \quad (15)$$

where

$\pi$  = surface pressure, dyne cm.<sup>-1</sup>

$\gamma_0$  = surface tension of the pure liquid, dyne cm.<sup>-1</sup>

$\gamma$  = surface tension of the film-covered surface, dyne cm.<sup>-1</sup>

The surface tension arises from the unbalanced molecular attraction which tends to pull molecules into the interior of a liquid phase.

Manual Measurement of  $\pi$ 

The direct measurement of  $\pi$  is accomplished with the null-deflection surface balance developed by Langmuir (98) and modified by Adam and Jessop (99). The sensing part of this device consists of a movable float that separates the clean reference area from the film-covered area of the surface. This float is shown schematically in Fig. 13 (and Fig. 15) and it is connected to a torsion wire balance system. The gaps between the float and the trough edges are sealed with flexible ribbons to prevent film leakage to the reference surface. Once the monolayer molecules are close enough to interact, the float is pulled to the left as the test area is reduced. This area is reduced in a stepwise manner by moving the compression barrier to the left. The torsion wire is rotated manually to return the float to the null position after each reduction in area. The extent of the rotation is read directly from a vernier scale that moves over a circular disk calibrated in degrees. This torsion wire rotation is converted to  $\pi$  through the use of Equation (16)

$$\pi = (C\theta_r)/(L_f) \quad (16)$$

where

$\pi$  = surface pressure, dyne cm.<sup>-1</sup>

$C$  = torsion wire constant, dyne degree<sup>-1</sup>

$\theta_r$  = rotation of torsion wire, degree

$L_f$  = effective length of float, cm.

The effective float length is given by Equation (17)

$$L_f = l + (W)/(2) \quad (17)$$

where

$\underline{L}_f$  = effective length of float, cm.

$\underline{l}$  = actual length of float, cm.

$\underline{W}$  = combined width of gaps occupied by flexible ribbons, cm.

### Manual Measurement of $\underline{A}$

The average cross-sectional area of the monolayer molecules,  $\underline{A}$ , is given by Equation (18)

$$\underline{A} = (pg)/(\underline{N}c^2) \quad (18)$$

where

$\underline{A}$  = average cross-sectional area of monolayer molecules,  $\text{A.}^2 \text{ molecule}^{-1}$

$\underline{p}$  = test area length, cm.

$\underline{g}$  = test area width, cm.

$\underline{N}$  = number of molecules on test area

$\underline{c}$  = A.-cm. equivalence,  $10^{-8} \text{ cm. A.}^{-1}$

The length of the test area is experimentally measured with a metric scale attached to the trough.

### Construction of $\pi$ - $\underline{A}$ Isotherm

The values of  $\pi$  and  $\underline{A}$  are plotted on ordinary coordinate paper with  $\pi$  as a  $f(\underline{A})$ . The  $\pi$ - $\underline{A}$  isotherm is obtained by drawing a smooth curve through the data points.

### DESIGN OF AUTOMATIC RECORDING SURFACE BALANCE

The automatic recording surface balance was designed to perform the manual operations described in the preceding section. It provides continuous area reduction at a known, reproducible, adjustable rate and it provides continuous recording of  $\pi$  as a  $f(\underline{A})$ . The instrument is similar to the one described by Anderson

and Evett (57). Notable changes in the design are as follows: the electrical balancing system was simplified and updated; the trough and barrel torsion balance combination was replaced by a Cenco Horizontal Hydrophile Balance with a trough 65-cm. long, 14-cm. wide and 1.5-cm. deep; the platinum flexible ribbons were replaced with Teflon; and a magnetic damper was added to the torsion balance system.

The manually operated compression barrier was replaced with one driven by an adjustable speed, reversible synchronous motor. Likewise, the manual balancing of the torsion balance system was replaced with an electrical balancing-recording system.

The edges of the trough, the ends of the support frame, and the Lucite compression barriers were covered with polyfluorocarbon tape. Paraffin was used to coat the remainder of the exposed area of the trough, the float and its accessories, and the heads of the screws used in the attachment blocks. Solvent saturated paper towels were used to clean the smooth side of the plastic tape. The sequence of solvents was methanol followed by n-hexane.

Schematic diagrams of the complete assembly (Fig. 14), the trough and torsion balance assembly (Fig. 15), and the electrical balancing system (Fig. 16) are given in this section. Also included is an abridged electrical parts list (Table XII).

The trough and barrier drive were mounted on separate slabs of 1 inch-thick aluminum tooling plate. These slabs were located on separate benches and cushioned with foam rubber blankets. A Lucite dust shield with a full-length access door was used to cover the trough and a Lucite overflow tray was placed under the trough. The tray was slightly larger than the trough and open at one end to a sink.

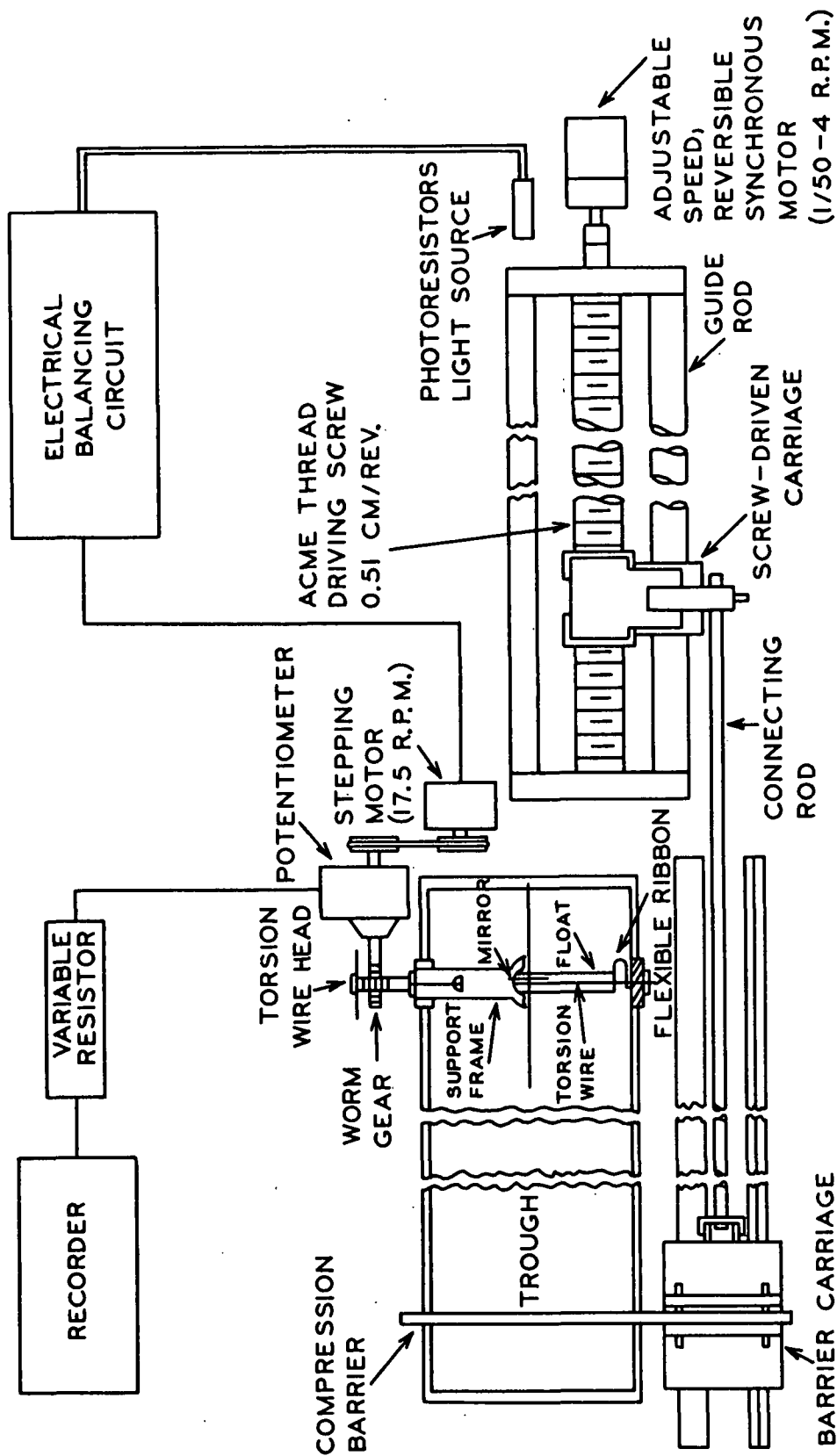


Figure 14. Schematic Diagram of Complete Assembly

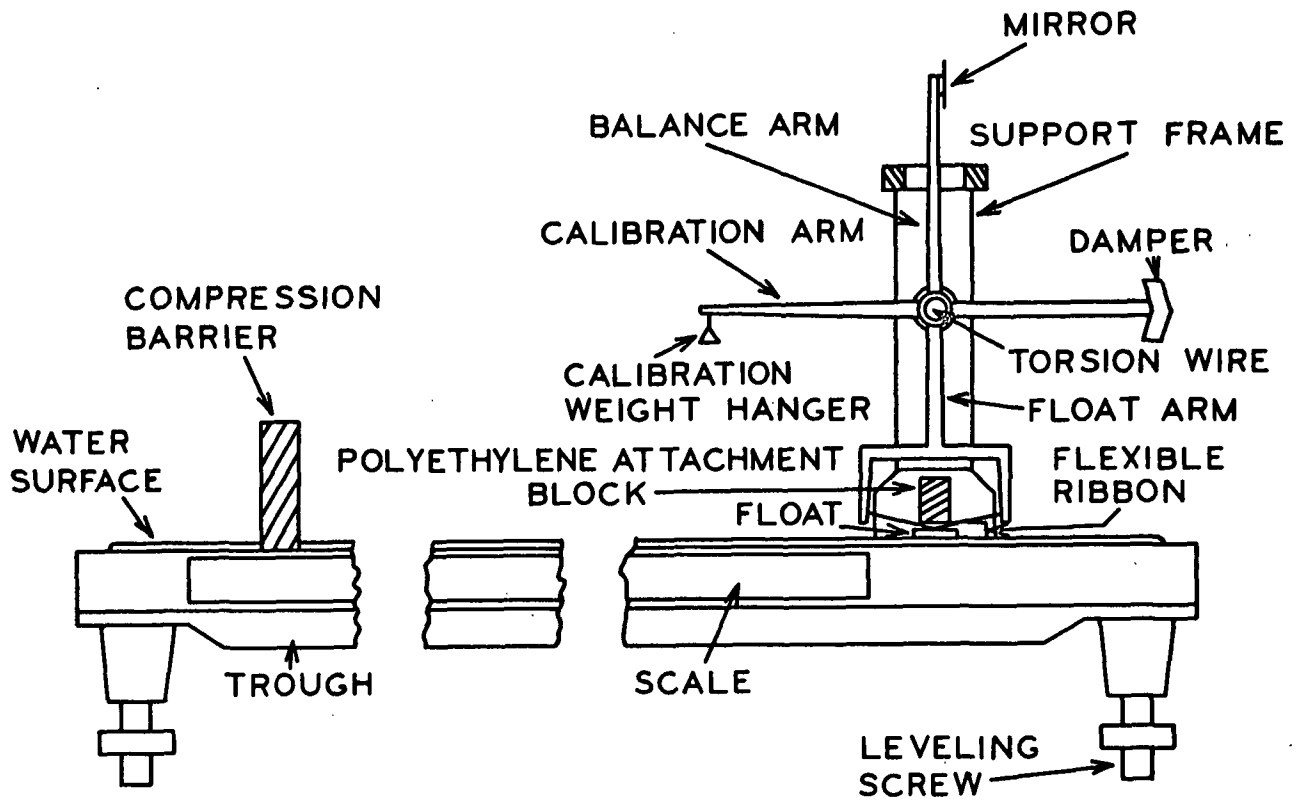


Figure 15. Schematic Diagram of Trough and Torsion Balance Assembly

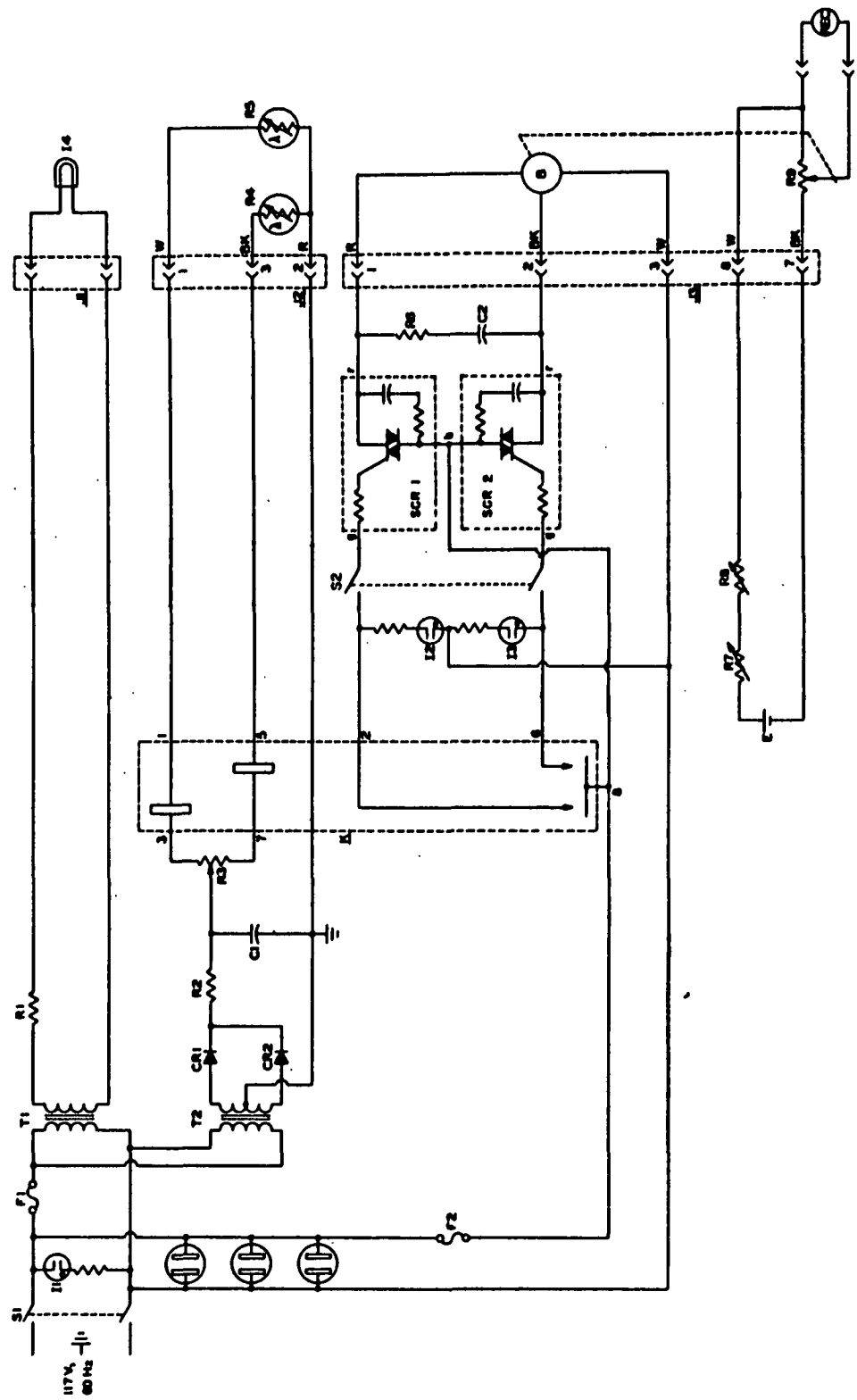


Figure 16. Schematic Diagram of Electrical Balancing System

TABLE XII  
ABRIDGED ELECTRICAL PARTS LIST

Diagram Designation	Identification
B	Slo-Syn motor, type SS50PI
C1	1000 mfd, 15 v.
C2	2.6 mfd, 330 VAC
CR1, CR2	Type 1N1692
E	Dry cell, 1.5 v., size C
F1, F2	3AG, 1/2 A, S-B
I1, I2, I3	Neon 51
I4	Type 1130 (In I&N type 2099 Illuminating Device)
J1	Superior type DF30BC binding posts
J2	Amphenol type 91-PC3F (use 91-MC3M on cord)
J3	Jones type S-308-RP (use P-308-CCT on cord)
K	Barber-Colman type AYIZ7358-100
R1	0.6 ohm
R2	20 ohm, 2W
R3	ADJUST, 1000 ohms, 2 W, linear
R4, R5	Clairex type CL-707L
R6	250 ohms, 25 W
R7	.300K potentiometer
R8	SCALE, 25K, 2 W, linear
R9	2.2K, 10-turn, 0.1% linear
S1	POWER
S2	RUN-ADJUST
T1	Stancor type P-6456
T2	Stancor type RT-201 (taps selected to give 8.7 v. across C1)
SCR1, SCR2	G-E triac subassemblies, type 100G1

## OPERATION OF AUTOMATIC RECORDING SURFACE BALANCE

Determination of  $\pi$ -A Isotherm

The operation of the automatic balance during the determination of a  $\pi$ -A isotherm is outlined in this section. References are made to the schematic diagrams in the preceding section.

After the trough is leveled and filled and the substrate swept, switch S2 is opened to disconnect the balance motor. Switch S1 is turned on to supply power to all components. Light from the illuminating lamp, I4, is directed to the balance-indicating mirror attached to the balance arm of the torsion balance. The light reflected from this mirror strikes the photosensitive resistors, R4 and R5. These are part of the bridge comprised of R4, R5, and the two coil windings of the Micropositioner relay, K. The balance or direction of unbalance of the bridge may be observed on the indicator lamps I2 and I3. Any needed adjustments are made by changing the position of the illuminating light on the photoresistors.

The spreading solution is deposited on the test surface between the barrier and the float. Six minutes are allowed for reaction. Switch S1 is turned off. Switch S2, the chart recorder drive switch, and the driving screw motor switch are turned on. Switch S1 is turned on and the recorder chart and the compression barrier start simultaneously. When the test area has been reduced to a value at which  $\gamma$  decreases, the float is pulled toward the clean reference surface. This causes the light reflected from the mirror to change position on the photosensitive resistors. Simultaneously, the balance of the bridge of which these are a part is affected. The unbalance of the bridge causes the closure of the relay contacts from which the stepping-type balance motor, B, is operated. This motor turns in the direction dictated by the unbalance of the bridge until the bridge is balanced. At this point, the relay contacts open and the motor stops.

The balance motor is mechanically coupled to potentiometer R9 which in turn is directly geared to the torsion wire of the surface balance. The position of the slider of R9 is a measure of the force applied to keep the surface balance in the null position. Dry cell E, range resistor R7, and SCALE calibrating potentiometer R8 impress a voltage across R9 suitable for driving a 30 mV potentiometric recorder. The chart recorder drive speed range is  $1/8$  to  $4$  inch  $\text{minute}^{-1}$ .

### Calibration

The time axis of the chart recorder is directly proportional to the average area of the monolayer molecules ( $\bar{A}$ ). The deflection of the pen is directly proportional to the force required to keep the surface balance in the null position.

For the correlation of  $\bar{A}$  and chart paper length, the driving screw motor and the recorder chart drive motor are started and stopped simultaneously. These motors are allowed to run for various time periods. The length of chart and the reading on the trough scale are recorded for each run. Barrier positions are converted to molecular areas by Equation (18) and the chart length is plotted as a  $f(\bar{A})$  to obtain an area calibration curve.

The torsion balance system is calibrated in terms of recorder pen deflection. The balance is filled to the operating level, switch S2 is opened, and switch S1 is closed. Various weights are hung on the calibration lever arm of the balance at the same distance from the torsion wire as the float. The pulley attached to potentiometer R9 is turned by hand until the electrical bridge is balanced as shown by the indicator lamps I2 and I3. The pen deflection caused by the movement of the potentiometer slider is registered on the chart recorder paper. The scale expansion of the recorder is set with the SCALE calibration potentiometer R8

(coarse) and the chart recorder scale potentiometer (fine). A plot of pen deflection as a function of ( $\text{calibration weight}/\underline{L}_f$ ) yields the surface pressure calibration curve.

#### SAMPLE $\pi$ -A ISOTHERMS

Sample  $\pi$ -A isotherms obtained with the automatic recording surface balance are shown in Fig. 17. Isotherm A is for the TABSH monolayer on sulfuric acid. Isotherm B is for the monolayer formed when TABSH is spread on an aluminum sulfate substrate with  $[Al] = 3.16 \times 10^{-3} M$ . The quantity,  $[Al]$ , represents the total molar concentration of aluminum species present in the system. The values of  $A_{10}$ ,  $A_{K,EX}$ , and  $\pi_{K,EX}$  were measured from isotherms. The average area of the monolayer molecules when  $\pi = 10 \text{ dyne cm.}^{-1}$  is denoted by  $A_{10}$  (66). The values,  $A_{K,EX}$ , and  $\pi_{K,EX}$ , are the coordinates of the extrapolated collapse point of the monolayer. This point is obtained by extrapolation of the approximately linear portions that lie immediately on either side of the knee of the isotherm (44) (see arrow in Fig. 17).

The chart recorder potentiometer was set so that at  $\pi = 20.0 \text{ dyne cm.}^{-1}$  the pen deflection = 110 mm. With this setting, the operational sensitivity of the balance =  $0.19 \text{ dyne cm.}^{-1} \text{ mm.}^{-1}$ . The operational sensitivity is the reciprocal of the slope of the surface pressure calibration curve (66).

#### EFFECT OF AREA REDUCTION RATE ON $\pi$ -A MEASUREMENTS

Anderson and Evett (57) reported the successful use of area reduction rates ( $\frac{dA}{dt}$ ) in the range between 0.1 and 2.0  $A.^2 \text{ molecule}^{-1} \text{ minute}^{-1}$ . Consequently, a convenient rate within this range was selected for preliminary work with the monolayers described in the preceding section. The rate used was 1.43  $A.^2 \text{ molecule}^{-1} \text{ minute}^{-1}$  and it is one half of the maximum possible rate of the instrument. Since the time required to complete a  $\pi$ -A isotherm at this rate was inconveniently long, the maximum rate was tried for the monolayers.

The values of  $A_{10}$ ,  $A_{K,EX}$ , and  $\pi_{K,EX}$  obtained with both rates are given in Table XIII.

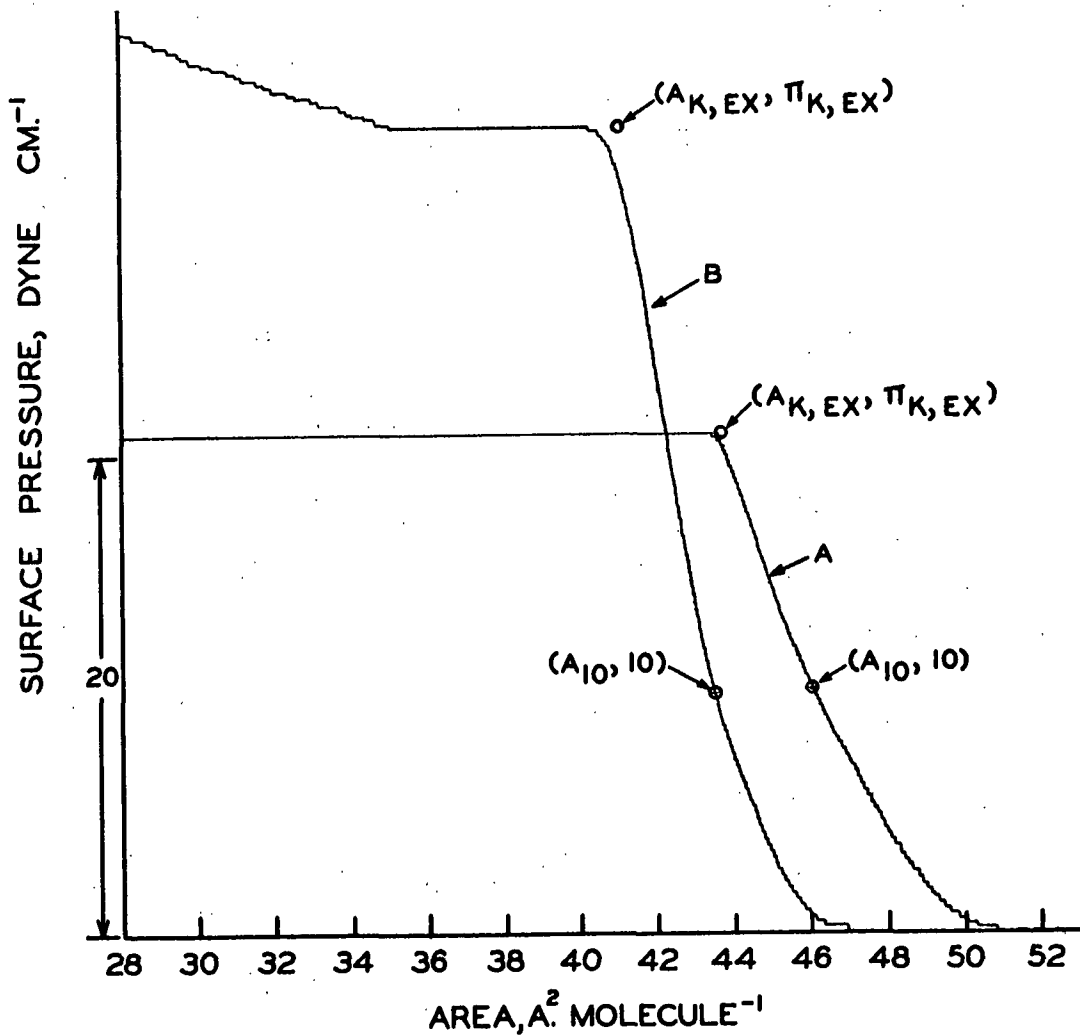


Figure 17. Sample Surface Pressure-Area Isotherms Obtained with Automatic Recording Surface Balance. Isotherm A is for the TABSH Monolayer on a Sulfuric Acid Substrate. Isotherm B is for the Monolayer Formed when TABSH is Spread on an Aluminum Sulfate Substrate with  $[Al] = 3.16 \times 10^{-3} M$ . Both Substrates were at  $20^\circ C$ . with  $pH = 4.00$ , Reaction Time = 6 Minutes, and  $\frac{dA}{dt} = 2.86 A.^2 \text{ Molecule}^{-1} \text{ Minute}^{-1}$

TABLE XIII

$\underline{A}_{10}$ ,  $\underline{A}_{K,EX}$ , AND  $\pi_{K,EX}$  VALUES OBTAINED AT TWO AREA REDUCTION RATES<sup>a</sup>

Substrate	Area Reduction Rate, A. <sup>2</sup> molecule <sup>-1</sup> minute <sup>-1</sup>	$\underline{A}_{10}$ , A. <sup>2</sup> molecule <sup>-1</sup>	$\underline{A}_{K,EX}$ , A. <sup>2</sup> molecule <sup>-1</sup>	$\pi_{K,EX}$ , dyne cm. <sup>-1</sup>
H <sub>2</sub> SO <sub>4</sub>	1.43	45.7	43.3	20.5
H <sub>2</sub> SO <sub>4</sub>	2.86	46.0	43.6	20.5
Al <sub>2</sub> (SO <sub>4</sub> ) <sub>3</sub> <sup>b</sup>	1.43	43.6	41.2	33.4
Al <sub>2</sub> (SO <sub>4</sub> ) <sub>3</sub>	2.86	43.4	41.0	33.5

<sup>a</sup>Substrates were at 20°C. with pH = 4.00 and reaction time = 6 minutes.

<sup>b</sup>[Al] = 3.16 x 10<sup>-3</sup>M.

Values obtained at the higher rate are not appreciably different from those obtained at the lower rate. As a result, the rate, 2.86 A.<sup>2</sup> molecule<sup>-1</sup> minute<sup>-1</sup>, was used for all subsequent  $\pi$ -A isotherm determinations.

#### REPRODUCIBILITY OF $\pi$ -A MEASUREMENTS

The values of  $\underline{A}_{10}$ ,  $\underline{A}_{K,EX}$ , and  $\pi_{K,EX}$  for TABSH monolayers on sulfuric acid substrates are shown in Table XIV.

The standard error is less than  $\pm 0.03$  for all three quantities.

Table XV shows the values of  $\underline{A}_{10}$ ,  $\underline{A}_{K,EX}$ , and  $\pi_{K,EX}$  for the monolayers formed when TABSH is spread on aluminum sulfate substrates with [Al] = 3.16 x 10<sup>-3</sup>M.

The standard error is less than  $\pm 0.1$  for all three quantities.

TABLE XIV

$\underline{A}_o$ ,  $\underline{A}_{K,EX}$ , AND  $\underline{\pi}_{K,EX}$  VALUES FOR TABSH MONOLAYERS  
ON SULFURIC ACID SUBSTRATES<sup>a</sup>

Sample Number	$\underline{A}_o$ , A. <sup>2</sup> molecule <sup>-1</sup>	$\underline{A}_{K,EX}$ , A. <sup>2</sup> molecule <sup>-1</sup>	$\underline{\pi}_{K,EX}$ , dyne cm. <sup>-1</sup>
TABSH-86	45.9	43.5	20.7
TABSH-91	45.8	43.6	20.8
TABSH-93	45.8	43.6	20.5
TABSH-97	46.0	43.8	20.6
TABSH-99	45.9	43.6	20.6
TABSH-101	46.0	43.6	20.6
TABSH-103	45.9	43.6	20.5
TABSH-109	45.9	43.6	20.8
TABSH-112	46.0	43.6	20.5
TABSH-114	46.0	43.6	20.5
TABSH-117	46.0	43.8	20.6
TABSH-122	46.0	43.6	20.5
TABSH-126	46.0	43.8	20.7
TABSH-128	46.0	43.7	20.8
TABSH-130	46.2	43.8	20.7
TABSH-132	46.2	43.8	20.7
TABSH-134	46.2	43.8	20.8
TABSH-138	46.1	43.7	20.6
TABSH-140	45.9	43.6	20.6
TABSH-142	46.2	43.8	20.6
TABSH-146	46.0	43.7	20.5
TABSH-148	46.0	43.7	20.6
TABSH-150	46.0	43.7	20.7
TABSH-154	46.1	43.8	20.6
Average values	$46.00 \pm \sigma$ $= 46.00 \pm 0.12$	$43.68 \pm \sigma$ $= 43.68 \pm 0.10$	$20.63 \pm \sigma$ $= 20.63 \pm 0.10$

<sup>a</sup>Substrates were at 20°C. with pH = 4.00, reaction time = 6 minutes, and  $\frac{dA}{dt} = 2.86$  A.<sup>2</sup> molecule<sup>-1</sup> minute<sup>-1</sup>.

TABLE XV

$\underline{A}_{10}$ ,  $\underline{A}_{K,EX}$ , AND  $\pi_{K,EX}$  VALUES FOR THE MONOLAYERS FORMED  
WHEN TABSH IS SPREAD ON ALUMINUM SULFATE SUBSTRATES<sup>a</sup>

Sample Number	$\underline{A}_{10}$ , A. <sup>2</sup> molecule <sup>-1</sup>	$\underline{A}_{K,EX}$ , A. <sup>2</sup> molecule <sup>-1</sup>	$\pi_{K,EX}$ , dyne cm. <sup>-1</sup>
TABSH-104	43.1	41.0	33.7
TABSH-127	43.4	41.0	33.5
TABSH-169	43.4	41.0	33.5
Average values	$43.30 \pm \sigma$ $= 43.30 \pm 0.17$	41.0	$33.57 \pm \sigma$ $= 33.57 \pm 0.11$

<sup>a</sup>Substrates were at 20°C. with pH = 4.00,  $[Al] = 3.16 \times 10^{-3} M$ , reaction time = 6 minutes, and  $\frac{dA}{dt} = 2.86 A.^2 \text{ molecule}^{-1} \text{ minute}^{-1}$ .

## APPENDIX IV

## ANALYSIS OF COLLECTED MONOLAYER MATERIAL

## ISOLATION

Collection Trough

The two collection troughs were constructed with 1/2 inch-thick Lucite sheets, polyfluorocarbon tape, and paraffin. Each collection trough consisted of a trough surrounded by an overflow channel connected to a drain. A schematic diagram of the larger collection trough is given in Fig. 18.

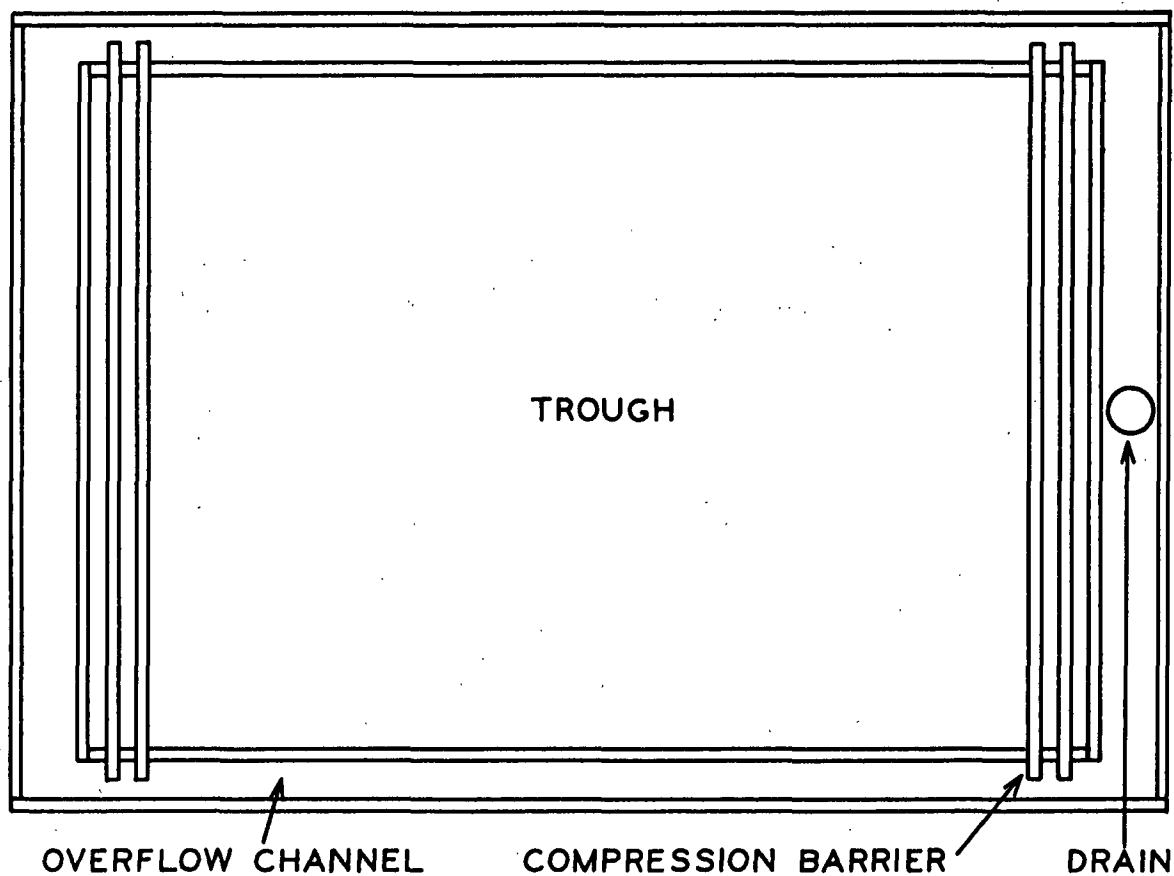


Figure 18. Schematic Diagram of Collection Trough Used to Prepare Monolayers for Analysis

The trough of the smaller collection trough was 69-cm. long, 25-cm. wide, and 1.2-cm. deep. The trough of the larger one was 107-cm. long, 71-cm. wide, and 1.2-cm. deep. Polyfluorocarbon tape was used to cover the compression barriers and the edges and sides of the troughs. The remainder of each trough and the edges of the tape were covered with paraffin. The tape was cleaned before use as described in Appendix III.

#### Effect of Washing on Free Acid Mole Fraction

The free acid mole fractions of washed and unwashed monolayer material collected from aluminum sulfate substrates with  $[Al] = 3.16 \times 10^{-3} M$  are given in Table XVI. These fractions were determined from the infrared spectra of the samples as described in the Results and Discussion section.

TABLE XVI

#### FREE ACID MOLE FRACTIONS OF WASHED AND UNWASHED MONOLAYER MATERIAL COLLECTED FROM ALUMINUM SULFATE SUBSTRATES<sup>a</sup>

Sample Number	Original $[Al]$ , $M$	Treatment	Free Acid Mole Fraction
H21	$3.16 \times 10^{-3}$	unwashed	0.51
H39	$3.16 \times 10^{-3}$	washed	0.50

<sup>a</sup>Both substrates were at 20°C. with pH = 4.00 and reaction time = 6 minutes; samples were dried at 20°C.

These results indicate that washing does not cause any significant change in the free acid mole fraction of this material. All samples for analysis except H21 were washed according to the procedure described in the experimental section.

Effect of Number of Skimmings and Substrate Age on Free Acid Mole Fraction

Samples of the first and last monolayers of a series collected from an aluminum sulfate substrate were compared by infrared analysis. Similar samples were compared for a substrate with  $[Al] = [C_2O_4]$ . The free acid mole fraction ( $X_{\text{TABSH}}$ ) values for these samples are given in Table XVII.

TABLE XVII

FREE ACID MOLE FRACTIONS OF FIRST AND LAST SKIMMINGS IN A SERIES<sup>a</sup>

Substrate		Skimming Number	Time After Mixing, <sup>b</sup> minutes	Free Acid Mole Fraction
$Al_2(SO_4)_3$ Original [Al], <u>M</u>	$H_2C_2O_4$ Original [C <sub>2</sub> O <sub>4</sub> ], <u>M</u>			
$3.16 \times 10^{-3}$	0	1	60	0.51
$3.16 \times 10^{-3}$	0	15	210	0.50
$3.16 \times 10^{-3}$	$3.16 \times 10^{-3}$	1	60	0.82
$3.16 \times 10^{-3}$	$3.16 \times 10^{-3}$	17	260	0.84

<sup>a</sup>Substrates were at 20°C. with pH = 4.00 and reaction time = 6 minutes; samples were washed and dried at 20°C.

<sup>b</sup>This is the time between addition of reagent stock solutions to water and collection of material.

The  $X_{\text{TABSH}}$  values of the material from these two substrates are not appreciably affected by the number of skimmings or substrate age.

Effect of Number of Skimmings on [Al] of Substrate

The depletion of [Al] caused by the removal of monolayer material was calculated for all substrates. The calculations were based on the salt mole

fraction of the monolayers and the presence of  $\text{Al}(\text{TABS})_2\text{OH}$  in the monolayer material. Table XVIII contains the results of these calculations.

TABLE XVIII

CALCULATED DEPLETION OF [Al] IN SUBSTRATES CAUSED  
BY REMOVING REACTED MONOLAYER MATERIAL<sup>a</sup>

Substrate			
$\text{Al}_2(\text{SO}_4)_3$ Original [Al], <u>M</u>	$\text{H}_2\text{C}_2\text{O}_4$ Original [ $\text{C}_2\text{O}_4$ ], <u>M</u>	Maximum Number of Skimmings	Depletion of [Al], <sup>b</sup> %
$1.78 \times 10^{-4}$	0	6	0.06
$3.16 \times 10^{-4}$	0	7	0.05
$5.63 \times 10^{-4}$	0	10	0.06
$1.00 \times 10^{-3}$	0	11	0.04
$1.78 \times 10^{-3}$	0	11	0.03
$3.16 \times 10^{-3}$	0	11	0.02
$5.63 \times 10^{-3}$	0	11	0.01
$1.00 \times 10^{-2}$	0	11	0.006
<sup>c</sup> $3.16 \times 10^{-3}$	0	15	0.02
$3.16 \times 10^{-3}$	$7.9 \times 10^{-4}$	11	0.02
$3.16 \times 10^{-3}$	$1.58 \times 10^{-3}$	11	0.01
$3.16 \times 10^{-3}$	$2.37 \times 10^{-3}$	11	0.01
$3.16 \times 10^{-3}$	$3.16 \times 10^{-3}$	6	0.004
$3.16 \times 10^{-3}$	$3.97 \times 10^{-3}$	6	0.002
$3.16 \times 10^{-3}$	$4.74 \times 10^{-3}$	6	0.001
$3.16 \times 10^{-3}$	$6.32 \times 10^{-3}$	6	0.001
<sup>c</sup> $3.16 \times 10^{-3}$	$3.16 \times 10^{-3}$	17	0.01

<sup>a</sup> Calculated for substrates at 20°C. with pH = 4.00 and reaction time = 6 minutes.

<sup>b</sup> Calculated depletion is based on the original [Al] and the salt mole fraction of the monolayer where  $\text{Al}(\text{TABS})_2\text{OH}$  is present in samples washed and dried at 20°C.

<sup>c</sup> These are representative values for the larger trough with a 11.5-l. capacity. The remaining sample numbers are for the smaller trough with a 2.6-l. capacity.

The calculated depletion of [Al] is 0.06% or less for all substrates.

Effect of Number of Skimmings and Substrate Age on Substrate pH

The pH of each substrate solution was determined after a set of skimmings had been collected. These results are shown in Table XIX.

TABLE XIX

pH VALUES OF SUBSTRATES AFTER REMOVAL OF SETS OF SKIMMINGS<sup>a</sup>

Substrate		Original pH	Number of Skimmings	Time After Mixing, <sup>b</sup> minutes	Final pH
Al <sub>2</sub> (SO <sub>4</sub> ) <sub>3</sub> Original [Al], M	H <sub>2</sub> C <sub>2</sub> O <sub>4</sub> Original [C <sub>2</sub> O <sub>4</sub> ], M				
1.78 x 10 <sup>-4</sup>	0	3.995	6	132	3.990
3.16 x 10 <sup>-4</sup>	0	4.000	7	144	3.995
5.63 x 10 <sup>-4</sup>	0	3.995	10	180	3.984
1.00 x 10 <sup>-3</sup>	0	4.005	11	192	4.000
1.78 x 10 <sup>-3</sup>	0	4.002	11	192	3.994
3.16 x 10 <sup>-3</sup>	0	4.000	11	192	4.000
5.63 x 10 <sup>-3</sup>	0	4.000	11	192	4.009
1.00 x 10 <sup>-3</sup>	0	4.000	11	192	4.038
<sup>c</sup> 3.16 x 10 <sup>-3</sup>	0	4.000	15	260	3.994
3.16 x 10 <sup>-3</sup>	7.9 x 10 <sup>-4</sup>	4.000	11	192	4.015
3.16 x 10 <sup>-3</sup>	1.58 x 10 <sup>-3</sup>	3.998	11	192	4.002
3.16 x 10 <sup>-3</sup>	2.37 x 10 <sup>-3</sup>	3.999	11	192	4.003
3.16 x 10 <sup>-3</sup>	3.16 x 10 <sup>-3</sup>	3.999	6	132	3.998
3.16 x 10 <sup>-3</sup>	3.97 x 10 <sup>-3</sup>	4.001	6	132	4.011
3.16 x 10 <sup>-3</sup>	4.74 x 10 <sup>-3</sup>	3.998	6	132	4.002
3.16 x 10 <sup>-3</sup>	6.32 x 10 <sup>-3</sup>	4.002	6	132	4.002
<sup>c</sup> 3.16 x 10 <sup>-3</sup>	3.16 x 10 <sup>-3</sup>	4.000	18	294	4.002

<sup>a</sup>Substrates were at 20°C. with reaction time = 6 minutes.

<sup>b</sup>This is the time between addition of reagent stock solutions to water and measurement of final pH.

<sup>c</sup>These are representative values for larger trough with a 11.5-l. capacity. The remaining sample numbers are for the smaller trough with a 2.6-l. capacity.

Only four substrates had a pH change greater than 0.2%.

## VACUUM DRYING CHAMBER

The vacuum chamber used to dry samples at 40°C. and 100°C. is shown in Fig. 19. The node is approximately 5-mm. larger in outside radius than the glass tubing. A Teflon sleeve (Matheson 32315-45) was used to seal the ground joint and the stopcock was equipped with a straight bore Teflon plug.

## REPRODUCIBILITY OF INFRARED ABSORBANCE RATIO VALUES

The absorbance of COOH at 1700 cm.<sup>-1</sup>,  $\frac{A_{\text{COOH}}}{A_{\text{CH}}}$ , and the absorbance of CH at 2910 cm.<sup>-1</sup>,  $\frac{A_{\text{CH}}}{A_{\text{CH}}}$ , were measured for samples subjected to infrared analysis. These measurements were used to form the absorbance ratio,  $\frac{A_{\text{COOH}}}{A_{\text{CH}}}$ , of the collected monolayer material. Values of this ratio for TABSH are shown in Table XX.

TABLE XX

ABSORBANCE RATIOS<sup>a</sup> FOR TABSH<sup>b,c</sup>

Sample Number	$\frac{A_{\text{COOH}}}{A_{\text{CH}}}$
H11A	1.09
H11B	1.05
H11C	1.05
H11D	1.10
H11E	1.10
H11F	1.05
H11G	1.10
Average value	$1.077 \pm \sigma$ $= 1.077 \pm 0.026$

<sup>a</sup>For the absorbance ratios, the absorbances of COOH at 1700 cm.<sup>-1</sup> and CH at 2910 cm.<sup>-1</sup> were used.

<sup>b</sup>This TABSH is the recrystallized material described in Appendix I.

<sup>c</sup>The material was dried at 20°C. as described in the experimental section.

STOPCOCK-STRAIGHT BORE  
IMPROVED 1:5 TEFLON PLUG

GROUND JOINT-FULL  
LENGTH - 40/50

NODE

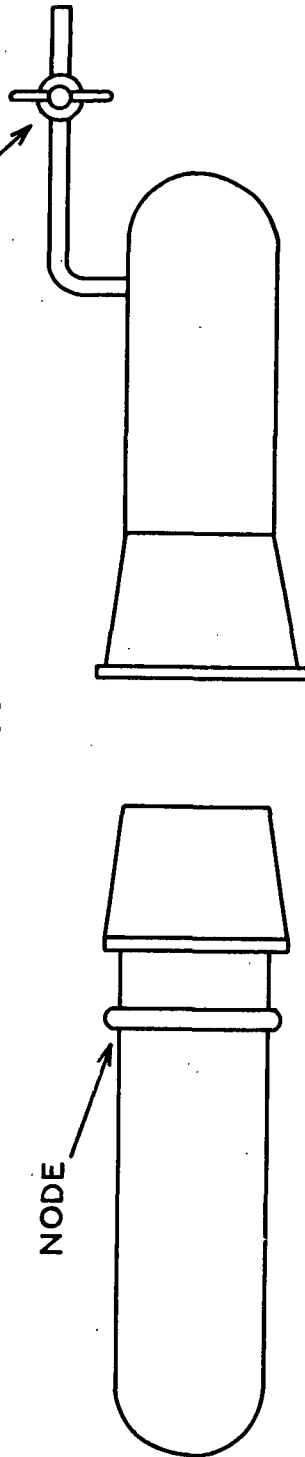


Figure 19. Schematic Diagram of Vacuum Drying Chamber

For these replicate samples, the standard error of the absorbance ratio is less than  $\pm 0.01$ .

## DETERMINATION OF TOTAL CARBON

### General Description

The Van Slyke manometric carbon analysis technique is thoroughly described by Van Slyke and his coworkers in their original papers (59-62). The organic sample is oxidized to carbon dioxide with a liquid combustion reagent (Appendix II). This carbon dioxide is absorbed in an aqueous solution of sodium hydroxide and hydrazine sulfate. After removal of the extraneous gases from the absorption chamber, the carbon dioxide is liberated from the absorption solution by the addition of lactic acid. The amount of carbon dioxide is calculated from the measurement of the gas pressure and temperature at a fixed volume.

### Recovery and Reproducibility

The Van Slyke manometric carbon determination was checked for recovery and reproducibility with sodium carbonate.

Carbon analysis results for this material are given in Table XXI.

The recovery of carbon is 99.35% and for replicate samples, the standard error is  $\pm 0.41$ .

## DETERMINATION OF OPTIMUM OPERATING VOLTAGE OF BERNSTEIN-BALLENTINE TUBE

The optimum operating voltage of the Bernstein-Ballentine tube was determined as described by Bernstein and Ballentine (63). A sample of radioactive carbon dioxide was transferred to the tube with methane. A curve of counts per minute versus voltage was determined over the voltage range in which counting occurs.

TABLE XXI

CARBON CONTENTS OF SODIUM CARBONATE STANDARD<sup>a</sup>

Sample Number	Expected Carbon, mg.	Carbon Found, mg.	Carbon Found, %
Na <sub>2</sub> CO <sub>3</sub> 10	2.142	2.122	99.09
Na <sub>2</sub> CO <sub>3</sub> 36	2.007	1.983	98.83
Na <sub>2</sub> CO <sub>3</sub> 16	2.039	2.005	98.31
Na <sub>2</sub> CO <sub>3</sub> 9	2.012	1.978	98.41
Na <sub>2</sub> CO <sub>3</sub> 35	2.078	2.058	99.08
Na <sub>2</sub> CO <sub>3</sub> 38	2.106	2.120	100.64
Na <sub>2</sub> CO <sub>3</sub> 13	2.103	2.126	101.10
Average value			99.35 ± σ =
			99.35 ± 1.09

<sup>a</sup>This material was dried at 110°C. for 2 hours.

This curve is given in Fig. 20. The voltage, 3600 v., at the midpoint of the approximately horizontal portion of the curve was selected as the optimum operating voltage.

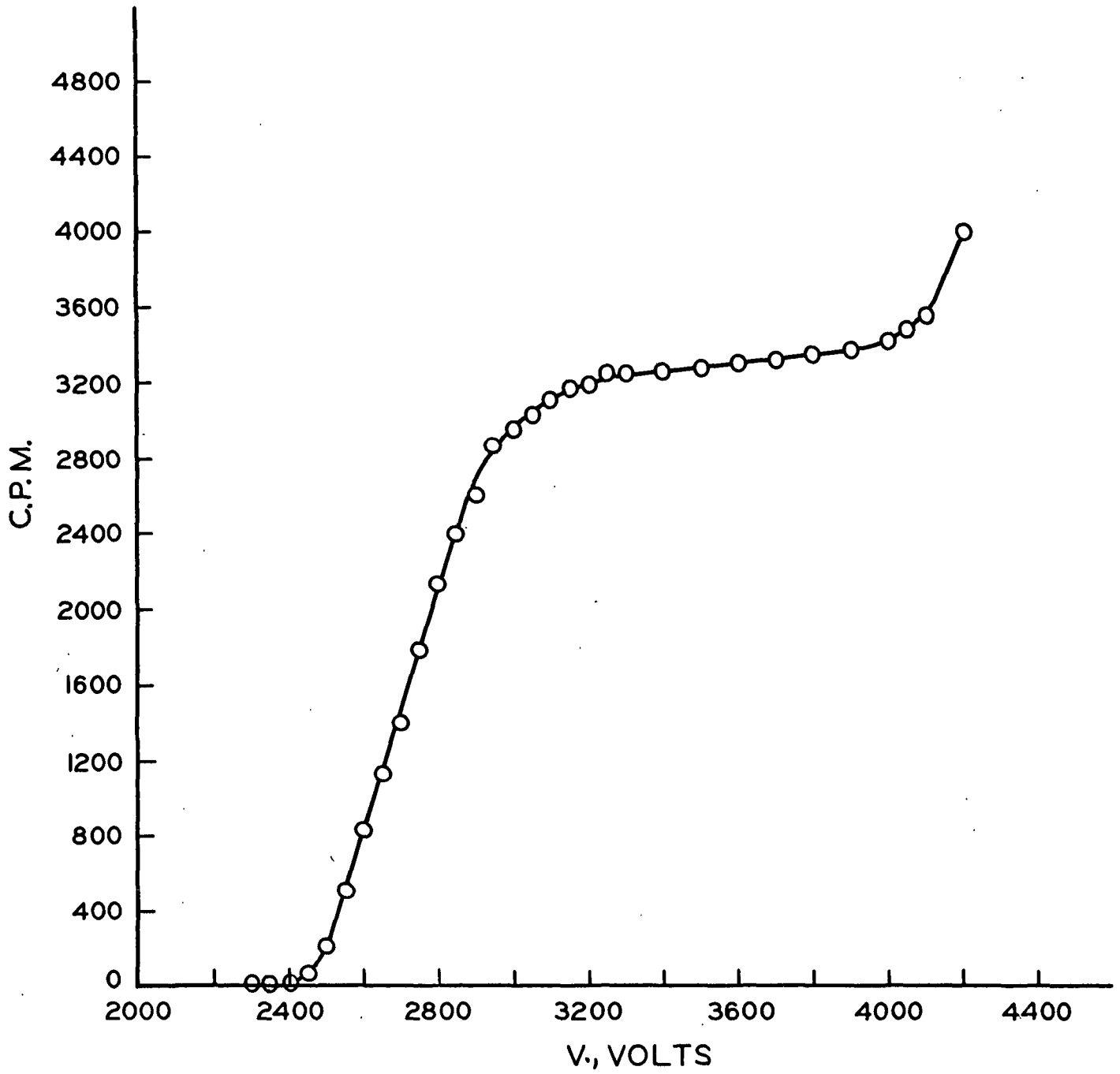


Figure 20. Counts Per Minute Versus Voltage For Bernstein-Ballentine Tube

## APPENDIX V

## DATA

TABLE XXII

pH VALUES FOR ALUMINUM SULFATE SUBSTRATES  
BEFORE ADJUSTMENT<sup>a</sup>

$\text{Log}_{10} [\text{Al}]$ in Substrate	pH
-3.75	4.53
-3.50	4.43
-3.25	4.34
-3.00	4.24
-2.75	4.13
-2.50	4.02
-2.25	3.91
-2.00	3.83
-1.75	3.72

<sup>a</sup>Substrates were at 20°C.

TABLE XXIII

pH VALUES FOR ALUMINUM SULFATE PLUS OXALIC  
ACID SUBSTRATES BEFORE ADJUSTMENT<sup>a</sup>

$[\text{C}_2\text{O}_4]/[\text{Al}]^b$ in Substrate, mole ratio	pH
0.25	2.94
0.50	2.62
0.75	2.44
1.00	2.32
1.06	2.29
1.25	2.22
1.50	2.15
2.00	2.03

<sup>a</sup>Substrates were at 20°C.

<sup>b</sup> $[\text{Al}] = 3.16 \times 10^{-3}\text{M}$  in all substrates.

TABLE XXIV

pH VALUES FOR OXALIC ACID SUBSTRATES BEFORE ADJUSTMENT<sup>a</sup>

$[\text{C}_2\text{O}_4], \text{M} \times 10^3$	pH
1.58	2.82
3.16	2.54
6.32	2.27

<sup>a</sup>Substrates were at 20°C.

TABLE XXV

$\underline{A}_0$ ,  $\underline{A}_{K,EX}$  AND  $\underline{\pi}_{K,EX}$  VALUES FOR THE MONOLAYERS FORMED

WHEN TABSH IS SPREAD ON OXALIC ACID SUBSTRATES<sup>a</sup>

$[C_2O_4]$ in Substrate, $\underline{M} \times 10^3$	$\underline{A}_0$ , A. <sup>2</sup> molecule <sup>-1</sup>	$\underline{A}_{K,EX}$ , A. <sup>2</sup> molecule <sup>-1</sup>	$\underline{\pi}_{K,EX}$ , dyne cm. <sup>-1</sup>
1.58	46.2	43.8	20.7
3.16	46.0	43.7	20.7
6.32	46.1	43.7	20.7

<sup>a</sup>Substrates were at 20°C. with pH = 4.00, reaction time = 6 minutes, and  $\underline{dA}/\underline{dt} = 2.86$  A.<sup>2</sup> molecule<sup>-1</sup> minute<sup>-1</sup>.

## APPENDIX VI

## SAMPLE CALCULATIONS

Sample calculations of  $X_{\text{TABSH}}$  and  $X_{\text{TABS}^-}$  are summarized below for the monolayer material collected from an aluminum sulfate substrate with  $[\text{Al}] = 3.16 \times 10^{-3} \text{ M}$  at  $20 \pm 1^\circ \text{C}$ . with  $\text{pH} = 4.00$ .

$$\text{Absorbance at } 2910 \text{ cm.}^{-1} = 0.730$$

$$\text{Absorbance at } 1700 \text{ cm.}^{-1} = 0.409$$

$$a_{\text{TABSH}}/a_{\text{R}} = 1.08 \text{ (Appendix IV)}$$

$$X_{\text{TABSH}} = \left( \frac{a_{\text{R}}}{a_{\text{TABSH}}} \right) \left( \frac{A_{\text{COOH}}}{A_{\text{CH}}} \right) = 0.52 \quad (12)$$

$$X_{\text{TABSH}} + X_{\text{TABS}^-} = 1.00$$

$$X_{\text{TABS}^-} = 1.00 - X_{\text{TABSH}} = 0.48$$